BIOLOGICAL AND CHEMICAL DESIGN FOR LIGNIN CONVERSION

A Dissertation

by

SHANGXIAN XIE

Submitted to the Office of Graduate and Professional Studies of
Texas A&M University
in partial fulfillment of the requirements for the degree of

DOCTOR OF PHILOSOPHY

Chair of Committee,	Joshua S. Yuan
Committee Members,	Dennis Gross
	Libo Shan
	Susie Y. Dai
Head of Department,	Leland S. Pierson III

August 2016

Major Subject: Plant Pathology

ABSTRACT

The efficient utilization of lignin for fungible fuels and products represents one of the most imminent challenges in modern biorefinery. My research thesis has mainly focused on developing and optimizing the lignin-to-lipid conversion route. Advanced ^{31}P nuclear magnetic resonance (NMR) lignin characterization technology, laccase based lignin pretreatment technology, proteomics and synthetic biology tools were applied to this study. First, the study demonstrated that the enzymes and microbes synergized to degrade different functional groups of lignin to promote the bioconversion. The *Rhodococcus opacus* cell growth increased exponentially in response to the level of laccase treatment, indicating the synergy between laccase and bacterial cells in lignin degradation. NMR analysis suggested that laccase, *R. opacus* cell and Fenton reaction reagents promoted the degradation of different types of lignin functional groups, elucidating the chemical basis for the synergistic effects. The cell-laccase fermentation led to a 17-fold increase of lipid production**.** Second, the study showed that enhanced electron transfer via electron mediators can promote the redox reaction to catalyze the lignin bioconversion by laccase. NMR analysis revealed that an efficient enzyme-mediator system can promote the cleavage of most intramolecular and intermolecular cross-links including the condensed chemical linkages, leading to the degradation of lignin to a large extent. The *R. opacus* PD630 growth was increased by 10^6 fold and the simple batch fermentation could achieve lipid titer at more than 1 g/L. Third, through systems biology-guided biodesign, I have optimized multiple steps of lignin degradation towards to lipid production. An efficient laccase secretion system was established in

PD630 for lignin depolymerization through different molecular levels including transcription, translation, signal peptide secretion efficiency and transporters. Moreover, lipid biosynthesis pathway of *R. opacus* PD630 was optimized based on the proteomics analysis, which led to significantly increased lipid accumulation. The two modules of lignin depolymerization and lipid biosynthesis were then integrated for efficient lignin conversion into lipid.

In summary, these studies enabled more efficient conversion of lignin and biorefinery waste to fungible products. The fundamental understanding of chemical and biological processes in lignin conversion can be exploited in different ways to enable various biorefinery product streams from biorefinery waste streams.

ACKNOWLEDGEMENTS

I would like to give thanks to my advisor Dr. Joshua Yuan, who not only gave me advice and support on my study and research, but also provided me invaluable help and support on my personal life. I am very appreciative for Dr. Yuan's advice on pursuing my successful academic career, realizing my personal ideal, and being good husband and father. The protocols for the research are easily found from the published literature and other publicly available sources. However, the attitude and habit to be a good scientist are difficult to learn from the papers. Therefore, I would like to thank Dr. Dennis Gross, Dr. Libo Shan and Dr. Susie Dai for their advice on developing my personal qualities to be a good scientist. I also would like to give my gratitude to Dr. Gross for his help on my initial bacterial transformation work, to Dr. Shan for her suggestion on my genetic molecular work, and to Dr. Dai for her help on my proteomics research. I also want to extend my gratitude to Dr. Arthur Ragauskas, Dr. Yunqiao Pu and Dr. Qinign Sun for their help on chemical characterization of lignin. Special thanks to Dr. Xiaoyu Zhang for her continuous support on my research, study and my personal living. Thanks also go to my former and current lab mates for their support throughout the course of this research, including Dr. Weibing Shi, Ms Furong Lin, Dr. Xin Wang, Dr. Yan Shi, Dr. Honhbo Yu and Miss Muzi Li. Finally, thanks for my parents and my wife. I may not be able to finish this study and research without their encouragement, support, patience and love.

NOMENCLATURE

2D	Two Dimensional
4-HBA	4-Hydroxybenzoic
AA	Auxiliary Activities
AAD	Ary-Alcohol Dehydrogenase
AAO	Ary-Alcohol Oxidase
ABTS	2,2'-Azino-bis(3-ethlbenzthiazoline-6-sulfonic acid)
BSA	Bovine Serum Albumin
C7BzO	3-(4-Heptyl)phenyl-3-hydroxypropyl dimethylammoniopropanesulfonate
CAZy	The Carbohydrate-Active Enzymes Database
CDH	Cellobiose Dehydrogenase
CFU	Colony Forming Unit
CLP	Consolidate Lignin Processing
DGG	Distiller's Dried Grains
DMSO	Dimethyl Sulfoxide
DNA	Deoxyribonucleic Acid
DOE	Department of Energy
EDTA	Ethylenediaminetetraacetic Acid
EISA	Energy Independence and Security Act
EOL	Ethanol Organosolv Lignin
FAME	Fatty Acid Methyl Ester

FAS	Fatty Acid Synthase
FDR	False Discovery Rate
G	Guaiacyl
GC/MS	Gas Chromatography/Mass Spectrometry
GLOX	Glyoxal Oxidase
GPC	Gel Permeation Chromatography
H	*p*-hydroxyphenyl
HBT	1-Hydroxybenzotriazole
HPLC	High Performance Liquid Chromatography
HSQC	Heteronuclear Single Quantum Coherence
LC-MS/MS	Liquid Chromatography–Mass Spectrometry/ Mass Spectrometry
KEGG	Kyoto Encyclopedia of Genes and Genomes
M_n	Number Average Molecular Weight
MnP	Manganese Peroxidase
M_w	Weight Average Molecular Weight
MudPIT	Multidimensional Protein Identification Technology
NBUS	Natural Biomass Utilization System
NHND	*endo-N*-Hydroxy-5-Norbornene-2,3-Dicarboximide
NMR	Nuclear Magnetic Resonance
NOE	Nuclear Overhauser Effect
Paa	Phenylacetate
PCR	Polymerase Chain Reaction

PDI	Polydispersity Index
PHA	Polyhydroxyalkanoates
PPS	Polymer Standards Service
QR	Quinone Reductase
R&D	Research and Development
RBS	Ribosomal Binding Site
RFS	Renewable Fuel Standard
RM	*Rhodococcus* Minimal
SDF	Simultaneous Depolymerization and Fermentation
SDS	Sodium Dodecyl Sulfate
TAG	Triacylglycerol
Tat	Twin-Arginine Translocation
TCA	Tricarboxylic Acid
TMDP	2–chloro–4,4,5,5–tetramethyl–1,3,2–dioxaphospholane
TSB	Trypticase Soy Broth
U.S.	United States
USDA	U.S. Department of Agriculture
VA	Veratryl Alcohol
WS/DGAT	Wax Ester Synthase/Acyl-CoA:Diacylglycerol Acyltransferase
PTT	Phosphopantotheinyl Transferase

TABLE OF CONTENTS

LIST OF FIGURES

Page

LIST OF TABLES

Page

1. INTRODUCTION AND LITERATURE REVIEW*

1.1. Lignin utilization as a major challenge for sustainable biorefinery

Bioethanol represents one of the most mature forms of biofuel to displace fossil fuels and mitigate global climate changes. Current U.S. bioethanol production (~15 billion gallons annually), derived primarily from corn, contributes ~10% to the gasoline transportation fuel supply. However, the U.S. Energy Independence and Security Act (EISA) bill contains provisions that increase the Renewable Fuel Standard (RFS) to 36 billion gallons by 2022, among which 22 billion gallons must be advanced biofuel derived from nonfood-based biomass, the majority of which will be lignocellulosic biofuels. The USDA/DOE Updated Billion Ton report reviewed these demands and concluded that these goals can be addressed using lignocellulosic biomass including: perennial crops, wheat straw, corn stover, other agricultural crop residues, forest residues, tree farms (i.e., hybrid poplar), secondary forest industry waste materials, and other energy crops.[1-3]

Despite the recent advances in processing carbohydrate in lignocellulosics, the utilization of lignin for fungible fuels or chemicals has yet to be achieved. As a main constituent of lignocellulosic biomass (15-30% by weight, up to 40% by energy), lignin

---

* Part of this chapter is reprinted with permission from: "Exploration of Natural Biomass Utilization Systems (NBUS) for advanced biofuel—from systems biology to synthetic design". Shangxian Xie, Ryan Syrenne, Su Sun and Joshua S. Yuan. Current Opinion in Biotechnology. 27:195-203. Copyright © 2013 Elsevier. "Lignin Conversion: Opportunities and Challenges for Integrated Biorefinery". Shangxian Xie, Arthur J. Ragauskas, and Joshua S. Yuan. Industrial Biotechnology. 12(3): 161-167. Copyright @ 2016 Mary Ann Liebert, Inc. publishers.

is the second most abundant biopolymer on Earth.[1, 4] Nevertheless, lignin has received little attention relative to cellulose in terms of R&D efforts in biofuel production. In 2004, the pulp and paper industry alone produced 50 million tons of extracted lignin, yet only approximately 2% of the lignin available from the pulp and paper industry is used commercially, with the remainder burned as a low value fuel.[5] Nearly 300 million tons of lignin may be available if the Billion Ton initiative is implemented, and the lignin-containing biorefinery residues represent a significant resource for the sustainable production of fuels and chemicals.

From a holistic point of view, the use of lignin-containing biorefinery waste stream will add in new bioproducts to enable the biofuel process to be integrated, sustainable, and cost-effective. Taken corn ethanol as an example, biorefinery for first generation biofuel actually produces multiple product streams, including DGG as the animal feed. In the same way, lignocellulosic biorefineries need to develop bioproduct streams other than ethanol for both sustainability and cost-effectiveness. Lignin utilization therefore is a major factor to enable integrated biorefinery to reduce cost, minimize carbon emissions, and maximize sustainability of lignocellulosic biofuels. Lignocellulosic biomass is naturally recalcitrant to deconstruction by microorganisms and enzymes.[6, 7] To facilitate the enzymatic saccharification of cellulose, biomass typically requires pretreatment at elevated temperatures (i.e., ~150–220 ^{o}C) and acidic, alkaline or neutral processing conditions.[6] Regardless of the exact bioprocessing technology employed, almost all biological processing platforms for the conversion of plant polysaccharides to bioethanol (or biobutanol) result in the formation of a

significant lignin process stream.[8] This lignin fraction can be frequently utilized as an energy resource for power/electrical generation, partially because there are few efficient chemical conversion processes available that can convert lignin into transportation biofuels or higher value chemical substrates. Although a certain amount of lignin (~30–40%) is needed for the thermal requirements of bioethanol production including pretreatment and alcohol distillation,[9] a modern biological cellulosic processing plant will have ~60% excess lignin. The utilization of this excess lignin as feedstock for renewable fuels offers a significant opportunity to enhance the overall operational efficiency and impact of a lignocellulosic biorefinery.

Technologies being pursued to convert lignin to fungible fuels include catalytic pyrolysis, hydrotreatment, alkaline fragmentation/alkylation and gasification. Several studies have dealt with chemical treatments to fragment lignin into smaller fragments (i.e., C6 to C22) that could be used as an additive to gasoline and/or diesel. Recent patents by Shabtai et al. describe a two-step method to yield a reformulated, partially oxygenated gasoline product, which includes a mixture of C6-C10 substituted phenyl/methyl ethers, cycloalkyl methyl ethers branched paraffins, and alkylated and polyalkylated cycloalkanes.[10] Further technical requirements/challenges are still needed for this approach to achieve cost-effectiveness. Catalytic hydrotreatment of lignin has also been examined as a means of acquiring a low DP lignin for biofuels application. Oasmaa et al. have reported that thermal treatment of softwood and hardwood lignin at 400 ºC for 40 min in the presence of a metal catalyst and hydrogen resulted in 49~71% yield of a bio-oil.[11] Pyrolysis is an alternative methodology that can convert lignin into a

bio-oil. As produced, the bio-oils are very complex mixtures and are generally chemically unstable, corrosive, and have a high O:C ratio which makes their direct use for fuels problematic. Even though thermochemical or chemical processes provide a potentially viable approach to a lignin-to-fuel platform, these methods are often hindered by the low quality fuel product needing up-grading, corrosive intermediates or end products, and significant cost for waste management. For example, the pyrolysis of lignin generates hundreds of different compounds, most of which are oxygenated.[12] This requires a costly hydro-deoxygenation step that is still being researched.[12] Further technical requirements/challenges are still needed for this approach to achieve cost-effectiveness. Several reviews have covered the thermochemical conversion of lignin from different aspect.[13, 14] Biotechnology represents an alternative with significant potentials.

1.2. Lignin bioconversion into various product streams by microorganisms

In nature, lignin is a complex aromatic heteropolymer composed of phenylpropane units cross-linked via a variety of chemically stable bonds, which makes it particularly difficult for microbial degradation.[15, 16] Nevertheless, natural biomass utilization systems (NBUS) evolved mechanisms for lignin degradation, often with at least two sequential steps: lignin depolymerization into aromatic compounds and subsequent degradation of aromatic compounds[16]. Extensive work has gone into understanding the mechanisms of lignin depolymerization in model systems such as white rot fungi and termites.[16-21]

1.2.1. Termite gut system

Termite gut has been referred to be the smallest bioreactor in the world and it has been reported that the lignocellulolytic biomass material is nearly 99% degraded in 24 hours in the termite gut.[22] It could carry out the whole process of lignocellulose degradation from the 'pretreatment' to 'conversion for energy' under a continuous and integrated processing. The chewed biomass was first processed in foregut and midgut, which carry out lignin degradation as implied by ours and other researchers' data.[23] The processed biomass is further passed into the hindgut for saccharification and fermentation.[24, 25] Recent studies established that forgut and midgut as the main locations for lignin depolymerization with the detailed mechanisms still debatable. On one side, multiple enzymes for lignin depolymerization have been characterized.[18, 26] Among these lignases, the laccase identified from termite gut has been applied in industrial process. On the other side, Fenton reaction was recently proposed to play an essential role in the lignin depolymerization. Overall, previous studies suggested that both enzymatic and other chemical processes are important for lignin depolymerization.

1.2.2. White and brown rot fungus

Among the studied NBUSs, wood-rot fungi are the most well-studied lignin-degradation microbes with the capacity to completely degrade lignin.[17, 27-30] Even though most white rot fungi can secrete cellulase and hemicellulase for carbohydrate utilization, the mechanisms for lignin degradation remains debatable; in particular, for the relative importance of three types of de-polymerization reactions. First, traditional studies revealed that white rot fungi can secrete four classes of ligninolytic enzymes including

heme peroxidases, manganese peroxidases, versatile peroxidases, and laccases.[31] Despite the importance of these enzymes, their large size impedes the penetration into the plant cell wall structure. Therefore, an additional class of enzymes, known as accessory enzymes is believed to play a critical role in lignin degradation. These enzymes include quinone reductases (QR), ary-alcohol dehydrogenases (AAD), cellobiose dehydrogenase (CDH), and H_2O_2 production enzymes for peroxidases, such as aryl-alcohol oxidase (AAO) and glyoxal oxidase (GLOX).[17, 32] These accessory enzymes work with the aforementioned major lignin degrading enzymes to create reactive radicals network for efficient lignin degradation. Metabolic profiling revealed that low-molecular-weight compounds such as oxlic acid, veratryl alcohol (VA), and ABTS (2,2'-azino-bis(3-ethlbenzthiazoline-6-sulfonic acid)) can serve as electron donors and facilitate the formation of radicals toward lignin depolymerization.[33] Besides enzymatic reactions, the non-enzymatic Fenton reaction was the third type of mechanism believed to play an important role in degradation of lignin by white rot fungi, as revealed by recent comparative studies.[34-37] The role of Fenton reactions in white rot fungi have correlated with recent studies in termite, where similar reactions also appear to play a role in lignin de-polymerization. The relative importance of each type of reaction, as it relates to actual lignin and biomass degradation, may also depend on the particular species and environment. Compared to white rot fungi, brown rot fungi (BRF) have higher enzymatic selectivity toward cellulose and hemicellulose and can depolymerize these compounds rapidly.[37, 38] The extensive species diversity of white and brown rot fungi

provided an ideal model for comparative 'omics' analysis to reveal the diverse mechanisms for biomass degradation.

Comparative genomics and transcriptomics analysis of white and brown rot fungi with different lignin degradation capacities has shed light into the mechanisms for lignin depolymerization and utilization in these NBUS. The genomic analysis of *Phanerochaete chrysosporium* revealed an impressive array of genes encoding secreted oxidases, peroxidases and hydrolytic enzymes that cooperate in wood decay.[28] Comparative analyses of 31 fungal genomes revealed a consistent result that fungal class II peroxidases plays a central role in lignin degradation and also suggested that lignin-degrading peroxidases expanded in the lineage leading to the ancestor of the white rot fungus.[17] The transcriptomic analysis of white rot fungus *Phanerochaete carnosa* growing on different feedstocks discovered the coordinative function of abundant lignocellulose degradation enzymes including manganese peroxidases, lignin peroxidases, cellulases, hemicellulases, glyoxal oxidase, P450 monooxygenases and glycosyl hydrolase family 61 proteins.[39] The studies shed light into the potential mechanisms for biomass degradation and utilization in white rot fungus.

1.2.3. Bacteria systems

Despite the strong lignocellulosic biomass utilization capacity of fungal species, there is not yet a robust commercial fungus-based biorefinery process for lignocellulosic biofuel, partially due to the challenges in genetic manipulation systems available for oleaginous and white rot fungi.[19] Bacteria and yeast have been the mainstream strains for fermentation process in lignocellulosic biofuel. In particular, *Zymomonas mobilis* and

Escherichia coli are classic bacterial strains for engineering sugar fermentation.[40] Despite the strength of yeast as a gold-standard for sugar fermentation, few yeast strains have a biomass degradation capacity. In contrast, many bacterial species have been widely studied for lignocellulosic biomass degradation and utilization capacity.

For the past three decades, significant progress has shed light into our understanding of the molecular mechanisms for cellulose and hemicellulose degradation within bacterial systems. Numerous researches have implicated the mechanisms of cellulose/hemicellulose degradation between aerobic and anaerobic bacteria differs significantly. Besides cellulose and hemicellulose degradation, lignin degradation capacity of bacterial strains has recently been explored for bioconversion of lignin into fungible fuels or chemicals. Extensive research has established that aromatic compounds can sustain the growth of multiple bacteria species from genus such as *Streptomyces, Rhodococcus, Nocardia, Sphingobium, Pseudomonas, Bacillus, Achromobacter*, *Cupriavidus, Phanerochaete* and others.[41-43] Even though it is generally believed that lignin depolymerization capacity in bacteria is weaker than that for white rot fungus, studies have shown that bacteria can also secret extracellular lignolytic enzymes for lignin depolymerization. Among these enzymes, laccase was thought to be the most widespread amongst bacterial species, according to the latest bacterial genome sequencing information.[44] For example, some of the *Streptomyces* strains can express both extracellular laccase and lignin peroxidase.[45, 46] A newly isolated strain *Cupriavidus basilensis* B-8 was reported to secret laccase as high as 815.6 U/L.[42] Besides the classic

ligninase, some of the lignin-degrading bacteria can also produce other type of enzymes with lignin degradation capacity including DyP-type peroxidase.[47]

Besides lignin depolymerization capacity, many bacteria evolved diverse and strong capacity to utilize aromatic compounds. For example, more than eight aromatic pathways was identified in *Rhodococcus sp.*, and these peripheral aromatic compound degradation pathways all funnel intermediate products toward acetyl-CoA.[48] Among these pathways, the β-ketoadipate pathway was considered a "major utility pathway" in the processing and degradation of lignin-derived aromatic compounds.[49] The β-ketoadipate pathway is biochemically and evolutionarily conserved distributed widely among different bacterial species.[50] One of the most important advantages of exploiting bacteria for biomass degradation is the available genetic manipulation tools to enable the engineering of specific high-value target compounds by integrating these various pathways.

Using some of these bacteria, recent advances have been made to support the overall concept of bioconversion of lignin into fungible fuels and products. Several studies have established that oleaginous bacteria *R. opacus* can utilize lignin as sole carbon source and can directly convert processed lignin into lipid.[51, 52] Highly recalcitrant and relatively pure substrates like kraft lignin and ethanol organosolv lignin (EOL) were used as substrates in these studies, indicating the capacity of lignin depolymerization thus exists in bacteria and can be further enhanced. At the meanwhile, other studies further demonstrated that *Pseudomonas putida* KT2440 could accumulate significant amount of polyhydroxyalkanoates (PHA), when it was grown on alkali

pretreated lignin-enriched biorefinery streams.[53] Moreover, recent studies showed the metabolic engineered *P. putida* KT2440 could accumulate significant amount of muconate from lignin-derived aromatics.[54] Overall, the studies manifested the feasibility to use various microorganisms to convert biorefinery waste into different types of bioproducts. The studies unveiled enormous opportunities for microbial conversion to enable integrated biorefinery.

1.3. Major steps of lignin bioconversion and challenges

Despite the progresses, the final bioproduct titer for most of the previous studies remained too low to be commercially relevant. Fundamental understanding of lignin bioconversion process is crucial to optimize each step of lignin conversion to improve efficiency. As aforementioned, lignin is a complex aromatic heteropolymer composed of phenylpropane units, which are cross-linked via a variety of chemically stable bonds. To be used as carbon source for microbes, lignin needs to be firstly depolymerized into small molecular aromatic compounds. The lignin-derived aromatic compounds can be catabolized by the microbes to channel the carbon to central metabolites like acetyl-CoA. In the third step, the central metabolites or key intermediates will be used to produce a certain bioproducts like lipid, PHA and others. Therefore, an efficient lignin conversion process basically needs coordinate and enhance all three steps in microorganisms for lignin depolymerization, aromatic compound catabolism, and valuable compounds biosynthesis (Figure 1-1).

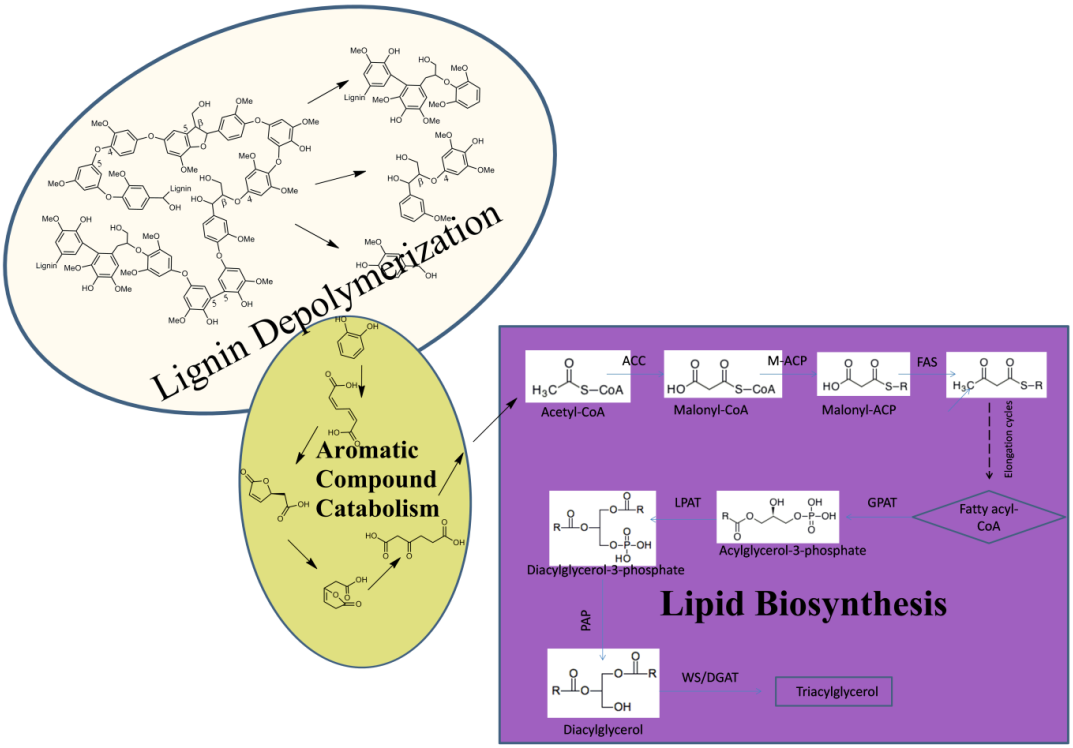

Figure 1-1. The three major steps for conversion of lignin into high value products. The bioconversion of lignin by microbes normally is carried out in three major steps including lignin depolymerization, aromatic compound catabolism and target product biosynthesis. In this figure, lignin-to-lipid bioconversion is chosen as a model to graphically explain the major steps for lignin bioconversion.

First, the relatively weak lignin depolymerization capacity of bacteria needs to be augmented to improve their growth rate and yield on processed lignin. Second, biosynthetic pathways need to be engineered so that valuable bioproducts accumulate to higher levels under a wider range of fermentation conditions. Third, the three steps of lignin depolymerization, aromatic compound degradation, and bioproduct production need to be balanced to enable rapid growth to a high cell density with reasonable bioproduct accumulation. The progresses and challenges in optimization of each of these three steps were discussed.

1.3.1. Lignin depolymerization

Lignin depolymerization is the first step in converting lignin to valuable products and is also probably the most challenging step.[55, 56] Lignin depolymerization is drastically different from depolymerization or saccharification of cellulose and hemicellulose. On one side, cellulose and hemicellulose saccharification often involves hydrolysis reactions with glycosyl hydrolases (GH), whereas lignin depolymerization heavily relies on the redox reaction involving electron transfer and redox potential. On the other side, cellulose contains glucose monomers linked by β-1,4-glucosidic bond, whereas lignin monomers were connected with more than ten types of very different chemical linkages. Even though some bacteria could use the lignin-derived aromatic compounds, lignin depolymerization capacity of most of these bacteria are relative weak as compared to white rot fungus or termites.

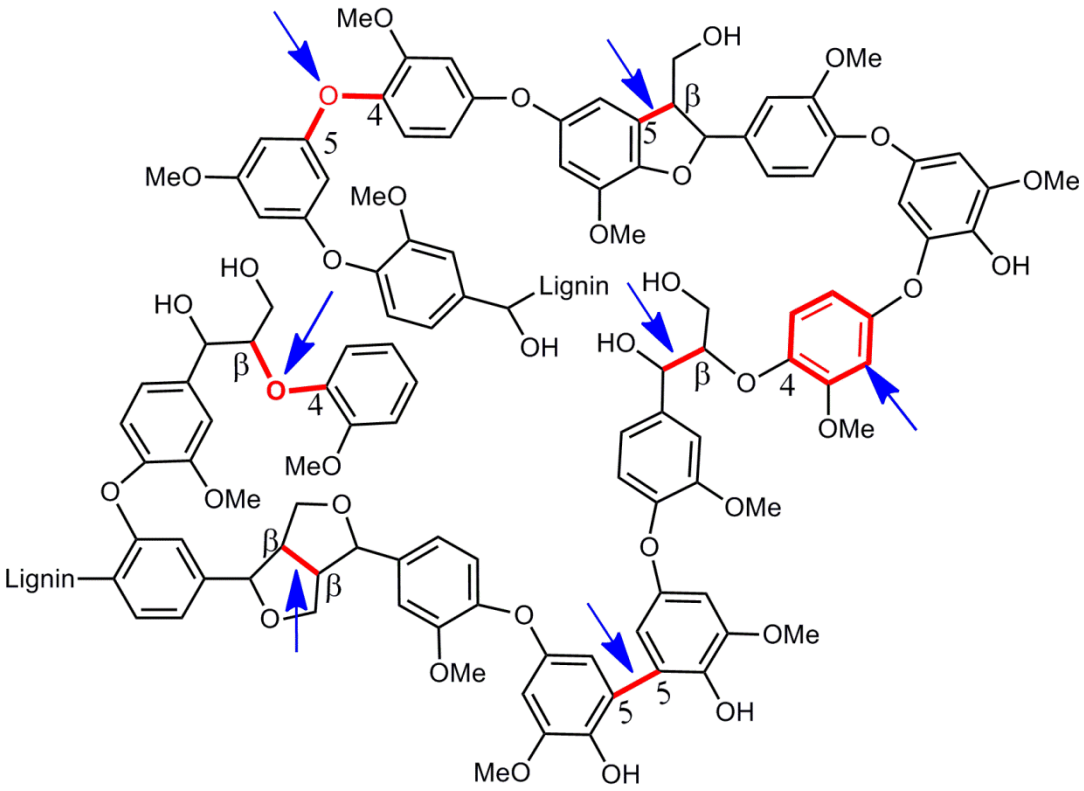

Figure 1-2. The proposed lignin depolymerization mechanisms by laccase. The proposed lignin depolymerization mechanisms by laccase. The figure presented an example of the possible structure for native lignin. The major inter-unit linkages in native lignin included the β-O-4, 5-5, β-β, 4-O-5 and β-5 bonds. The red bold linkages and blue arrows indicated the putative chemical bonds that could be cleaved by laccase based on previous studies.[52, 57, 58]

In order to achieve higher product titer and efficient lignin utilization, it is critical to have an efficient lignin depolymerization process to degrade lignin heteropolymers into aromatic compounds that can be used by microorganisms. Lignin depolymerization can be achieved with both biological and chemical approaches. Biological or biochemical lignin depolymerization often involves lignin degradation enzymes or Fenton reaction to catalyze the oxidation of lignin for breaking a broad range of chemical linkages within lignin. Among the major lignin depolymerization enzymes, laccase was recently chosen to study the synergy between enzymatic and bacterial degradation of lignin due to the self-sustainable generation of radicals for redox reactions and the capacity to cleavage broad chemical bonds in lignin (Figure 1-2).[52, 57] Previous study has established that the laccase and *R. opacus* cells synergized to degrade the lignin with complementary chemical functions.[52] Basically, ^{31}P NMR analysis suggested that laccase and *R. opacus* PD630 selectively degrade different chemical linkages to synergize the lignin depolymerization. Based on the mechanistic study, a new SDF (Simultaneous Depolymerization and Fermentation) process is developed to significantly increase cell growth and lipid yield for lignin fermentation by *R. opacus*. Besides laccase, Fenton reaction and other enzymes like lignin peroxidase and magnesium peroxidase could also be explored for lignin degradation in the future. However, it has been indicated that the synergy between Fenton reaction and bacterial cells is not as effective as laccase, probably due to the lack of continuous supply of H_2O_2 in the system. In fact, for both peroxidase and Fenton reaction, the key limitation is the requirement for a sustainable redox environment. In other words, both peroxidase and

Fenton reaction relies on the continuous supply of H_2O_2 and/or other radicals to sustain the reaction for lignin depolymerization. Such a requirement could be fulfilled by cells with capacities to produce H_2O_2 and other radicals or co-factors. Besides supplying the external enzymes, engineering microorganisms to produce lignin degradation enzymes for lignin depolymerization is another major direction for the future. It is worth mentioning that most of the biological lignin depolymerization processes are achieved under aerobic condition through redox reaction. Therefore, oxygen supplement will be another important consideration for efficient biological lignin degradation.

Besides biological and biochemical lignin depolymerization, chemical fractionation of lignin is another major approach explored for lignin bioconversion. Chemical fractionation of lignin has been thoroughly reviewed in several recent publications, even though the combination of chemical fractionation and bioconversion was barely discussed.[59, 60] In fact, most of these chemical fractionation methods cannot be readily applied to generate aromatics for bioconversion, because of the often toxic products to inhibit the microbial growth. Nevertheless, several chemical approaches have been effective in producing fractionated biorefinery waste or kraft lignin for improved bioconversion. Linger *et al.* have developed a NaOH-anthraquinone-based method to pretreat biorefinery waste under high pressure (30–40 psi). The method can be effectively integrated with *P. putida* KT2440 bioconversion of biorefinery waste for PHA and cis,cis-muconate production.[54, 61] In addition, Wei *et al.* showed that O_2 pretreatment could reduce the recalcitrance of alkali lignin and make it more processible for *R. opacus* DSM1069 bioconversion of kraft lignin for lipid.[62]

Despite the advances in lignin depolymerization, an efficient bioconversion process with higher titer relies on more effective lignin depolymerization or fractionation. On one hand, the biological or chemical approaches compatible with microbial fermentation needs to be developed and optimized. Multiple enzyme and treatment approaches need to be integrated. Eventually, the engineering of microorganisms to secrete lignin degradation enzymes could be particularly enabling for a consolidated lignin processing. On the other hand, the processibility of lignin needs to be taken into consideration for both lignin depolymerization and subsequent conversion. Our preliminary studies indicated that the lignin depolymerization efficiency by either enzymatic or chemical treatment could be significantly impacted by the type of lignin used. Chapple *et al.* also demonstrated that the lignin monomer composition affected the lignocellulose degradability.[63, 64] Consequently, the composition of residue lignin from biorefinery waste could be modified by either altering the biomass pretreatment process or redirecting the lignin biosynthesis pathway in plant feedstock to form certain type of lignin. It will be intriguing to study how different feedstock lignin modification strategies could increase the processibility and compatibility of lignin for microbial bioconversion.

1.3.2. Aromatic compound catabolism

The second step for lignin bioconversion is the catabolism of aromatic compounds derived from lignin by microorganisms, where bacterial species have further advantages for manipulation and enhancement. The recent available sequences on various microbes helped to advance our understanding of the molecular mechanisms for

microbial aromatic compounds catabolism. The best studied among the Gram-positive bacteria are *Rhodococcus* and among the Gram-negative bacteria, *Pseudomonas*. A large number of aromatic compound catabolic pathways have been characterized in bacteria including those responsible for growth on benzene, benzoate, (tere) phthalates, biphenyl, styrene, phenylacetate and vanillin.[65-70] Generally speaking, the bacterial aromatic catabolism is arranged with two types of pathways: a large number of "peripheral aromatic" pathways funneling a range of natural and xenobiotic compounds into a restricted number of "central aromatic" pathways.[71] For example, the peripheral Van pathway transforms vanillin and vanillate to protocatechuate, which in turn is transformed to central metabolites via β-ketoadipate pathway to integrate with TCA (tricarboxylic acid) cycle and produce acetyl-CoA.[65] Sainsbury *et al.* have demonstrated that an engineered strain of *R. sp.* RHA1 lacking vanillin dehydrogenase accumulates vanillin, when incubated with Kraft lignin or lignocellulose.[72] Mohn and Eltis have also identified the transporters for aromatic compound conversion, and suggested that the capacity of the transporters in bacterial cell membrane for aromatic compound transportation is another key limiting factor for efficient aromatic compounds catabolism.[73]

As noted above, lignin is a complex aromatic heteropolymer and a diverse range of aromatic compounds are often released after lignin depolymerization. It is therefore critical for the microbes to process the diverse range of aromatic compounds for lignin conversion. Meanwhile, many lignin-derived compounds are strong inhibitors for microbial growth, especially when they reach a certain concentration in the medium.

These compounds included phenol, vanillin, 4-hydroxybenzoic acid, and coumaric acid.[74, 75] One of the approaches to address this challenge is to screen and select the suitable strains for degrading a broad range of aromatic compounds. For example, Shi et al. screened and identified a beta-proteobacterium *C. basilensis* B-8 which has high capacity in lignin-derived aromatic compounds catabolism.[42] Extensive microbial strain screening and characterization works need to be carried out to identify the suitable strains with broad range of aromatic compound degradation capacity and high tolerance to the inhibitors.

In addition, understanding of molecular and genomic mechanisms for aromatic compound degradation and the tolerance of lignin-derived inhibitors is important for designing efficient conversion of aromatic compounds. The entire microbial aromatic compounds catabolism pathways should be balanced from "peripheral aromatic" pathways to "central aromatic" pathways target different lignin derived aromatic compounds. Further progresses should be made in characterizing pathways and expressing heterologous enzymes in target microbes to enable their improving aromatic compound catabolism capacity. For example, expression of the genes from SYK-6 (*ligA*, *ligB*, *ligC*) conferred the ability to convert protocatechuate into a novel polymer-based material in *P. putida*.[76] The tolerance of the strain to the lignin-derived inhibitors could also be improved by molecular adaptation and metabolic engineering. Yoneda *et al.* found that the adaptively evolved *R. opacus* to phenol tolerance showed significantly upregulated phenol degradation pathways and putative transporters.[77] Consequently, the inhibitor tolerance could be enhanced by reverse genetic engineering to overexpress the

inhibitor transporter and the genes in degradation pathways. These examples highlight the potential for using systems and synthetic biology to modify the microbial aromatic compounds utilization toward efficient lignin bioconversion in bacteria. Overall, both strain screening and metabolic engineering will be important in obtaining suitable bioconversion strain with broader range of aromatic compound degradation capacity toward lignin bioconversion.

1.3.3. The biosynthesis of valuable compounds

The final metabolic step for lignin bioconversion is to channel the carbon flux toward certain target products. A diverse range of target bioproducts can be sought for lignin bioconversion. Traditional bioproducts are carbon storage compounds like PHA and lipid, which are derived from central metabolism intermediates like acetyl-CoA. However, considering the aromatic monomers of lignin, other products can be derived from the intermediates of aromatic compound degradation.

From a metabolic flux perspective, multiple steps of lignin degradation pathways can be engineered to produce valuable products (Figure 1-3). For example, the deletion of vanillin dehydrogenase in *R. sp.* RHA1 resulted in the accumulation of vanillin, an aromatic compound broadly used in food additives.[72] Recently, Vardon *et al.* demonstrated that *P. putida* KT2440 could be engineered to accumulate significant amount of cis,cis-muconate, an intermediate of catechol metabolism in β -ketoadipate pathway, by blocking its funneling into next intermediate muconolactone.[54] The engineered *P. putida* KT2440 could accumulate 0.7 g/L muconate grown on lignin-enriched biorefinery stream.

The ‘peripheral’ and ‘central’ aromatic compound degradation pathway will eventually funnel the carbon from aromatic compounds into central metabolites like acetyl-CoA and pyruvate.[78] These central metabolites from primary metabolism can be widely used for synthesis of various target metabolites including lipid, PHA, terpene, and others. Kosa *et al.* showed that *R. opacus* DSM 1069 and PD630 strains, under nitrogen limiting conditions, convert lignin-derived compounds, such as 4-hydroxybenzoic (4-HBA) and vanillic acid into triacylglycerols (TAGs).[56] They further demonstrated the EOL can be converted into TAG as biofuel precursor too. In the same way, processed biorefinery waste has been converted to PHA for bioplastics as shown by Linger *et al.*[53] Despite the progress, the titers for the current lignin conversion systems are all very low as compared to the carbohydrate-based system, making it difficult for commercial applications. Even though many bacteria have naturally evolved pathway to accumulate bioproducts for carbon storage, it is critical to have systems level understanding of how these pathways are regulated under lignin substrate. The systems biology-guided biodesign can be an effective approach to increase the titer to achieve economic biorefinery streams.

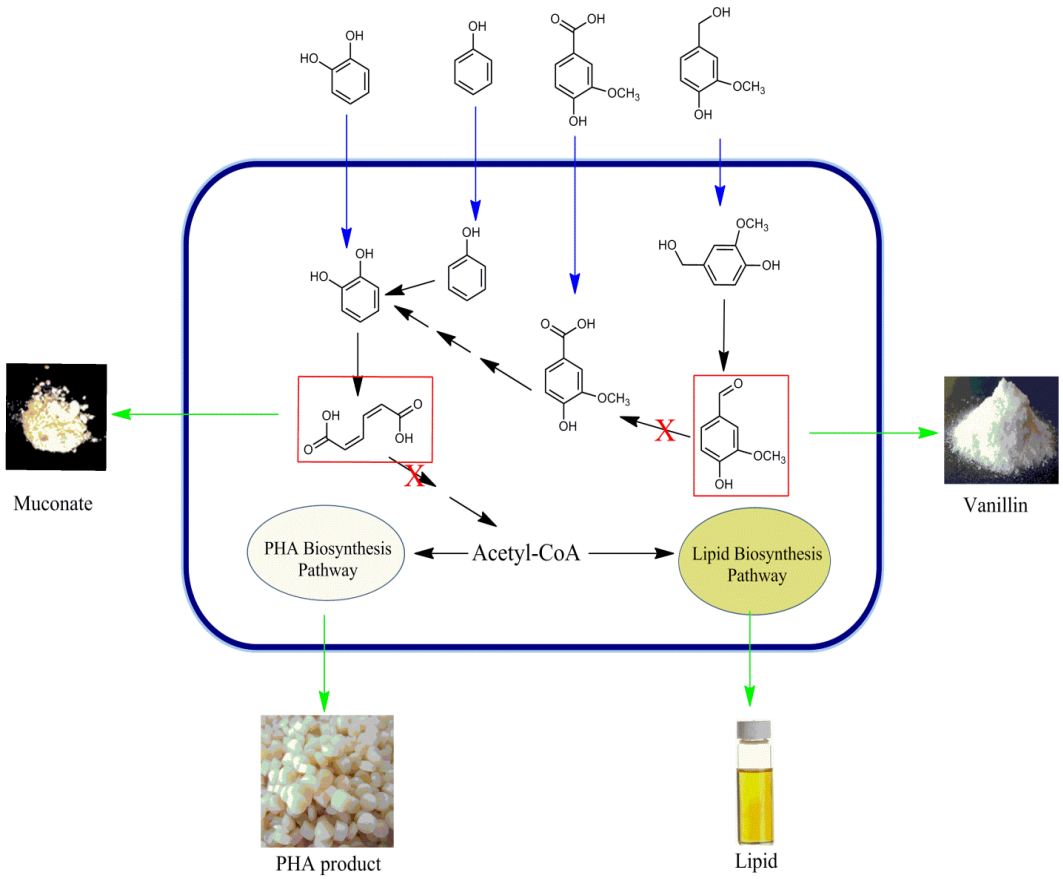

Figure 1-3. The metabolic pathways in microbes for producing valuable chemicals from lignin-derived aromatic compounds. In this figure, only several aromatic compounds were displayed and catechol branch of β-ketoadipate pathway was selected as an example to illustrate the metabolic pathway for the production of high value chemicals.

2. SYNERGISTIC ENZYMATIC AND MICROBIAL LIGNIN CONVERSION*

2.1. Introduction

As a main constituent of lignocellulosic biomass, lignin is the second most abundant biopolymer in the terrestrial plants.[1, 4, 7, 79] Despite the abundance, the utilization of lignin has been particularly challenging due to its recalcitrance nature.[79] In nature, lignin is a complex aromatic heteropolymer composed of phenylpropane units cross-linked via a variety of chemically stable bonds to confer recalcitrance of plant cell wall.[15, 16] The utilization of the lignin in the biorefinery waste streams as feedstock for biofuels and bioproducts represents a unique opportunity to improve cost-effectiveness, carbon and energy efficiency of biorefineries.[16, 79] Bioconversion recently emerged as a potentially effective strategy for lignin processing.[21, 51, 62] Despite the lignin recalcitrance, many nature biomass utilization systems including white rot fungi and termites evolved capacity to degrade and utilize lignin.[16, 21, 80, 81] Among the different systems, *R. opacus* bacteria have recently been established with the capacity to convert lignin into lipid,[51, 56, 62, 82] yet the industrial application of the platform is hindered by the low yield of target compounds. The challenge can be addressed by integrating the enzymatic and chemical depolymerization with bacterial conversion to achieve a SDF process. It is thus critical to understand if and how the enzymatic depolymerization can be synergized with bacterial conversion. Moreover, it is also important to achieve in-depth understanding of the scientific principles, chemical, and biological mechanisms

---

*Reprinted with permission from: "Synergistic enzymatic and microbial lignin conversion" Cheng Zhao, Shangxian Xie (Co-first author and Corresponding author), Yunqiao Pu, *et al*. Green Chemistry. 18(5): 1306-1312. Copyright @ 2016 Royal Society of Chemistry.

involved in lignin degradation in an enzyme-cell combined system. In this article, the aim is to address these scientific questions by investigating the potential synergistic enzymatic and microbial conversion of lignin.

Lignin depolymerization is the key step to enable the bioconversion of the phenolic heteropolymer, in a way similar to saccharification in cellulose conversion.[7, 16] However, unlike cellulose with the β-1,4-glucosidic link as the chemical bond and glucose as the monomer, lignin contains diverse aromatic monomers and various types of chemical bonds or interunit linkage such as β-O-4, α-O-4/β-5 (phenylcoumaran), β-β (resinol), dibenzodioxocin, 4-O-5, and 5-5.[83] The requirement of redox reaction to cleave these bonds further complicated the deploymerization process. Previous studies have well characterized three lignin depolymerization system including laccase-based, peroxidase-based and Fenton reaction-based systems.[16, 17, 21] Model lignin degradation organisms like white rot fungi have all three lignin depolymerization systems, yet bacteria like *Rhodococci* generally have one or two of these systems, with a lower efficiency as compared to the white rot fungi and termites. In this research, the mechanisms in natural biomass utilization systems will be reverse designed by combining the laccase and Fenton reaction system to evaluate how the combination of enzyme, chemical, and cell treatment will synergize the lignin depolymerization and promote lignin utilization by bacteria.

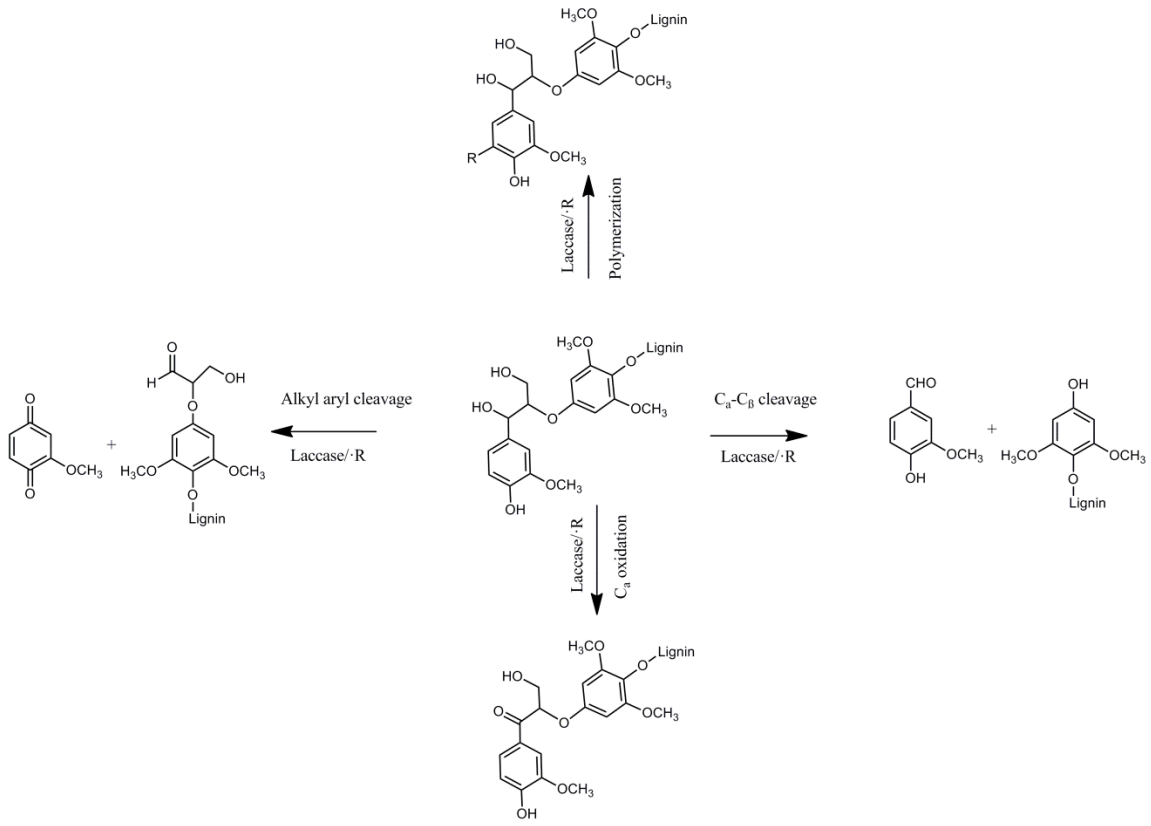

Figure 2-1. The role of electron mediators in facilitating laccase-based oxidation of lignin. Laccase could both polymerize and depolymerize lignin via redox reactions. The initial oxidative attack to lignin by laccase was targeted at the phenolic structures, which generated the phenoxyl radicals (•R). The released phenolic fragments could serve as a reaction mediator for further lignin oxidization. On one side, the phenoxyl radicals could degrade the non-phenolic lignin structure through C_{α}-C_{β} cleavage, C_{α} oxidation, alkyl aryl cleavage and even aromatic ring cleavage. On the other hand, the radicals could also lead to the oxidation reaction to polymerize aromatic compound monomers.

Laccase is chosen for the enzyme-cell system due to its capacity to self-generate radicals, which distinguished laccase-based lignin depolymerization from Fenton reaction and peroxidase (Figure 2-1). For both Fenton reaction and peroxidase, the reactions will depend on the radicals that are often generated and recycled by other enzymatic systems. Laccase provided a potentially self-sufficient system for lignin degradation. However, the unique mechanism imposed a fundamental scientific question: how would laccase and cell synergize during the lignin utilization? In other words, considering that both polymerization and depolymerization activities exist for laccase, can the cells consume aromatic compounds generated from the lignin oxidation to promote the reaction toward depolymerization? In this article, these questions were addressed by demonstrating the enzyme-cell synergy on lignin degradation at both biological and chemical levels.

2.2. Material and methods

2.2.1. Lignin and bacteria strain

Kraft lignin (catalog#370959) and laccase from *Trametes versicolor* (catalog# 51639) was purchased from Sigma-Aldrich (St. Louis, MO, USA). *R. opacus* PD630 (DSM-44193) was purchased from the Leibniz Institute DSMZ-German Collection of Microorganisms and Cell Cultures (Braunschweig Germany). The strain was recovered in 5 mL Trypticase Soy Broth (TSB) at 28 °C for 2 days. The culture medium was then mixed with 1 mL glycerol, dispensed to 1.5 mL tubes, and chilled in liquid nitrogen for storage. The strain was stored in -80 °C.

2.2.2. Medium preparation

Two types of media were used for the fermentation. The *Rhodococcus* Minimal (RM) medium was prepared as follows. 1.4 g $(NH_4)_2SO_4$ and 1.0 g $MgSO_4 \cdot 7H2O$ were added into 962 mL ddH_2O, and then sterilized by autoclave at 121°C for 20 min. The solution was then cooled down to room temperature, and then added 1mL 15 g/L sterile $CaCl_2 \cdot 2H_2O$, 1.0 mL sterile trace element solution, 1.0 mL sterile stock A solution, and 35.2 mL sterile 1.0 M phosphate buffer. The solution is then finalized to 1000 mL.

For lignin fermentation medium, 0.5 g kraft lignin, 0.14 g $(NH_4)_2SO_4$, 0.1 g $MgSO_4 \cdot 7H_2O$ were added into about 90 mL ddH_2O. The pH was adjusted to 12.5 to dissolve the lignin. After the lignin was completely dissolved, the solution was neutralized with HCl to pH 7.0 and adjusted to the total volume of 96.2 mL followed by autoclaved.. The solution was further cooled down to room temperature and added 0.1 mL 15g/L sterile $CaCl_2 \cdot 2H_2O$, 0.1 mL sterile trace element solution, 0.1 mL sterile stock A solution, and 3.52 mL sterile 1.0 M phosphate buffer. The solution was finalized at 100 mL.

The trace element solution was made of 0.5 g $FeSO4 \cdot 7\ H_2O$; 0.4 g $ZnSO4 \cdot 7\ H_2O$; 0.02 g $MnSO4 \cdot H_2O$; 0.015 g H_3BO_3; 0.01 g $NiCl_2 \cdot 6H_2O$; 0.25 g EDTA; 0.05 g $CoCl_2 \cdot 6H_2O$; 0.005 g $CuCl_2 \cdot 2H_2O$, and ddH_2O to make up to 1 L. The solution was then sterilized by filtration through a 0.22 μm filter.

The stock A solution was made by mixing 2.0 g $NaMoO_2 \cdot 2H_2O$, 5.0 g FeNa·EDTA, and ddH_2O to 1L, and further sterilized by filtration through a 0.22 μm filter. The 1 M phosphate buffer was made by adding 113 g K_2HPO_4, 47 g KH_2PO_4 and

ddH2O to make up to 1 L, and further sterilized by filtration. Both the stock A solution and the phosphate buffer were prepared freshly.

2.2.3. Lignin fermentation

The seed culture was prepared by inoculating a single colony of *R. opacus* PD630 into 20 mL TSB medium, and cultivated at 28 °C to OD_{600} 1.5. The cultured strain were harvested by centrifuging and washed twice with equal volume of RM medium without lignin. The washed cells were resuspended in 20 mL RM medium without lignin. 1 mL of resuspended cells was added to 100 mL of lignin fermentation medium. For laccase and Fenton reaction treatments, the enzyme and chemicals were added at the same time of strain inoculation. The fermentation was carried out in 250 mL flask capped with eight layers of cheesecloth and one layer of kraft paper at a shaking speed of 200 rpm to keep the fluent air circulation, which helps to maintain the oxygen in solution. The fermentation was carried out at 28 °C for 144 h.

2.2.4. Lignin concentration analysis by Prussian Blue assay

The pH for the sample was adjusted to 12.5 with 10 M NaOH to completely dissolve the lignin. In order to completely dissolve lignin, the lignin sample was mixed at speed of 180 rpm for 1 h. The total volume was adjusted to 100 mL by adding RM minimum medium. The samples were further diluted to an optimal concentration using ddH_2O to adjust the final absorbance at 700 nm to be within the range of 0.7-1.5. The lignin concentration was then measured with Prussian Blue reagents to read the absorbance at 700 nm with UV/vis spectrophotometer.[64, 84] Approximately 1.5mL of the diluted samples was transferred into 2 mL tubes. 100 μL of 8 mM $K_3Fe(CN)_6$ was added

into the tube and followed by the immediate addition of 100 μL 0.1 M $FeCl_3$. The samples were mixed thoroughly by shaking the tube for 5 minutes. The samples were transferred to 1 cm cuvette to obtain the absorbance at 700 nm by spectrophotometer, using the ddH_2O sample as blank control. Standard curve was established with the same reagents and known concentration of lignin. All experiments were carried out in triplicate.

2.2.5. Cell concentration determination

To determine the number of living cell, 100 μL of fermentation culture was serial diluted and plated on Tryptic Soy agar plate. The numbers of colonies were counted from the plates and converted to colony forming unit/mL (CFU/mL).

2.2.6. Total lipid extraction

Total lipid of the bacterial *R. Opacus* PD630 after lignin fermentation was extracted with chloroform-methanol using modified Folch lipid extraction method.[85] 100 mL fermentation culture was centrifuged at 2500 g for 5 min, and the supernatant was collected. The pellet was re-suspended with 100 mL 0.9% NaCl solution, and was centrifuged at 2500 g for 5 min. The supernatant was collected and combined with previous one. Repeat twice the resuspension and centrifugation step. The collected 300 mL supernatant was centrifuged at 10,000 g for 30 min to pellet cells. The pelleted cells were lyophilized for 24 h. 3 mL chloroform: methanol (2:1) solution was added to cells to homogenize the cells for 3 h, followed by 3000 rpm centrifugation to make pellets. The supernatant was transfer to the freshly weighted tubes. Subsequently, 0.6 mL distilled water was added. After phase separation, the upper phase was discarded. The

organic phase containing total lipid was rinsed with chloroform: methanol: water (3:48:47). The upper phase was removed and the organic phase was dried down under N_2 stream and the lipid was weighted.

2.2.7. Lignin characterization by gel permeation chromatography

The lignin gel permeation chromatography (GPC) analysis was performed after acetylation on a PSS-Polymer Standards Service (Warwick, RI, USA) GPC SECurity 1200 system, featuring Agilent HPLC 1200 components equipped with four Waters Styragel columns (HR1, HR2, HR4 and HR6) and an UV detector (270 nm).[62]

Specifically, lignin was acetylated in a mixture of acetic anhydride/ pyridine (1:1 v/v, 2.0 mL) for 24 h at room temperature. The reaction mixture was diluted with ethanol (30 mL) and stirred for 30 min and then concentrated under lower pressure. The addition and removal of ethanol was repeated to remove trace acetic acid and pyridine from the samples. The samples were then dissolved in chloroform and added dropwise into diethyl ether to precipitate the samples followed by centrifugation. After air drying, the acetylated samples were dried for 24 h in a vacuum oven at 40°C prior to GPC analysis. Tetrahydrofuran was used as the mobile phase in GPC analysis and the flow rate was 1.0 mL/min. The molecular weights of the derivatized lignin samples were acquired by using a calibration curve established with standard narrow polystyrene samples.

2.2.8. Lignin structure analysis by NMR

All the NMR experiments were carried out at a Bruker Avance III 400-MHz NMR spectrometer. Heteronuclear single quantum coherence (HSQC) and ^{31}P NMR

measurements of lignin samples were carried out following literature methods.[86, 87] HSQC spectra were acquired using deuterated dimethyl sulfoxide (500 μL) as solvent for lignin samples (~ 60 - 100 mg) at 45 ºC with the following acquisition conditions: 11-ppm spectra width in F2 (1H) dimension with 2048 data points (232.7-ms acquisition time), 220-ppm spectra width in F1 (13C) dimension with 256 data points (5.8-ms acquisition time); a 1.5-s pulse delay; a $^{1}J_{C\text{-}H}$ of 145 Hz; and 96 scans. The central solvent peak (δ_C 39.5 ppm; δ_H 2.5 ppm) was used for chemical shift calibration. For quantitative ^{31}P NMR analysis, lignin (ca. 20 mg) was dissolved in a solvent of pyridine/$CDCl_3$ (1.6/1.0 v/v, 500 μL) and derivatized with 2-chloro-4,4,5,5-tetramethyl-1,3,2-dioxaphospholane. The spectrum was acquired using an inverse-gated decoupling pulse sequence (Waltz-16), a 90° pulse, and a 25-s pulse delay. N-hydroxy-5-norbornene-2,3-dicarboximide was used as the internal standard. 128 scans were accumulated for each sample. NMR data were processed using the TopSpin 2.1 software (Bruker BioSpin) and MestreNova (Mestre Labs) software packages.

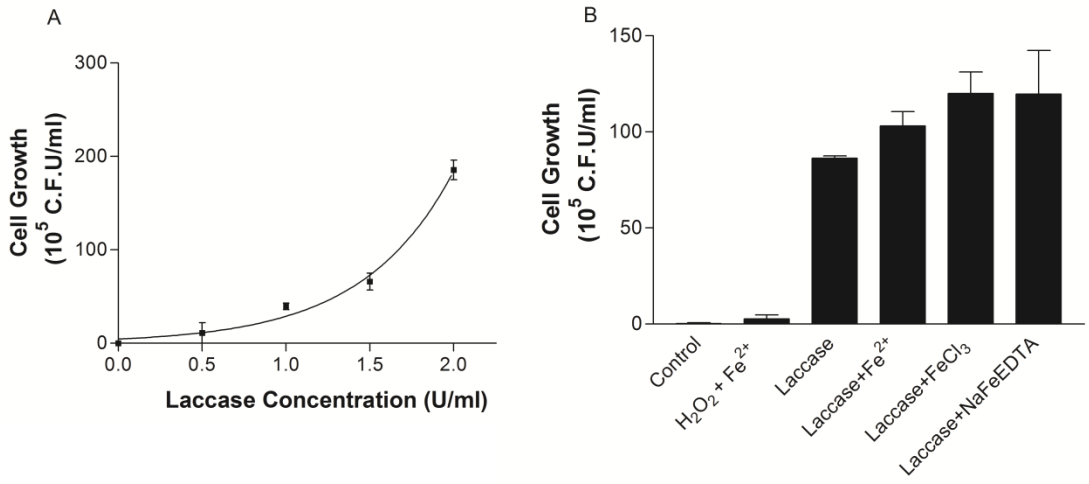

Figure 2-2. The increase of cell growth in response to laccase and other treatments. A. laccase promotes *R. opacus* PD630 cells growth using lignin as carbon source. *R. opacus* PD630 showed an exponential increase of cell growth associated with laccase concentration. B. Fenton reaction has limited synergistic effect with laccase treatment to promote *R. opacus* PD630 cells growth in lignin fermentation. Except the no laccase control, all treatments contain laccase at a concentration of 1.0 U/ml in fermentation medium. Control: only the *R. opacus* PD630 cells were added to fermentation medium; H_2O_2+Fe^{2+}: *R. opacus* PD630 cells supplied with 0.2 mM $FeSO_4$ and 0.067 mM H_2O_2; Laccase: *R. opacus* PD630 cells supplied with laccase; Laccase+Fe^{2+}: *R. opacus* PD630 cells supplied with laccase, 0.2 mM $FeSO_4$ and 0.067 mM H_2O_2; Laccase+$FeCl_3$: *R. opacus* PD630 cells supplied with laccase, 0.2 mM $FeCl_3$ and 0.067 mM H_2O_2; Laccase+ NaFeEDTA: *R. opacus* PD630 cells supplied with laccase, 0.2 mM NaFeEDTA and 0.067 mM H_2O_2.

2.3. Results and discussions

2.3.1. Laccase treatment significantly promote the cell growth on lignin

Laccase treatment significantly promoted the cell growth of *R. opacus* PD630 on lignin. As shown in Figure 2-2A, the laccase treatment significantly promoted the PD630 cell growth on kraft lignin as the sole carbon source. The CFU of *R. opacus* PD630 cells after six days of growth increases exponentially in response to the activity of laccase in the enzyme-cell system. The cell growth was very slow without laccase treatment due to the relatively low initial inoculation. However, with the increased concentration of laccase, the CFU after six days of cultivation can achieve an exponential increase to 1.85×10^7/mL at 2 U/mL of laccase treatment. Considering that kraft lignin is mostly insoluble, laccase treatment might lead to the depolymerization and solubilization of lignin to provide more carbon source for *R. opacus* PD630 cells, which in turn promoted the cell growth. The result clearly indicated the synergy between laccase and cells, and such synergy was confirmed by further chemical analysis.

2.3.2. Fenton reaction has less synergy with cell system

As aforementioned, Fenton reaction is another type of widely studied lignin degradation mechanisms.[21] Fenton reaction is believed to play an important role for lignin deoplymerization in termite gut and wood-degrading fungus.[21, 35, 37, 88] It therefore was examined if synergistic effect can be achieved for laccase treatment and Fenton reaction during bacterial lignin conversion. The classic model for Fenton reaction is that ferrous iron is oxidized by hydrogen peroxide to ferric iron, forming hydroxyl radical which could attack lignin. Considering that some iron ions may lead to the precipitation

of lignin, the chelated iron ions using EDTA were also used in the Fenton reaction experiment. Taken these into considerations, different types of iron ions and H_2O_2 were combined with laccase to study their effect on lignin conversion by *R. opacus* PD630. As compared to the laccase plus cell treatment, different types of iron ions have limited effects in promoting cell growth when combined with laccase plus *R. opacus* PD630 cell (Figure 2-2B). While all types of iron-laccase combination treatment increased the CFU at six days after fermentation, the impacts on cell growth is marginal as compared to that of laccase plus cell treatment. In addition, there was no significant difference observed in cell growth among different types of iron used in the treatment. Even though some synergy can be found for Fenton reaction, laccase, and cell system, the results indicated that laccase by itself has a much stronger synergy with *R. opacus* PD630 for cell growth on lignin as compared to that of Fenton reaction.

Furthermore, study of Fenton reaction alone with cells demonstrated a much more limited synergistic effect for cell growth ($H_2O_2 + Fe^{2+}$) as compared to that of laccase and cells. To reveal that if this limited effects of Fenton reaction on lignin conversion was caused by the radical elimination by catalase, the catalase activities under different conditions were detected. The results indicated that *R. opacus* PD630 did not express significant catalase during lignin fermentation (Figure 2-3). In nature, Fenton reaction depends on the quinone and other mediators, as well as the enzyme system to regenerate these mediators, to eventually reduce the ferric iron to ferrous iron for the sustainable reaction. In addition, iron catalyzed radicals are necessary for effective Fenton reaction. The relatively limited synergistic effects between laccase and Fenton

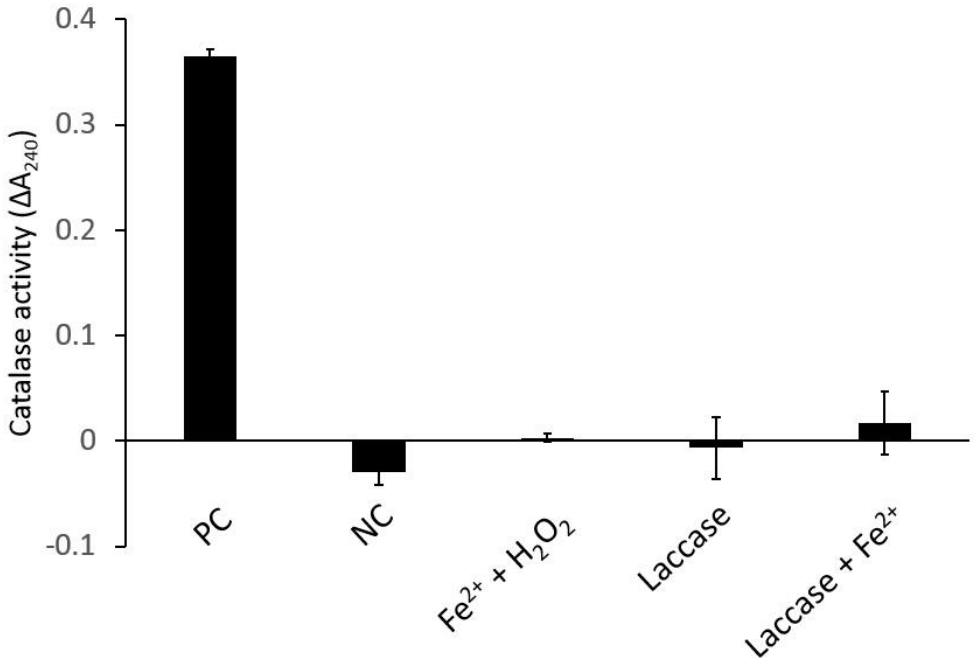

Figure 2-3. The catalase activity of *R. opacus* PD630 supernatant during lignin fermentation under different treatment conditions. The catalase activity was measured by reading the absorbance changes at 240 nm after mixing of 1 µL supernatant with 300 µL 0.036% (w/w) H_2O_2. PC, positive control containing 2 units catalase (Sigma, C1345); NC, negative control, which is the supernatant of lignin medium without fermentation; Fe^{2+}+H_2O_2, the supernatant of *R. opacus* PD630 after lignin fermentation with 0.2 mM $FeSO_4$ and 0.067 mM H_2O_2 treatment; Laccase, the supernatant of *R. opacus* PD630 after lignin fermentation with 1 U/mL laccase treatment; Laccase+ Fe^{2+}, the supernatant of *R. opacus* PD630 after lignin fermentation with 1 U/mL laccase and 0.2 mM $FeSO_4$ treatment.

2.3.3. Changes of lignin molecular weight during cell-laccase co-fermentation

Comprehensive lignin characterization was carried out to determine the key factors contributing to synergistic effects between laccase and *R. opacus* PD630 cells. GPC analysis was carried out to evaluate the changes of molecular weight under different fermentation conditions.[89] Five different conditions were compared as shown in Table 2-1, and these conditions included reference lignin sample without any bacterial or laccase treatment (no cell, Treatment I), lignin after the bacterial fermentation (cell only, Treatment II), lignin after bacterial fermentation with laccase treatment (cell + laccase, Treatment III), lignin after bacterial fermentation with laccase and ferrous iron treatment (cell + laccase + Fe^{2+}, Treatment IV) , and lignin after bacterial fermentation with laccase and Fenton reaction treatment (cell + laccase + Fe^{2+} + H_2O_2, Treatment V). These five fermentation conditions represented different combination of bacterial, enzymatic and chemical treatments, including PD630 only, PD630 with laccase enzyme, and PD630 with both laccase and Fenton reaction.

Table 2-1. GPC analysis of lignin molecular weight upon different treatments.

Lignin Sample	M_n	M_w	Polydispersity index
I[a]	1.73×10^3	8.08×10^3	4.66
II[b]	1.67×10^3	7.58×10^3	4.55
III[c]	2.12×10^3	2.68×10^4	12.7
IV[d]	2.15×10^3	3.30×10^4	15.3
V[e]	2.12×10^3	1.90×10^4	8.98

[a] I No cell; [b] II Cell only; [c] III Cell + Laccase; [d] IV Cell + Laccase + Fe^{2+}; [e] V Cell + Laccase + Fe^{2+} + H_2O_2.

As shown in Table 2-1, PD630 plus laccase treatment (Treatment III) led to the most significant increase in molecular weight as compared to the cell-only (Treatment II) and no-cell reference (Treatment I). The number average molecular weight (M_n) for cell-only fermentation (Treatment II) was not significantly different from no-cell reference (Treatment I), indicating that *R. opacus* PD630 has limited capacity for lignin depolymerization. However, a significant increase in M_n and M_w (weight average molecular weight) was observed when adding laccase into the fermentation (Treatment III vs. Treatment II). No significant differences in M_n were found among Treatment III, IV and V, indicating limited synergy of Fenton reaction and laccase on lignin degradation. In addition, even though PDI and M_w had relatively larger variation, the trends were the same as that of M_n, where *R. opacus* PD630 and laccase together led to the most significant increase of molecular weight. The slightly decrease of M_w for samples with Treatment V (cell, laccase, Fe^{2+}, and H_2O_2) was probably due to the effects of Fenton reaction to promote the degradation of some high molecular weight lignin.

The results was consistent with the slightly increased cell growth upon laccase, Fe^{2+} and H_2O_2 treatment as well as the functional group degradation data in the later part of the study.

The overall increase of lignin molecular weight upon cell and laccase treatment could be due to two reasons. On one side, laccase treatment might have significantly improved the usage of low molecular weight lignin, when combined with *R. opacus* PD630 fermentation. On the other side, the increase of M_w and M_n might also be due to the lignin polymerization caused by laccase. The laccase and cell synergy might have various impacts on different types of lignin. For low molecular weight lignin, the synergy between cell and laccase might have promoted the lignin degradation and subsequent consumption of degraded products. The rapid consumption of low molecular weight lignin could promote cell growth and leave high molecular weight lignin in the system. The overall effects will be both less low molecular weight lignin and potential re-arrangement of high molecular weight lignin structure. Nevertheless, an additional control experiment indicated that GPC analysis of laccase-only treated lignin showed a similar elution profile of gel permeation chromatograph as compared to the untreated control lignin, suggesting no considerable difference in the molecular weights of total lignin after laccase-only treatment. In addition, the increased cell growth and lignin consumption, as well as the subsequent NMR analysis all suggested that laccase and *R. opacus* PD630 synergy could have led to more efficient consumption of low molecular weight lignin. The consumption of low molecular weight lignin could result in relatively

higher molecular weight lignin in the fermentation system, and the composition changes well correlated with the increased M_n and M_w.

2.3.4. Laccase and *R. opacus* PD630 cell synergized lignin degradation as revealed by functional group contents

In complementary to GPC analysis, ^{31}P NMR spectra of the lignin samples from the aforementioned five treatments were analyzed to evaluate how laccase, cell, and Fenton reaction impacted the lignin degradation (Table 2-2). The changes of hydroxyl group contents in lignin was determined by ^{31}P NMR spectra of the lignin derivatized with TMDP (2–chloro–4,4,5,5–tetramethyl–1,3,2–dioxaphospholane) as described in the Materials and supplies section. TMDP reacts with the hydroxyl groups of lignin to form phosphitylated derivatives that can be detected by ^{31}P NMR.[86] In particular, the aliphatic hydroxyl, phenolic, and carboxylic acids groups of lignin were identified based on characteristic chemical shifts[89] and then quantified by peak integration as shown in Table 2-2.

Table 2-2. Decrease of lignin functional groups after different treatments.

Functional Group		Integration region (ppm)	Examples	hydroxyl contents/(mmol/g lignin)				
				I[a]	II[b]	III[c]	IV[d]	V[e]
Aliphatic OH		150.0-145.2	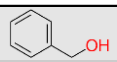	2.38	2.32	1.88	1.98	1.99
C_5 substituted condensed Phenolic OH	β-5	144.6-142.9	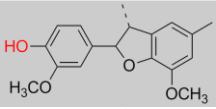	0.15	0.02	0.02	0.01	0.01
	4-O-5	142.9-141.6	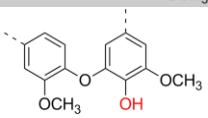	0.01	0.02	0.01	0.02	0.01
	5-5	141.6-140.1	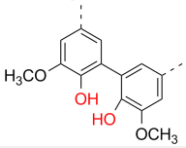	0.00	0.05	0.02	0.03	0.03
Guaiacyl phenolic OH		140.1-138.8	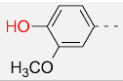	1.32	1.40	0.98	1.00	1.02
Catechol type OH		138.8-138.2	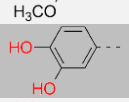	0.04	0.02	0.01	0.02	0.02
p-hydroxy-phenyl-OH		138.2-137.3	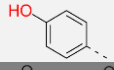	0.08	0.06	0.02	0.03	0.03
Carboxylic acid OH		136.6-133.6	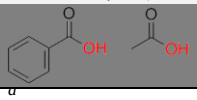	0.50	0.15	0.16	0.29	0.06

[a] I No cell; [b] II Cell only; [c] III Cell + Laccase; [d] IV Cell + Laccase + Fe^{2+}; [e] V Cell + Laccase + Fe^{2+} + H_2O_2.

R. opacus PD630 cell, laccase, and Fenton reaction could all lead to lignin degradation as indicated by decreased functional group contents from ^{31}P NMR analysis. As shown in Table 2-2, *R. opacus* PD630 cell-only treatment (Treatment II vs. I) resulted in a substantial decrease of β-5 condensed phenolic OH and carboxylic OH groups, while other OH functional groups barely degraded. The results suggested that *R. opacus* PD630 alone could cause lignin structural changes, yet the lignin degradation capacity is very limited in terms of the types of chemical bonds and the degree of functional group reduction. With the addition of laccase into fermentation using *R. opacus* PD630 (Treatment III vs. II), the lignin had a further significant decrease in the

contents of aliphatic OH and guaiacyl phenolic OH groups, the two most abundant hydroxyl groups in kraft lignin. For example, the degradation of aliphatic OH group was increased from 2.5% (Treatment II, cell-only) to 21% (Treatment III, cell + laccase). Moreover, the addition of Fenton reaction agents (Treatment IV and V) led to no further decrease of these functional groups (except for carboxylic OH group at the treatment V). As compared to the untreated control lignin, a slight decrease of aliphatic and guaiacyl phenolic OH groups was observed in laccase-only treated lignin, as revealed by ^{31}P NMR analysis. Lund and Ragauskas also observed a decrease in the content of condensed and guaiacyl phenolic groups upon treatment of lignin with laccase alone.[90] In summary, the results revealed that the enhanced lignin hydroxyl groups decrease was mainly due to laccase combined *R. opacus* PD630 cell fermentation, suggesting the synergy of laccase with *R. opacus* PD630 cell treatment for the lignin degradation.

The two dimensional (2D) ^{1}H-^{13}C HSQC was another method used to understand the mechanism of lignin degradation. HSQC spectra of lignin were measured for the aforementioned treatments. Signals from guaiacyl (G) and *p*-hydroxyphenyl (H) units were readily observed in the aromatic regions (Figure 2-4), confirming that the kraft lignin is a typical G/H type of softwood lignin with G as the major monolignol units.

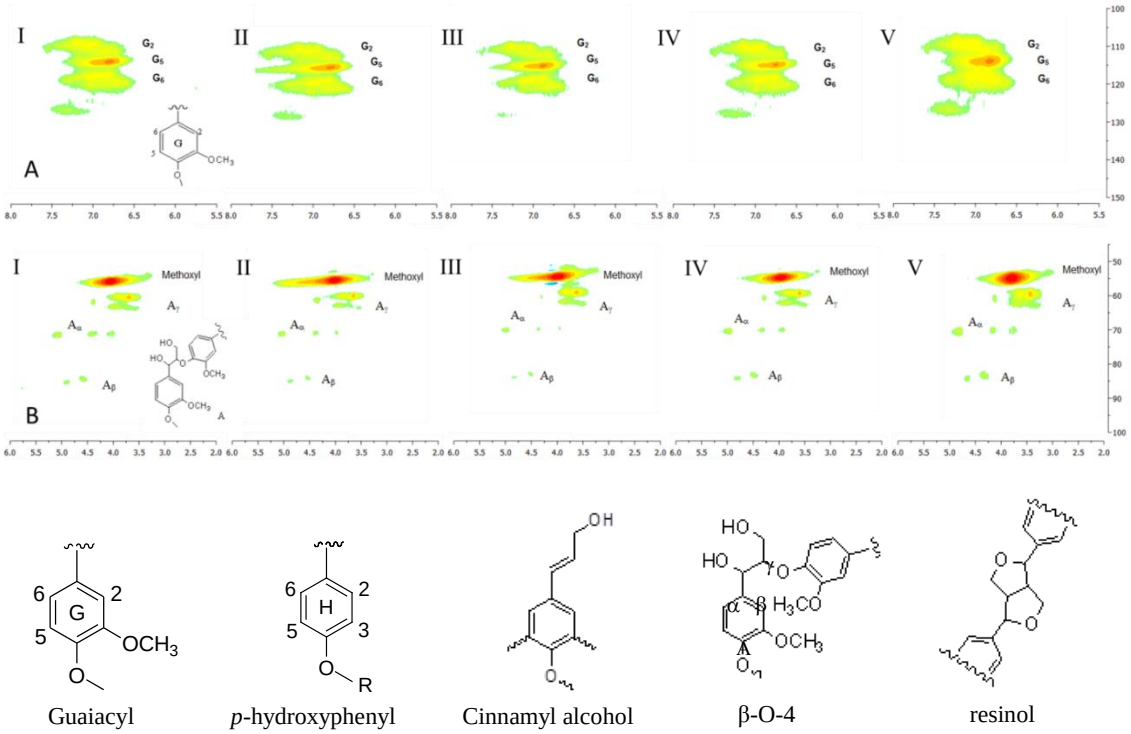

Figure 2-4. HSQC analysis of lignin after different treatments. The aromatic region (A) and aliphatic region (B) of HSQC NMR spectra of lignin obtained after treatments: (I) no cell, (II) cell only, (III) laccase, (IV) laccase and Fe^{2+}, and (V) laccase and Fenton reagent (Fe^{2+}+H_2O_2). The diagnostic signals in guaiacyl units for a softwood lignin were well observed at δ_C/δ_H of 110.8/7.06 (G_2), 115.1/6.78 (G_5), and 119.8/6.81 (G_6) ppm, with the existence of *p*-hydroxyphenyl (H) unit (i.e., its $C_{2/6}/H_{2/6}$ correlation signal δ_C/δ_H around 128.1/7.20 ppm). In the aliphatic region, the interunit linkage of β-O-4 was evident with its signals at 71.2/4.81 (C_α/H_α, A_α), 84.2/4.32 (C_β/H_β, A_β), and 59.8/3.48 ppm (C_γ/H_γ, A_γ), respectively. Signals for resinol subunits were also observed with its C/H correlations around $\delta c/\delta_H$ 85.0/4.66 (C_α/H_α), 3.06/53.9 (C_β/H_β), and 70.9/3.78,4.15 (C_γ/H_γ) ppm.

Semi-quantitative analysis of HSQC spectra showed that the cell plus laccase treated lignin had a slightly decrease of H unit (~4 %) and resinol subunits (~1.6 %) when compared to the control lignin sample, suggesting preferable degradation of these lignin structures in the treated lignin. In addition, the cell plus laccase treatment also resulted in a decrease of ~4.7 % in the relative abundance of end group cinnamyl alcohol. The reduction of cinnamyl alcohol can partially contribute to the decrease of aliphatic hydroxyl group content, which further supported the ^{31}P NMR results that the lignin from the cell plus laccase treatment had the lowest aliphatic hydroxyl group content.

Overall, the results revealed synergistic lignin degradation by *R. opacus* PD630 cell, laccase, and Fenton reaction. Among the different treatments, the fermentation with laccase and cell together led to the significant degradation of the most abundant functional groups in lignin such as aliphatic OH and guaiacyl phenolic OH. The results indicated that laccase and *R. opacus* PD630 could synergistically promote lignin degradation, which was consistent with the increased cell growth (Figure 2-2), lignin molecular weight upon laccase treatment (Table 2-1), and Prussian Blue assay (Figure 2-5A). As shown in Figure 2-5A, lignin degradation was significantly improved when fermented with both laccase and *R. opacus* PD630 cell.

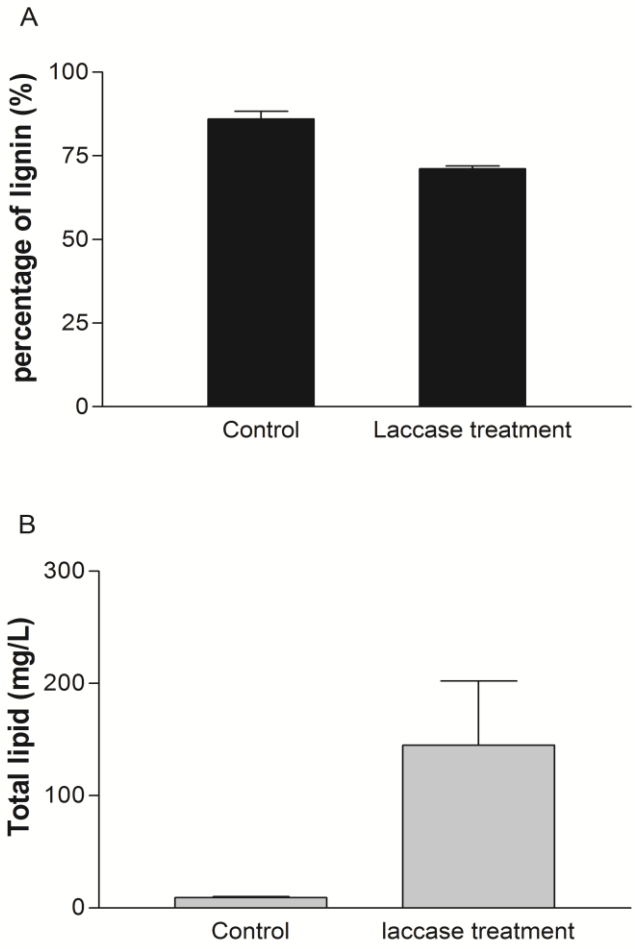

Figure 2-5. Lignin degradation and lipid yield of *R. opacus* PD630 with and without laccase treatment. A, Laccase treatment promoted the lignin degradation as indicated in Prussian blue assay. B, Laccase increased lipid yield from *R. opacus* PD630. For the control group, *R. opacus* PD630 cells was added to fermentation medium without laccase treatment. For laccase treatment, the cells and laccase were added to fermentation medium simultaneously.

2.3.5. Simultaneous depolymerization and fermentation significantly improved the lipid production

It has been established that *R. opacus* PD630 fermentation of lignin produces lipid, including TAG as the biodiesel precursor.[51] The SDF by the cell-laccase system not only promoted the cell growth and lignin degradation, but also led to significantly increased lipid production by 17 fold to 145 mg/L on insoluble kraft lignin (Figure 2-5B). The increase of lipid content suggests that efficiently degraded lignin monomers provide *R. opacus* cells with sufficient carbon source to accumulate lipid.

2.3.6. Potential mechanisms for synergy between laccase and cells

The NMR and lignin quantification analysis revealed synergistic degradation of lignin by both *R. opacus* PD630 cells and laccase with the following important features. First, the degradation of lignin by *R. opacus* PD630, laccase, and Fenton reaction were functional group specific. Unlike cellulose degradation with glucose as the single subunit, lignin is heteropolymer with diverse aromatic monomer units.[15, 16] These different monomers were further connected by various types of chemical bonds and linkages.[2] The changes of various OH functional groups as shown in Table 2-2 indicated that *R. opacus* PD630, laccase, and Fenton reaction each could favorably degrade different chemical structures, which might be the foundation for synergistic effects for cell-enzyme fermentation. Second, based on ^{31}P NMR analysis, laccase played an essential role for lignin degradation, because the enzyme specifically degraded both aliphatic OH and guaiacyl phenolic OH groups, the two types of most abundant hydroxyl groups in lignin.[91, 92] Third, the strong synergy of laccase and *R. opacus* cells

on lignin degradation indicated that the efficient consumption of degradation products generated by laccase promoted the depolymerization direction of the reaction. Four aspects of data were consistent to support the conclusion including the degradation of different hydroxyl functional groups, the significant improvement of cell growth upon laccase treatment, the increases in molecular weight, and the overall higher lignin consumption by the cell-laccase treatment. These features could be exploited for designing efficient conversion or modification of lignin toward various functional products.

2.4. Conclusion

Overall, the study unveiled an effective synergy between *R. opacus* PD630 cells and laccase for lignin degradation at both chemical processing and cell growth level. As compared to Fenton reaction, laccase treatment in the study has a much more significant impact on lignin degradation. The synergistic lignin degradation for laccase and cells was revealed at both chemical and biological level in terms of selective degradation of different functional groups and increased cell growth. The mechanistic study could enable a SDF process to significantly improve lignin utilization and cell growth. Laccase thus not only serves as a good enzyme for SDF, but also can potentially be engineered for consolidated lignin processing.

3. LIGNIN PREPROCESSING BY LACCASE-MEDIATOR SYSTEM ENHANCES BIOCONVERSION

3.1. Introduction

Lignin valorization represents one of the most significant challenges for the sustainability and profitability of lignocellulosic biorefinery.[1, 16, 79] Lignin is the second most abundant biopolymer in nature and a major waste from lignocellulosic biorefinery, pulping and paper industry. The utilization of the lignin-containing biorefinery waste for valuable products will improve CO_2 mitigation, net energy gain, waste management, and cost-effectiveness of biofuel.[79] The fundamental challenge for lignin depolymerization lies in the fact that lignin is a complex substituted polyphenol derived from hydroxycinnamyl monomers with various degrees of methoxylation forming a racemic, cross-linked, and highly heterogeneous aromatic macromolecule.[16, 21, 79] Enzymatic lignin depolymerization invokes the oxidative combustion of lignin mediated by various small molecule oxidants produced by various enzymes , such as laccase and manganese peroxidase (MnP), which can react directly with lignin to generate radical sites within the substrate and initiate bond scission reactions.[16]

It has been recently demonstrated that laccase and *R. opacus* PD630 cell can synergize effective lignin degradation and conversion.[52] Despite the progresses, enzymatic lignin depolymerization still render very low yield of fragmented and soluble lignin, partially due to the limitations on efficient electron transfer. In case of laccase, laccase can self- generate radicals by releasing the phenolic compounds from lignin to create a sustainable redox environment to achieve lignin depolymerization and

modification (Figure 3-1). However, the phenolic radicals released during lignin oxidation by laccase were very limited and often insufficient to mediate the electron transfer for the efficient cleavage of different chemical bonds. The fundamental scientific challenge for effective enzymatic lignin depolymerization thus is to improve electron transferring during the redox reaction.

Traditionally, various laccase-mediator systems have been exploited to improve lignin removal in paper pulping, to degrade hazardous aromatics for environmental remediation, and to modify lignocellulosics in biorefinery pretreatment.[93-96] Despite the progresses, the application of a laccase-mediator system in lignin conversion and the understanding of chemical mechanisms for recalcitrant lignin depolymerization by electron mediators are both still very limited. First, even though laccase-mediator system has been used for delignification in paper pulping, the concept of using an enzyme-mediator system for solubilization of purified lignin toward bioconversion is yet to be proven. No study has established a process for lignin solubilization and conversion using an efficient laccase-mediator system. It is still unclear if development of such a process is attainable, as different electron mediators have various impacts on enzymatic oxidation of lignin, making the outcome of biological-chemical catalytic system unpredictable. Second, the molecular and chemical mechanisms for electron mediators to facilitate lignin depolymerization during the solubilization of purified lignin are yet to be revealed. Previous studies mostly exploited model compounds to illustrate how an

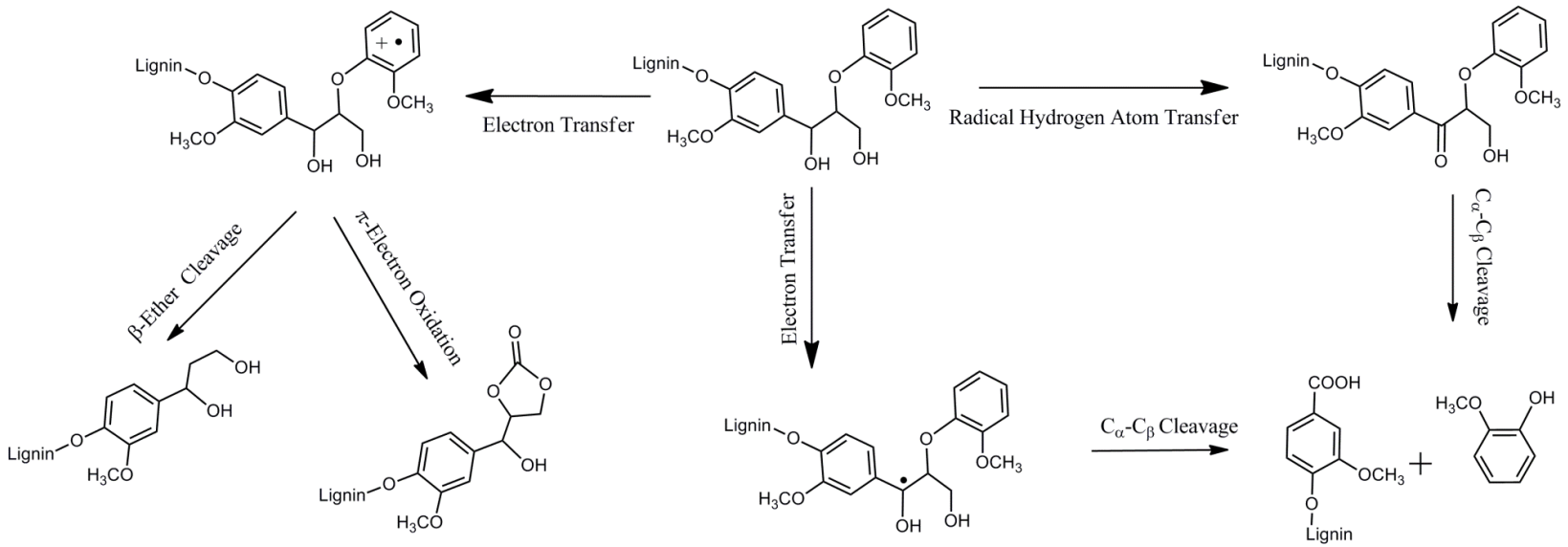

Figure 3-1. The proposed lignin depolymerization mechanisms by a laccase-mediator system as summarized from previous studies.

electron mediator could facilitate the cleavage of certain chemical bonds in the model compounds.[97, 98] Some studies also investigated the effects of laccase-mediator system on the lignin-carbohydrate complex during the delignification of paper pulp.[99] However, very few studies have comprehensively revealed what chemical groups the laccase-mediator system can efficiently degrade in purified lignin, which has hindered the application of such a system in lignin conversion and processing. Third, no research has established how the fragmented lignin out of laccase-mediator treatment can be integrated with microbial fermentation for bioconversion. Neither do we know if the solubilized lignin derived from laccase-mediator treatment can be compatible for microbial fermentation.

In this study, each of these three challenges have been addressed both to establish an effective lignin conversion platform with the advanced chemical design and to elucidate the fundamental mechanisms for the efficient lignin degradation by laccase-mediator system. The outcome both reveals chemical mechanisms with broad scientific impacts on biomass utilization and delivers an effective bioprocess to achieve record level of bioproduct yield for lignin bioconversion.

3.2. Material and methods

3.2.1. Lignin depolymerization by laccase-mediator

The alkali lignin (catalog number 370959) and laccase from *Trametes versicolor* (catalog number 51639) used in this study were both purchased from Sigma-Aldrich (St. Louis, MO, USA). For lignin depolymerization experiment, 6% (w/v) of lignin was loaded in 35 mM phosphate buffer (pH 7.0) and mixed with laccase with a loading of

150 U per gram of lignin and 1mM of the proper electron mediator as discussed in the manuscript. The mixture was incubated for 24 hours at 50 ℃ with a shaking speed of 180 rpm. The solubilized lignin after laccase-mediator depolymerization was collected by centrifuging at 10,000 g for 15 min. The collected solubilized lignin was used for further Gas Chromatography–Mass Spectrometry (GC/MS) analysis, Prussian Blue assay and lignin fermentation. The insoluble lignin from the pellet after centrifuge was washed twice with double distilled water and dried at 65 ℃ to reach constant weight. The weight loss of the insoluble lignin was calculated to determine the lignin solubilization efficiency. The dried insoluble lignin was also characterized by GPC and ^{31}P-NMR.

3.2.2. GC/MS analysis of the solubilized lignin

The monomer composition of the solubilized lignin was analyzed by GC/MS with the method modified from previous study.[100] 3 mL of solubilized lignin was extracted with 9 mL of ethyl acetate by vigorously shaking for 2 hours. The organic layer was collected and dewatered using anhydrous sodium sulfate. 1 mL of the dewatered solution was collected after centrifuging at 4,000 g for 10 min and dried under nitrogen gas stream. The dried residue was mixed with 100 µL dioxane, 10 µL pyridine and 50 µL trimethylsilyl. The mixture was incubated at 60 ℃ for 15 min with periodic shaking to completely dissolve the residue. 1 µL of the silylated compounds were injected into SHIMADZU-QP2010 SE GC/MS equipped with a ZB-5MSi column (thickness 0.25 µm; length 30m; diameter 0.25 mm). The column temperature program was set as: 50 ℃ hold for 5 min; 50-300 ℃ (10 ℃/min, hold time: 5 min). The low

molecular compounds were identified by searching against the NIST library available with the instrument.

3.2.3. Lignin concentration analysis by Prussian Blue assay

The concentration of total solubilized lignin in the solution after laccase-mediator treatment or bacterial fermentation was estimated by Prussian Blue assay.[64, 84] The solubilized lignin was first diluted to an optimal concentration using ddH_2O to a final volume of 1.5mL and mixed with 100 µL of 8 mM $K_3Fe(CN)_6$ and 100 µL 0.1 M $FeCl_3$. The samples were mixed immediately and reacted for exact 5 min. The samples were transferred to 1cm cuvette to record the absorbance reading at 700 nm by spectrophotometer. Standard curve was established with the same reagents and known concentration of catechol. All experiments were carried out in triplicate.

3.2.4. Lignin characterization by GPC

The molecular weight of the soluble and insoluble fraction of lignin before and after treatment was analyzed by GPC. The lignin (20 mg) was first acetylated by incubating with acetic anhydride/ pyridine (1:1 v/v, 1.0 mL) for 24 h in a sealed flask under an inert atmosphere at room temperature according to the literature.[101] After 24 h, the solution was diluted with 20 mL of ethanol and stirred for an additional 30 min, after which the solvents were removed with a rotary evaporator followed by drying in a vacuum oven at 40 °C. Prior to GPC analysis the acetylated lignin sample was dissolved in tetrahydrofuran (1.0 mg/mL), filtered through a 0.45 µm filter, and placed in a 2 mL auto-sampler vial. The molecular weight distributions of the acetylated lignin samples were then analyzed on an Agilent GPC SECurity 1200 system equipped with four

Waters Styragel columns (HR1, HR2, HR4, HR6), an Agilent refractive index (RI) detector, and an Agilent UV detector (270 nm). Tetrahydrofuran was used as the mobile phase in GPC analysis and the flow rate was 1.0 mL/min. A standard polystyrene sample was used for calibration. The Mn and Mw were determined by GPC. Average data of Mw, Mn and polydispersity index (PDI) were presented based on two different tests on each lignin sample.

3.2.5. Lignin characterization by NMR

The more detailed changes in chemical linkages of lignin by different treatment were analyzed by NMR. HSQC-NMR were acquired at a 500 MHz Varian VNMRS using 50 mg lignin dissolved in 500 uL dimethyl sulfoxide-d6 (DMSO-d_6) employing a standard sequence "Gradient HSQCAD" with 0.15s acquisition time, a 1.0 s pulse delay, a $^{1}J_{C\text{-}H}$ of 146 Hz, 48 scan and acquisition of 1024 data point (for ^{1}H) and 256 increments (for ^{13}C). The central solvent peak was used for chemical shift calibration.

Quantitative ^{13}C NMR spectra of acetylated lignin samples were acquired at room temperature. The hydroxyl functional group analysis was carried out following a published report.[102] Deuterated acetone was used as solvent. An inverse-gated decoupling pulse sequence was used to avoid nuclear overhauser effect (NOE), and 10, 240 scans – 30,720 scans were collected to achieve a satisfied signal-to-noise ratio.

For quantitative ^{31}P NMR analysis, 20 mg lignin was dissolved in 500 μL pyridine/$CDCl_3$ (1.6/1.0 v/v) solvent containing chromium acetylacetonate (relaxation agent) and *endo*-*N*-hydroxy-5-norbornene-2,3-dicarboximide (NHND, internal standard), then derivatized with 2-chloro-4,4,5,5-tetramethyl-1,3,2-dioxaphospholane.

The spectrum was acquired using an inverse-gated decoupling pulse sequence (Waltz-16), a 90° pulse, and a 25-s pulse delay. 128 scans were accumulated for each sample. NMR data were processed using the software of TopSpin 2.1 (Bruker BioSpin) and MestreNova (Mestre Labs) packages.[86]

3.2.6. Strain and culture medium

R. opacus PD630 (DSMZ 44193) was purchased from the DSMZ-German Collection of Microorganisms and Cell Cultures at the Leibniz Institute. The culture medium was modified from previous publication[103] which contained (per liter): 1.4 g $(NH_4)_2SO_4$, 1.0 g $MgSO_4 \cdot 7H2O$, 0.015 g $CaCl_2 \cdot 2H_2O$, 35.2 mL sterile 1 M pH 7.0 phosphate buffer (113 g/L K_2HPO_4 and 47 g/L KH_2PO_4), 1.0 mL sterile trace element solution (0.5 g/L $FeSO4 \cdot 7\ H_2O$, 0.4 g/L $ZnSO4 \cdot 7\ H_2O$, 0.02 g/L $MnSO4 \cdot H_2O$, 0.015 g/L H_3BO_3, 0.01 g/L $NiCl_2 \cdot 6H_2O$, 0.25 g/L EDTA, 0.05 g/L $CoCl_2 \cdot 6H_2O$ and 0.005 g/L $CuCl_2 \cdot 2H_2O$), 1.0 mL sterile stock A solution (2.0 g/L $NaMoO_2 \cdot 2H_2O$ and 5.0 g/L FeNa·EDTA) and certain carbon source.

3.2.7. Lignin fermentation

R. opacus PD630 was pre-cultured in aforementioned minimum medium with 0.5% glucose as carbon source at 28 °C to OD_{600} 1.5. The cells were harvested by centrifugation and washed twice with equal volume of the culture medium without carbon source. 5 ml of the resuspended cells were inoculated to 50 ml of aforementioned minimum medium with 1% of lignin as sole carbon source. The fermentation was set up at 28 °C with shaking speed of 200 rpm, and the samples were harvested periodically for bacterial growth assay and lipid extraction.

3.2.8. Cell growth and total lipid yield measurement

Considering that the cells and untreated lignin (with significant portion of insoluble contents) cannot be readily separated, it is difficult to measure either the OD600 or dry cell weight of *R. opacus* PD630 grown on untreated insoluble kraft lignin. Therefore, the growth of *R. opacus* PD630 on both untreated kraft lignin and treated soluble lignin were estimated according to the CFU.

The total lipid of *R. opacus* PD630 after lignin fermentation was extracted in the form of fatty acid methyl ester (FAME) according to the method described in our previous study.[104] The bacteria cells were harvested by centrifugation after lignin fermentation and incubated with 20 mL methanol at 65 °C for 30 min. 1 mL of 10 M KOH was added and incubated at 65 °C for 2 h. After the incubation, the sample was moved out from water bath and cooled down to room temperature. 1 mL of sulfuric acid was then added drop by drop and incubated at 65 °C for another 2 h. 8 mL of hexane was added and incubated with periodically shaking for 5 min to extract the lipid. The hexane layer was collected to pre-weighted glass tube after centrifugation and this hexane extraction step was repeated once. The hexane was evaporated under nitrogen gas stream and the lipid yield was calculated according to tube weight change. The CFU analysis revealed a higher fold of cell growth increase as compared to the lipid yield, which could be due to the larger variation in measuring lipid yield using weight-based methods at the low lipid titer on untreated lignin.

3.3. Results and discussions

3.3.1. Electron mediators could promote enzymatic lignin depolymerization and solubilization in a mediator-specific way

An efficient laccase-mediator system was first designed to solubilize >35% of insoluble kraft lignin. Kraft lignin is among the most recalcitrant and insoluble lignin. In general, laccase itself could only carry out oxidative attack on the phenol structure, which accounts for only a small portion of lignin.[105] To achieve effective lignin depolymerization, it is necessary to establish an efficient laccase-mediator system, where the electron mediator can facilitate the redox transfer during the oxidation by laccase and the subsequent non-enzymatic attack on non-phenolic lignin (Figure 3-1).[105-107] However, different mediators may have various impacts on the laccase-based lignin depolymerization reaction and could promote either polymerization or depolymerization reactions. The impact of electron mediators on lignin depolymerization is therefore subject to debate. In order to address these challenges, four different types of mediators were firstly screened in combination with a well-studied commercial laccase from *Trametes versicolor.* In order to well integrate with downstream bioconversion by bacteria *R. opacus* PD630, the pH for lignin depolymerization by laccase-mediator system was adjusted to 7. As shown in Figure 3-2A, the weight loss analysis revealed that most of the electron mediators significantly promoted lignin depolymerization. As compared to the laccase only treatment control, essentially all electron mediators can increase the soluble fraction of kraft lignin in water (Figure 3-2A).

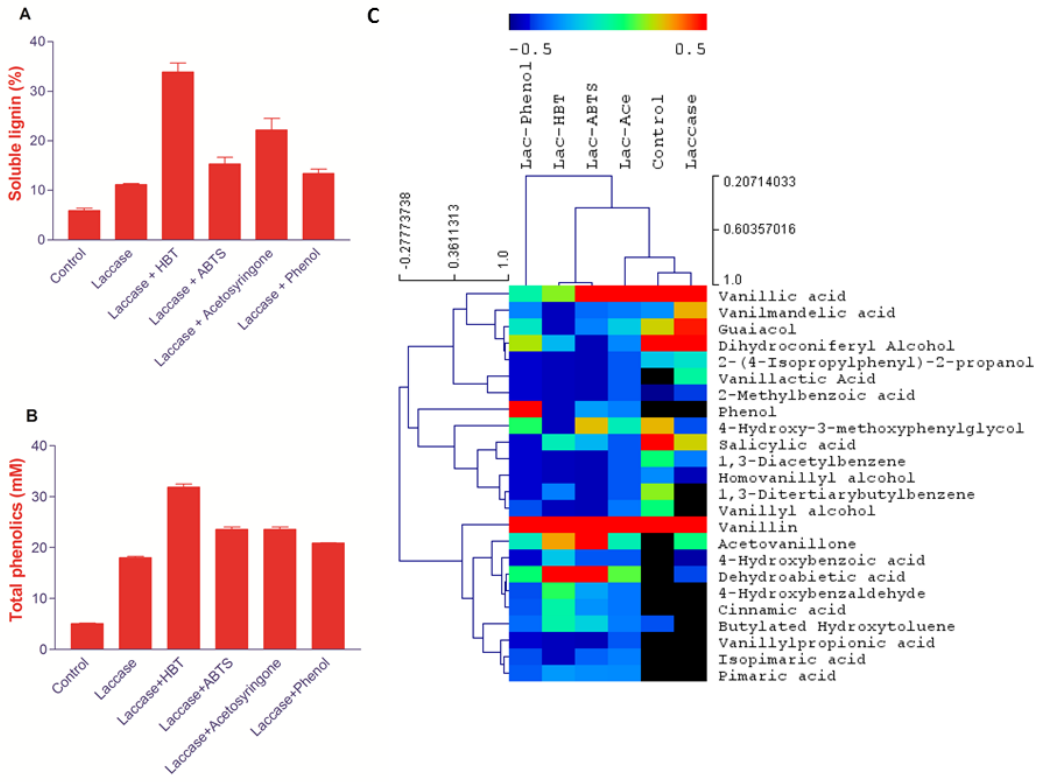

Figure 3-2. The solubilization of kraft lignin by different laccase-mediator systems. (A) The percentage of the solubilized lignin as calculated from the weight loss of the kraft lignin after the different laccase-mediator treatments; (B) The estimated total soluble aromatic compounds in solution determined by Prussian Blue assay; (C) The hierarchical cluster heatmap of the relative abundance of the monomer aromatic compounds in the solubilized lignin solution as detected by GC/MS analysis. Each row of the heatmap represented one detected compound and each column represented one sample (or treatment). The presented values were normalized within the sample and thus represented relative abundance of the compounds.

However, the efficiency for lignin depolymerization varies substantially among different mediators (Figure 3-2). For example, the laccase-HBT (1-hydroxybenzotriazole) system could lead to the most efficient lignin depolymerization with more than 35% of the kraft lignin released into water. Only about 15%, 22% and 13% of lignin was solubilized, when ABTS (2,2'-azino-bis(3-ethylbenzothiazoline-6-sulphonic acid)), acetosyringone, and phenol were used as mediators, respectively. The data from weight loss analysis was further confirmed by Prussian Blue assay of total aromatic compounds solubilized (Figure 3-2B). As shown in Figure 3-2B, the laccase-HBT system led to the highest concentration of aromatic compounds in water. The GC/MS analysis was further carried out to analyze the soluble monomer compounds released after lignin depolymerization by different laccase-mediator systems (Figure 3-2C). The heatmap presents the cluster analysis of normalized relative quantity of the various monomer compounds in the solution phase. The GC/MS analysis revealed that laccase in combination with various mediators released different aromatic monomer compounds, indicating the selective targeting of different chemical linkages during lignin oxidation.

Table 3-1. The number-average molecular weights (Mn) and weight-average molecular weights (Mw) of soluble lignin samples.

Samples	Mn	Mw
Control lignin	561	1918
Laccase lignin	135	646
Lac-HBT lignin	192	370

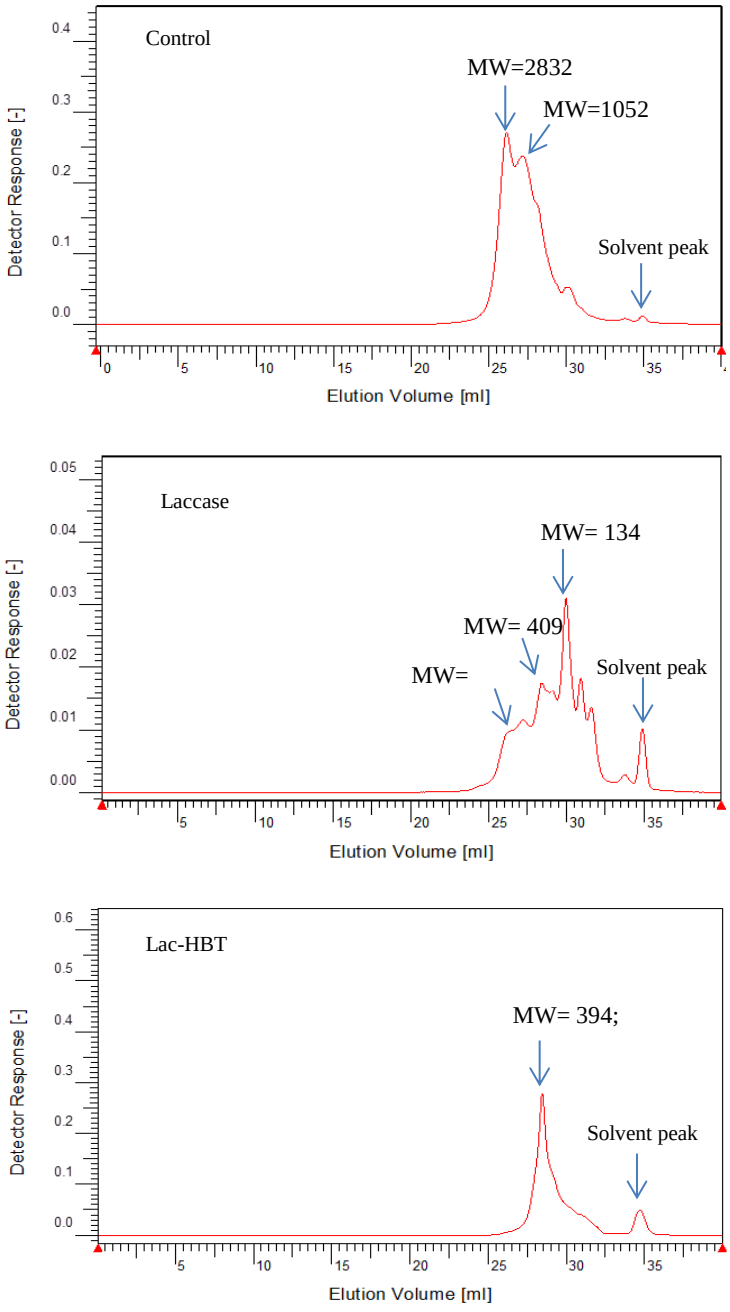

Figure 3-3. GPC chromatogram of soluble fractions of control, laccase-treated and laccase-HBT treated samples. Control: the soluble fraction of kraft lignin released without laccase treatment; Laccase: the soluble fraction of kraft lignin released with the laccase only treatment; Lac-HBT: the soluble fraction of kraft lignin released after laccase-HBT treatment.

GPC analysis was carried to further confirm the enhanced release of low molecular weight compounds by laccase-mediator systems. The soluble fractions of lignin under laccase and laccase-HBT treatments were compared with that of the untreated lignin. As shown in Figure 3-3 and Table 3-1, GPC analysis of the soluble fraction showed that the released soluble products had a number-averaged and weight-average molecular weights of 135 g/mol and 646 g/mol for laccase treated lignin, 192 g/mol and 370 g/mol for laccase-HBT treated lignin, respectively. The results further confirmed the release of low molecular weights products. The result indicated that laccase-mediator systems can promote the lignin depolymerization and release of low molecular weight lignin. Overall, the results highlighted two features for electron mediators to promote redox reactions toward enzymatic lignin depolymerization. First, an efficient laccase-mediator system could substantially promote lignin fragmentation and solubilization. Second, various mediators have different efficiency and selectivity for facilitating the lignin depolymerization reactions. We therefore focused on the most efficient mediator, HBT, to study the chemical mechanisms for electron mediators to promote lignin degradation and to investigate the feasibility of coupling laccase-mediator-based lignin solubilization with microbial bioconversion.

3.3.2. The lignin depolymerization by an efficient laccase-mediator system increased molecular weight of the insoluble lignin

In an effort to determine the effect of laccase-mediator system on the molecular weight distribution of kraft lignin, GPC was employed to analyze the insoluble portion of lignin before and after the laccase-mediator treatment.

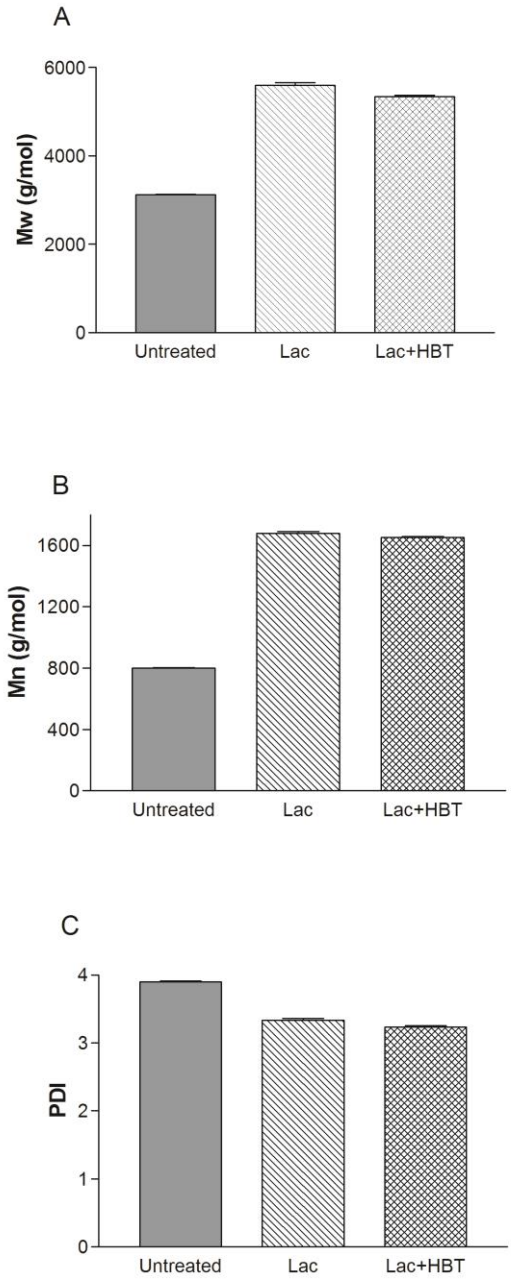

Figure 3-4. Molecular weight properties of the insoluble fraction of kraft lignin after laccase and laccase-HBT treatments as revealed by GPC analysis. The changes of Mw (A), Mn (B) and PDI (C) for kraft lignin after the laccase-HBT (Lac+HBT) treatment and laccase only (Lac) treatment.

There was a significant increase of molecular weights of insoluble lignin after the laccase and laccase-HBT treatment. M_w of lignin increased from 3122 to 5595 and 5337 g/mol for laccase and laccase-HBT treatment, respectively. M_n of lignin increased from 801 to 1678 and 1652 g/mol for laccase and laccase-HBT treatment, respectively. (Figure 3-4A, 3-4B). GPC analysis also revealed the decrease of PDI in the insoluble fraction of the treated lignin (Figure 3-4C), which could be attributed to the behavior of M_n and M_w. PDI was obtained through dividing M_w by M_n, and any changes on those two parameters could result in the altered PDI. The decreased PDI suggested that the insoluble lignin after laccase and mediator treatment became more uniform in molecular weight distribution.

On one side, the increase in average molecular weights and uniformity could result from repolymerization and re-arrangement of lignin structure by laccase.[108] On the other side, the increased molecular weights could also be attributed to the better fragmentation of lower mass lignin and the solubilization of such released small molecular weight compounds during lignin depolymerization. Considering that the laccase and mediator treatments led to increased solubilization of kraft lignin (Figure 3-2), it is likely that the degradation of low molecular weight lignin at least contributed partially to the increased molecular weight for insoluble lignin. The slight decrease of M_w and M_n of laccase-HBT treated lignin as compared to that of laccase only treatment may attribute to the more efficient degradation of low weight lignin into soluble part. The ^{31}P-NMR analysis further verified that the degradation of abundant chemical groups contributed to the increased molecular weight and uniformity of insoluble lignin.

3.3.3. Electron mediator promoted the enzymatic degradation of different functional groups and cleavage of abundant linkages

To further investigate the fundamental mechanisms of lignin solubilization during laccase and laccase-HBT treatments, quantitative ^{31}P NMR technique was applied to monitor the changes of aliphatic, phenolic hydroxylic and carboxylic functional groups in kraft lignin. The ^{31}P NMR analysis of insoluble fraction of kraft lignin provided an accurate and quantitative way to illustrate the effects of laccase-HBT system on lignin chemical bonds cleavage.

Table 3-2. The abundance of functional groups in lignin before and after laccase and laccase-HBT treatment as revealed by ^{31}P NMR analysis.

Chemical shift range (ppm)	Assignment	Consistency (mmol/g)		
		Untreated lignin	Lac	Lac+HBT
150.0 – 145.5	Aliphatic OH	2.57	2.33	1.90
144.70 – 142.92	β-5	0.53	0.41	0.29
142.92 – 141.70	4-O-5	0.37	0.35	0.26
141.70 – 140.20	5-5	0.59	0.51	0.40
140.20 – 138.81	Guaiacyl	1.90	1.37	1.10
138.18 – 137.30	p-hydroxylphenyl	0.22	0.21	0.12
136.60 – 133.60	Carboxylic acid OH	0.46	0.32	0.14
144.7---140.0	C5 substituted “condensed”	1.56	1.35	0.98

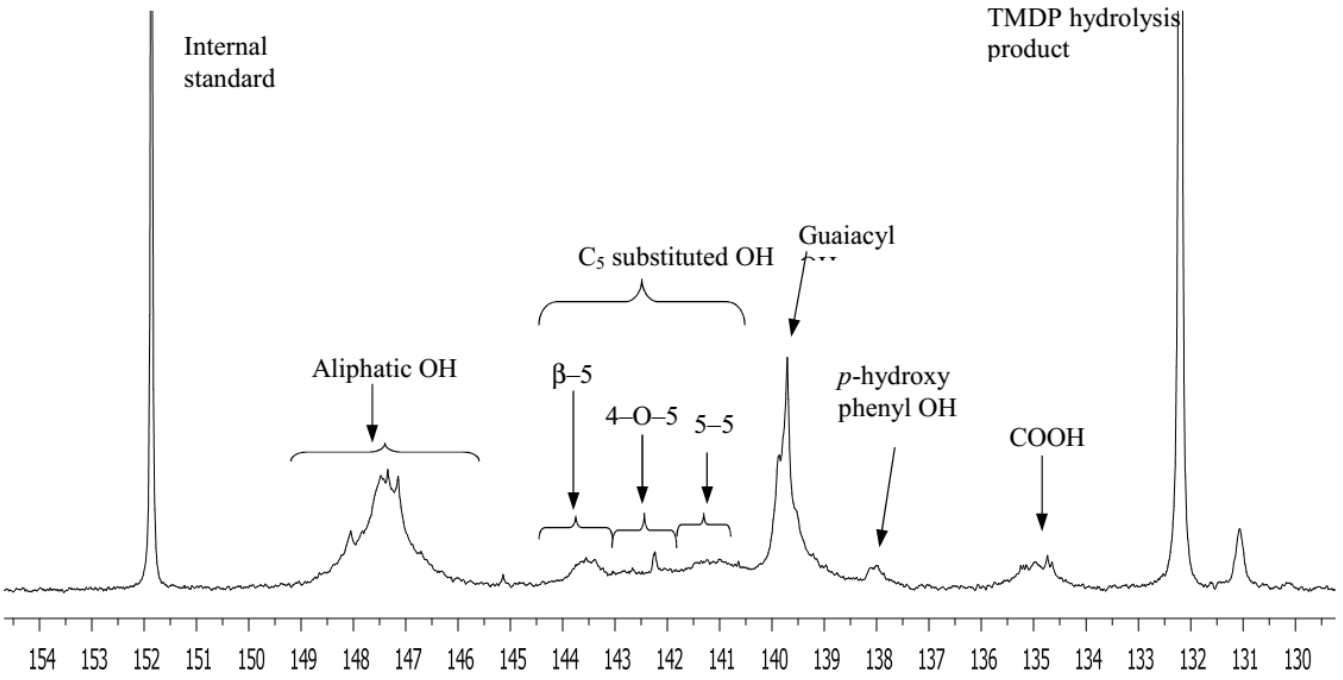

Figure 3-5. Analysis of hydroxyl groups in ^{31}P NMR spectrum of insoluble fraction of untreated kraft lignin after phosphitylation. Solvent: Pyridine/deuterated chloroform.

As shown in Table 3-2 and Figure 3-5, the kraft lignin used in the study was mainly composed of guaiacyl (G) and p-hydroxyphenyl (H) units, as revealed by the presence of G and H spectra signal and the absence of syringyl (S) spectra signal. The ^{31}P NMR revealed that laccase-HBT system treatment could lead to much more significantly decrease of non-condensed structures including guaiacyl, p-hydroxyphenyl and aliphatic OH structure by 42.1%, 45.5% and 26.1%, respectively, as compared to those of untreated lignin. The decrease of these functional groups by laccase alone treatment was much less significant, where only 27.9% decrease of guaiacyl group was observed, and no significant changes of p-hydroxyphenyl structure and aliphatic OH structure were found (Table 3-2). Moreover, the major interlinkages including β-5, 4-O-5 and 5-5 in kraft lignin were significantly decreased after laccase-HBT treatment by 45.3%, 29.7% and 32.2%, respectively. However, only 22.6% decrease of β-5 was observed in laccase alone treatment and no significant decrease of 4-O-5 and 5-5 linkages were observed (Table 3-2). Meanwhile, C5 condensed structure and carboxylic group in the insoluble lignin after laccase-HBT treatment were found significantly decreased as compared to those in untreated lignin and laccase-treated lignin. In order to further confirm the structure changes of the kraft lignin after laccase-HBT treatment, ^{13}C NMR analysis was carried out to further characterize the insoluble part of the kraft lignin with and without laccase-HBT treatment. The results showed a slight decrease of aliphatic and phenolic hydroxyl groups in laccase-HBT treated lignin samples, in agreement with ^{31}P NMR analysis (Figure 3-6, Table 3-3). All of these results strongly

suggested that laccase-HBT could depolymerize lignin in a much higher efficiency than that of laccase alone treatment.

Overall, the results indicated that the enhanced lignin fragmentation and solubilization was achieved by significantly improved cleavage of the aromatic interlinkages to release aromatic monomers and/or oligomers into water. Taken together with the lignin solubilization data and GPC analysis, the results highlighted that electron mediators like HBT could facilitate the electron transfer for attacking the abundant chemical groups and linkages to significantly increase the solubilization of kraft lignin.

Table 3-3. Quantitative estimation of hydroxyl group contents (number /Aryl group) in the insoluble acetylated lignin as determined by quantitative ^{13}C NMR after acetylation.

Structure	Control	Lac-HBT
primary OH	0.29	0.28
Secondary OH	0.21	0.19
Phenolic OH	0.59	0.49

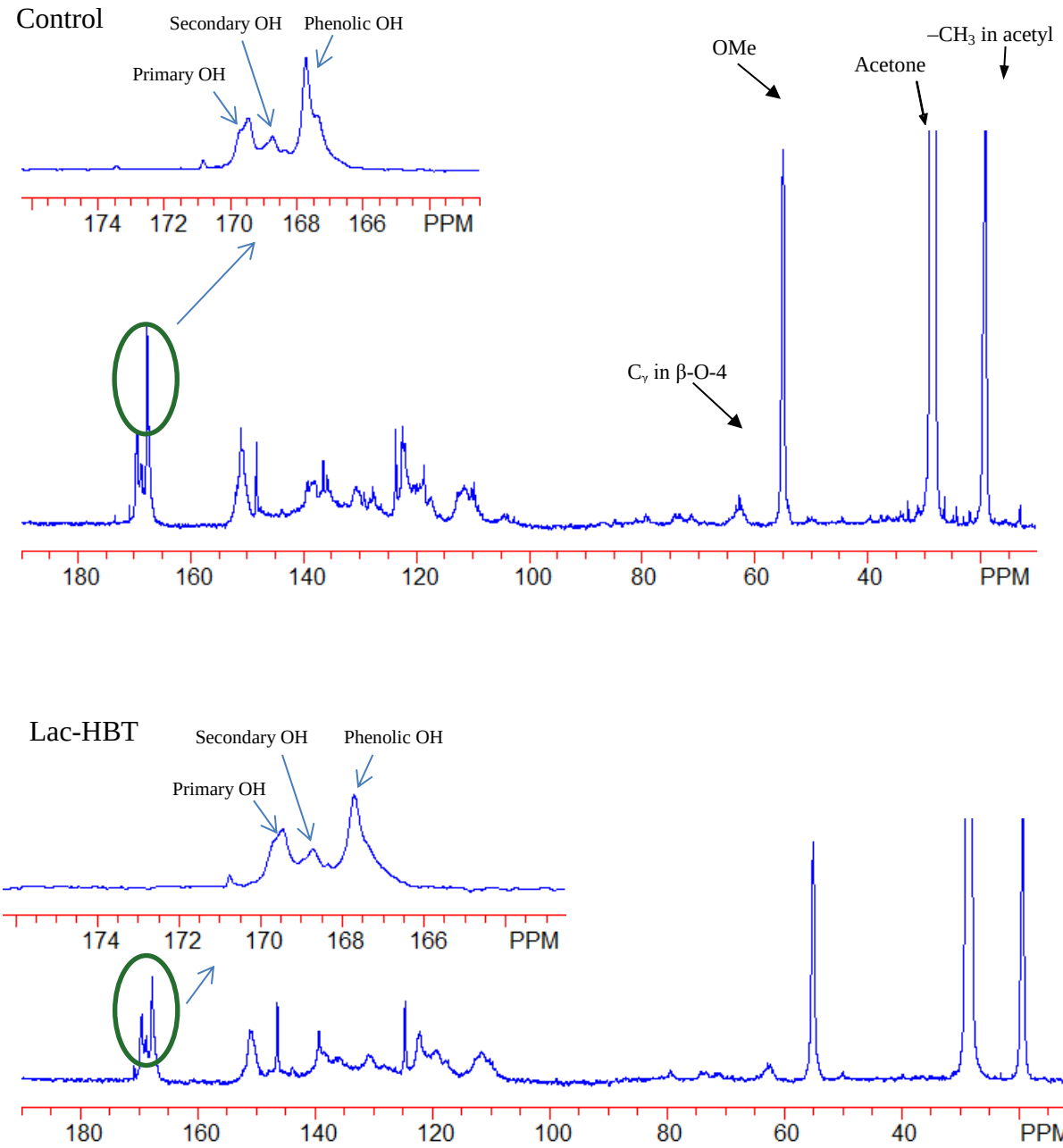

Figure 3-6. ^{13}C NMR spectra of insoluble acetylated residual lignin samples. Control: lignin without laccase treatment; Lac-HBT: lignin after laccase-HBT treatment. Solvent: deuterated acetone. An expansion of 162-176 ppm showing the primary, secondary and phenolic hydroxyl functional groups.

3.3.4. Lignin depolymerization by laccase-mediator system as demonstrated by HSQC-NMR

The electron mediator-facilitated lignin depolymerization was further confirmed by the HSQC-NMR, which provided semi-quantitative analysis of the kraft lignin after laccase treatment. The major inter-units observed in untreated kraft lignin were the β-O-4 (A), β-5/α-O-4 (B), and β-β (C) (Figure 3-7). The assessment of cross-peak intensity qualitatively indicated a decrease in intensity of both aliphatic region (β-aryl ether linkages, phenylcoumaran as well as resinol units) and aromatic region (the major guaiacyl unit) for both laccase and laccase-HBT treated lignins (Figure 3-7). The relative abundance of main interunit linkages in the untreated and laccase-HBT treated kraft lignin samples was determined by semi-quantitative analysis of HSQC spectra following reported procedures.[109, 110]**.** HSQC quantification of the main ether linkages gave a β-O-4: β-5/α-O-4: β-β ratio of 61.7: 17.3: 21.0 in the untreated softwood kraft lignin. The relative abundance of beta-O-4 linkage was slightly decreased in the laccase and laccase-HBT treated lignin when compared to that in the untreated kraft lignin (Figure 3-8).

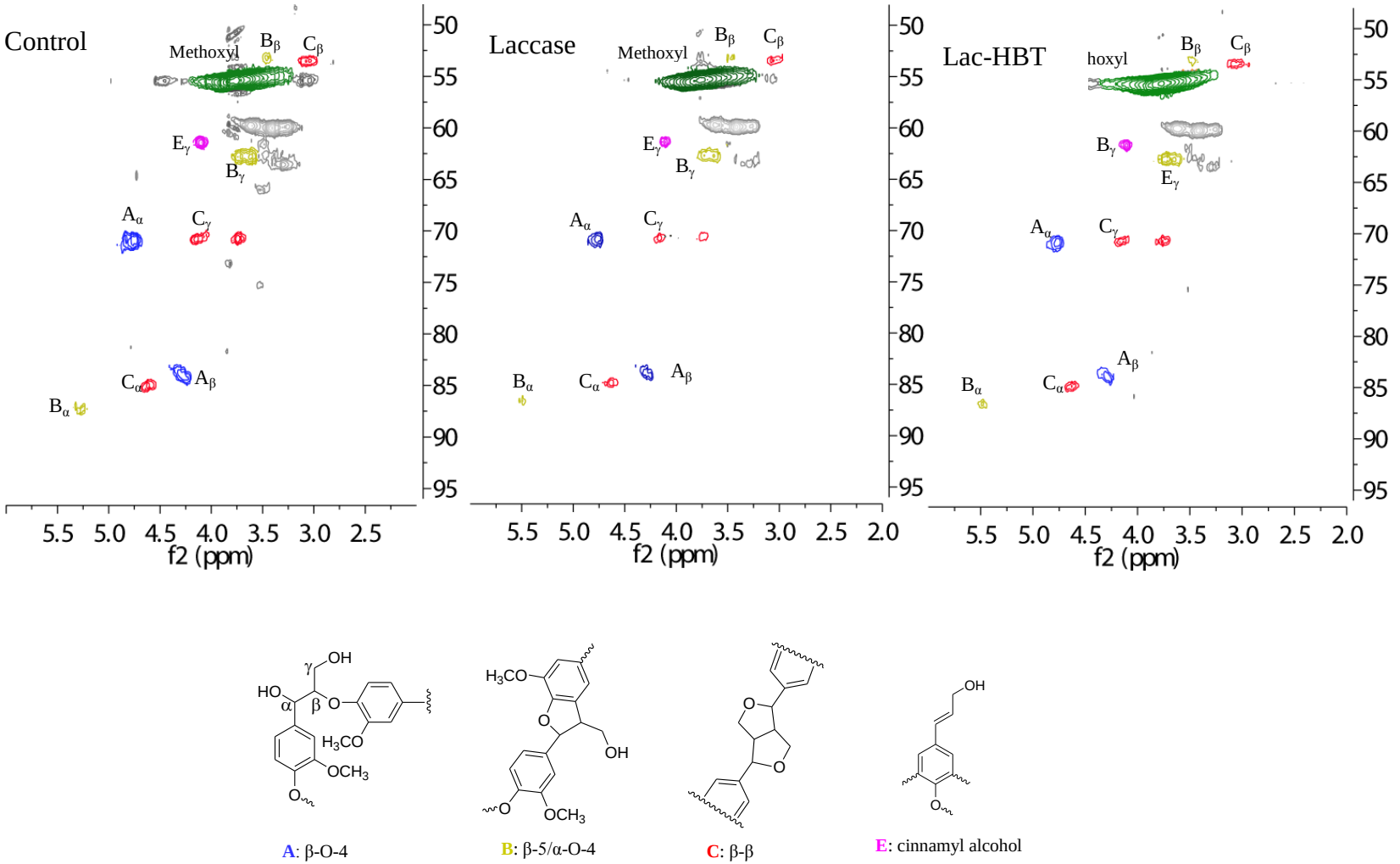

Figure 3-7. HSQC-NMR spectra (aliphatic regions) of the insoluble fractions from the untreated kraft lignin (Control), laccase only treated kraft lignin (Laccase) and laccase-HBT treated kraft lignin (Lac-HBT).

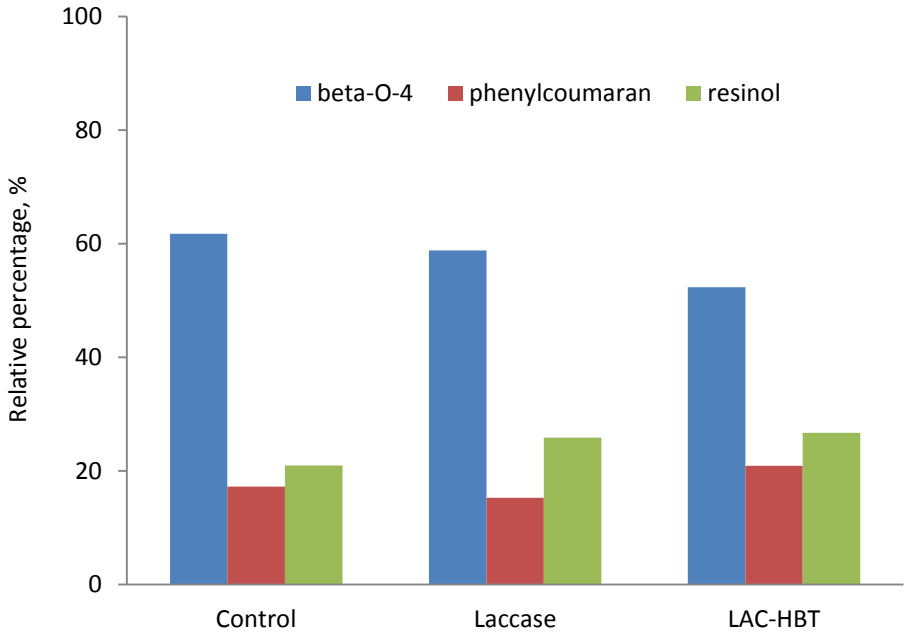

Figure 3-8. Relative abundance of interunit linkages as determined by 2D HSQC NMR. (Results expressed as percentage of total ether-linked side chains). Control: lignin without laccase treatment; Laccase: lignin after laccase only treatment; Lac-HBT: lignin after laccase-HBT treatment.

The result indicated that the efficient lignin depolymerization by laccase-HBT treatment might be related to the cleavage of β-O-4 linkage, which accounted over 50% of all ether linkages in lignin.[111] The HSQC data thus complemented the ^{31}P-NMR to demonstrate the breakdown of a broad range of abundant linkages by laccase and mediator treatment. The new laccase-mediator system thus provided an efficient platform to fragmentize and solubilize lignin for various applications.

3.3.5. The solubilized lignin by laccase-HBT system significantly promoted cell growth and lipid yield during bioconversion

It was further investigated that if the solubilized lignin from laccase-mediator system can be used for bioconversion. Although recent technology breakthroughs have enabled several chemical/physical methods to pre-process lignin for efficient fractionation,[61, 62, 112] the combination of these methods with bioconversion leads to limited increase of bioproduct yield from lignin as compared to that from model compounds.[54] Considering the potentially less toxic compounds produced by enzymatic lignin fragmentation as compared to chemical fragmentation, the compatibility of this laccase-mediator system with microbial bioconversion were investigated. The soluble fraction of laccase-HBT depolymerized kraft lignin was used as fermentation substrate for an oleaginous bacteria *R. opacus* PD630. The results highlighted that the lignin depolymerization by the laccase-mediator treatment could significantly promote lignin consumption and enable a record level of bioproduct yield on lignin. When the solubilized lignin was used as the sole carbon source for *R. opacus* PD630 fermentation, the cell growth was increased by 10^6 folds as compared to the cells grown on untreated

kraft lignin based on colony-forming unit (Figure 3-9A). The cell dry weight reached to 2.79 g/L, representing the highest yield for microbial fermentation of lignin. The lipid yield achieved 1.02 g/L, which was 10 time higher than the cells grown on untreated lignin (Figure 3-9B). The GC/MS analysis of the aromatic monomer compounds in the medium before and after fermentation indicated the consumption of several major compounds including cinnamic acid, 4-hydroxybenzaldehyde, 4-hydroxybenzoic acid, phenol, vanillin, and others (Figure 3-9C). In addition, several new aromatic compounds like 1,3-diacetylbenzene, octopamine and 1,4-cyclohexadiene were also found in the media after the fermentation. The results indicated that *R. opacus* PD630 not only utilized the aromatic monomers, but also degraded the aromatic oligomers to release monomers. Overall, the significant increase in lipid yield and cell growth indicated that the enzyme-mediator system for lignin fragmentation was very compatible with a variety of bioconversion platforms to process highly recalcitrant and insoluble lignin like kraft lignin.

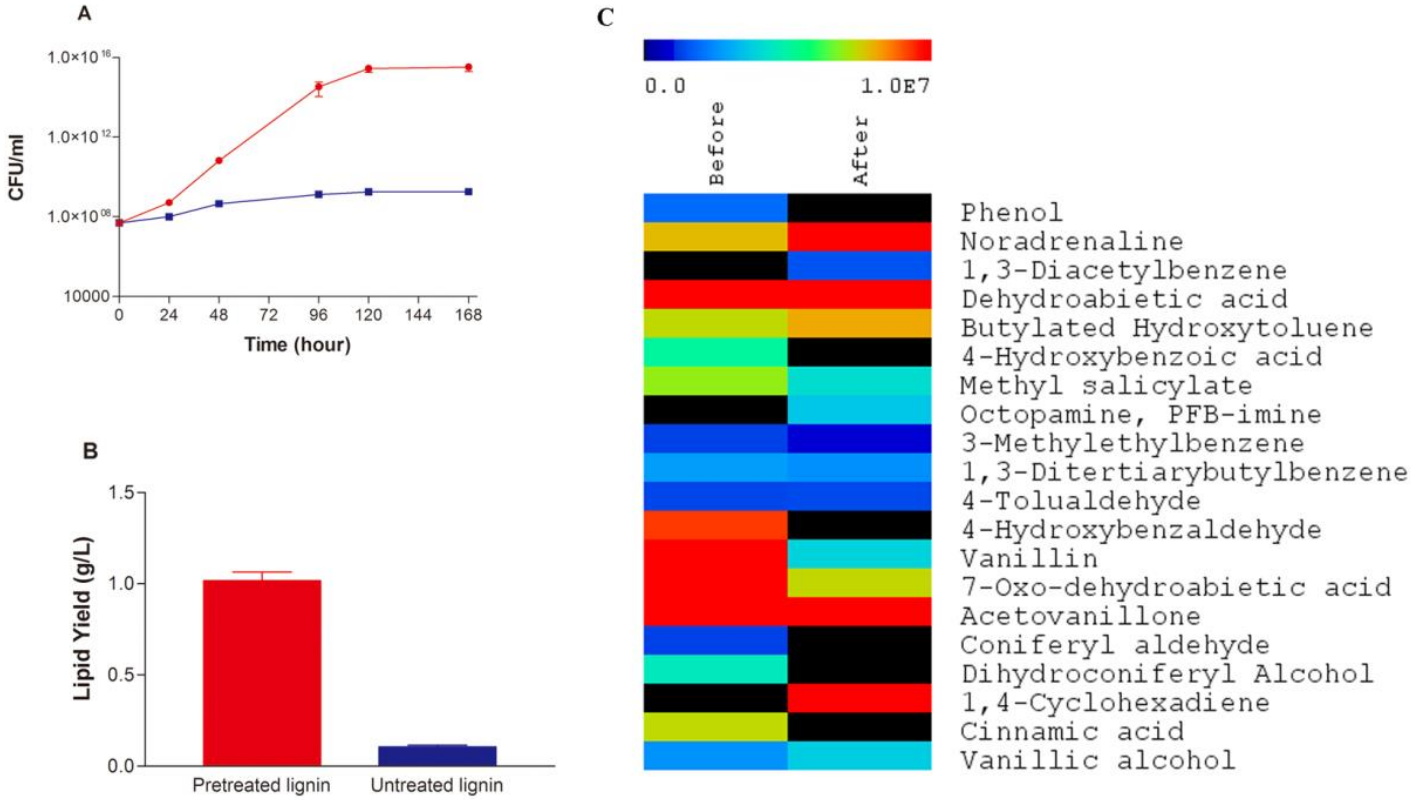

Figure 3-9. Bioconversion of solubilized fraction of kraft lignin out of the laccase-HBT treatment by *R.opacus* PD630. (A) The growth curve of *R.opacus* PD630 on solubilized lignin and untreated lignin. (B) The lipid yield of *R.opacus* PD630 after 7-days fermentation on solubilized lignin and untreated lignin. (C) The heatmap of the abundance of aromatic monomers in solubilized lignin before and after *R.opacus* PD630 as revealed by GC/MS analysis. The presented values were normalized within the sample.

3.3.6. The chemical mechanisms for efficient lignin depolymerization catalyzed by an enzyme-mediator system

The biological and chemical analyses suggested several aspects of the fundamental mechanisms for electron mediators to facilitate enzymatic lignin depolymerization. First, weight loss and Prussian Blue assay of lignin solubilization by enzyme-mediator systems suggested that the enhanced electron transfer could promote enzymatic depolymerization of insoluble and recalcitrant kraft lignin. The various electron mediators showed different selectivity and efficiency to interact with the same laccase for lignin depolymerization. Second, the NMR analyses revealed that the electron mediators like HBT can facilitate the electron transfer to promote the cleavage of a broad range of chemical linkages within lignin, which further resulted in the enzymatic degradation of different abundant functional groups and linkages. The enhanced redox reactions for chemical bond cleavage were the basis for more efficient enzymatic lignin depolymerization. Even though previous studies revealed the improved cleavage of certain chemical bonds by laccase-mediator system, this study for the first time revealed the cleavage of a broad range of chemical bonds as the basis for an efficient synergy between laccase and mediator. The fundamental mechanisms can be translated into broad applications including lignin conversion, selectively modification of lignin structure, and preparation of lignin for the synthesis of various carbon materials.

3.4. Conclusion

The scientific discovery has enabled an effective platform for lignin processing. First, the study established a lignin solubilization process by an efficient laccase-mediator system. Despite the abundance and importance, lignin utilization is hindered by the lack of efficient fragmentation and/or depolymerization methods to produce oligomers and monomers for bioconversion or chemical synthesis.[16, 79] Commercially available kraft lignin was used in this study to prove the principle of laccase-mediator enhanced microbial bioconversion, as kraft lignin is currently the most abundant source of lignin waste material and represents a relatively recalcitrant type of lignin. Further study indicated similar effects could be established for the lignin-containing biorefinery waste (Data not shown). The design of an efficient laccase-mediator system has enabled the solubilization of 35% of highly recalcitrant kraft lignin, resulting in a water soluble fraction as well as a more condensed and uniform insoluble fraction of lignin. The two fractions can be utilized for various purposes including microbial fermentation and materials synthesis. Second and more importantly, it has been demonstrated that the soluble lignin fraction is compatible with bioconversion using *R. opacus*. Bioconversion of lignin into various bioproducts has emerged as a powerful platform. For example, technical breakthroughs have established bioconversion can utilize EOL or lignin in biomass to produce lipid.[21, 51] However, the bioproduct yields from untreated lignin are usually very low as compared to those on model compounds.[51] Even though several chemical processes were developed for lignin depolymerization, the combination of these processes with microbial bioconversion still could not achieve bioproduct titer

higher than 1 g/L, assumingly due to the toxic compounds produced under extreme chemical conditions.[54, 61, 112] Enzymatic depolymerization of lignin serves as a viable alternative to produce fragmented products that are less toxic and more amenable to bioconversion. Another significant advantage for the enzymatic process is the relevant mild conditions, which will significant reduce the capital investment for the bioprocess stream in an integrated biorefinery setting. Despite the potential, enzymes like laccase can only lead to very limited lignin depolymerization. The enhanced electron transfer and resultant cleavage of abundant chemical linkages by proper mediators significantly improved enzymatic lignin depolymerization and subsequent release of soluble monomers and oligomers. The significant improved lipid yield and cell growth on laccase-HBT treated lignin indicated that the new enzyme-mediator platform could be broadly applied to bioconversion of lignin into different bioproducts.

4. BIODESIGN OF EFFICIENT LIGNIN CONVERSION

4.1. Introduction

Lignin valorization into fungible products represents one of the most significant challenges in modern biorefinery. Regardless of the exact biomass pretreatment methods used, essentially all bioprocesses of lignocellulosics will lead to a major lignin containing waste stream. Even though some of this lignin can be burned to power the biorefinery, the lignocellulosic biorefinery normally have about 60% of waste lignin. The utilization of this lignin for fungible biofuels and bioproducts represents a significant opportunity to enhance the sustainability and economics of lignocellulosic biofuel. In a similar way, the paper and pulping industry produces over 50 million ton of lignin waste annually, and only 2% of it are used commercially. Despite the significance, lignin valorization has been a highly challenging task due to the recalcitrant nature of the aromatic polymer with diverse monomers, variable chemical linkages, and the need of redox reaction for linkage breakage. Even though a thermochemical approach was developed to convert lignin, the process is complicated by the often corrosive products that need further catalytic steps with hydrogen to upgrade. Bioconversion of lignin recently emerged as a viable route for various bioproducts, yet the titer for essentially all bioproducts are too low to be commercially relevant. Our previous study established that enzyme and microbes like *R. opacus* PD630 can synergize to degrade lignin and improve conversion efficiency. Despite progress, the optimization of enzyme production system and carbon utilization remained to be the major challenge to achieve higher bioproduct titer toward commercial relevance. In particular, lignin depolymerization remains to be

the speed-limiting step for bioconversion, and the enhanced secretive production of lignolytic enzymes from microorganisms will be essential to develop either consolidate lignin processing (CLP) or simultaneous lignin depolymerization and fermentation.

From a broader perspective, the secretive production of enzymes and proteins from Gram positive bacteria like *R. opacus* PD630 represents another major challenge in biotechnology. Unlike gram negative bacteria which has both cytoplasmic membrane and outer membrane, Gram positive bacteria has only one cytoplasmic membrane and thus the protein can be more easily exported across the cell membrane and then released directly into extracellular environment. The membrane and cell wall structure determines that Gram positive bacteria might be exploited to express cellulytic and lignolytic enzymes extracellularly at a higher yield for either consolidated or enzymatic biomass conversion. The potential of Gram positive bacteria in protein production has been demonstrated by the high α-amylase production (17.6 g/L).[113] Despite the high protein titer in homologous protein expression, few bacterial species have the comprehensive enzymatic systems needed for lignin bioconversion. Moreover, no studies achieved secretive production of heterologous recombinant protein using Gram positive bacteria at over 5g/L. In this study, the challenges in lignin bioconversion were addressed by developing a highly efficient laccase secretive expression system based on system biology guided biodesign for lignin depolymerization. At the meantime, proteomics analysis enables us to discover the key genes to drive the carbon flux into lipid biosynthesis.

Overall, the integration of different biological functional modules including efficient ligninase secretive system and robust lipid biosynthesis system as well as mild chemical treatment design will deliver a revolutionary approach for utilizing the waste lignin from biorefinery for advanced biofuels.

4.2. Material and methods

4.2.1. Strain and medium

R. opacus PD630 (DSMZ 44193) was purchase from Leibniz Institute DSMZ-German Collection of Microorganisms and Cell Cultures (Braunschweig Germany). The culture medium was prepared as follow (per liter): 10g glucose or lignin (or other concentration stated in the paper), 1.4 g $(NH_4)_2SO_4$ (or other concentration stated in the paper), 1.0 g $MgSO_4$·7H2O, 0.015 g sterile $CaCl_2$·$2H_2O$ 1.0 mL sterile trace element solution (0.5 g/L FeSO4·7 H_2O; 0.4 g/L ZnSO4·7 H_2O; 0.02 g/L MnSO4·H_2O; 0.015 g/L H_3BO_3; 0.01 g/L $NiCl_2$·$6H_2O$; 0.25 g/L EDTA; 0.05 g/L $CoCl_2$·$6H_2O$; 0.005 g/L $CuCl_2$·$2H_2O$), 1.0 mL sterile stock A solution (2.0 g/L $NaMoO_2$·$2H_2O$, 5.0 g/L FeNa·EDTA), and 35.2 mL sterile 1.0 M phosphate buffer (pH 7.0).

4.2.2. Plasmids and genes

The gene for the small laccase from *Streptomyces coelicolor* was synthesized by GenScript with codon optimization according to the codon usage table of *R. opacus* PD630. The *Escherichia coli-Rhodococcus* shuttle vector pRST used for laccase heterologous expression in *R. opacus* PD630 was constructed with the *Rhodococcus* plasmid replication origin from pTip-RT1[114] and the fragment from pSET152[115] which contains *E.coli* plasmid replication origin and apramycin resistance gene. The *E. coli-*

Rhodococcus shuttle vector pBSNC9031 was constructed by using pBluescript SK as background and integrating with thiostrepton resistance gene *tsr* from *Streptomyces azureus* and synthesized (by GenScript) pNC903 sequence which contains *Rhodococcus* plasmid replication origin.[116]

4.2.3. Genetic transformation

The plasmid was transformed into *R. opacus* PD630 by electroporation using the modified method from previous studies.[117, 118] 0.1 mL of an overnight precultured strain in TSB medium was inoculated into 10 ml of fresh TSB medium supplemented with 0.5% (w/v) glycine in a 50-ml Erlenmeyer flask and incubated at 28° C to an optical density of 0.5 at 600 nm. The cells were then harvested by centrifuging, washed twice with ice-cold HS buffer (7 mM HEPES, 252 mM sucrose, pH 7.0) and concentrated 10-fold in ice-cold HS buffer. 1 µg purified plasmid DNA was mixed with 400 µl of competent cells and incubated at 40 ℃ for 10 min. The electroporation was then performed in electrocuvette with the following settings: 6.5 kV/cm, 600 Ω and 25 µF. The pulsed cells were immediately diluted with 1 ml of TSB medium and regenerated at 28 ℃ for 4 hours before being plated on appropriate selective medium (100 µg/mL thiostrepton for pBSNC9031 based plasmid and 80 µg/mL apramycin for pRST based plasmid).

4.2.4. Genomic DNA extraction

The genomic DNA of *R. opacus* PD630 was extracted according to the modified method from previous a publication.[119] The bacterial cells were harvested from 5 ml of

late exponential culture by centrifugation. The collected cell pellet was frozen at -20°C for one hour and resuspended in 250 μL fresh TE (10 mM Tris-HCl, 1 mM EDTA, pH 8) containing 10 mg/mL lysozyme and 0.1 mg/mL mutanolysin. The slurry was incubated at 37°c for 1–2 hour with gentle shaking. After the incubating, 50 μL 0.5 M EDTA, 50 μL 10% SDS, 50 μL 5 M NaCl and 10 μL proteinase K (fresh 20 mg/ml) were added respectively and incubated the mixture at 37°C for another 1 hour. 50 μL sodium perchlorate (1 g/mL) was added to the mixture and the DNA was extracted with equal volume of phenol: chloroform: isoamyl alcohol (25:24:1). The supernatant was collected after centrifuging and extracted again with 500 μL chloroform: isoamyl alcohol (24:1). The supernatant was collected after centrifugation and 0.6 mL isopropanol was added to precipitate the genomic DNA. The DNA pellet after centrifuging was washed briefly with 70% ethanol, then dried and resuspended in 50 μL TE buffer.

4.2.5. Lignin fermentation

R. opacus PD630 was pre-cultured in aforementioned minimum medium with 2% glucose as carbon source at 28 °C for 7 days. 5 mL of the bacterial culture was inoculated to 50 mL of aforementioned minimum medium with 1% of lignin as sole carbon source in the 250 mL Erlenmeyer flask. The fermentation was carried out at 28 °C with shaking speed of 200 rpm, and the samples were harvested periodically for bacterial CFU assay and lipid extraction.

4.2.6. Protein extraction

For the total intracellular protein extraction, the bacterial cell pellet collected from 10 mL culture medium was resuspended in 2 mL Alkali-SDS buffer (5% SDS; 50

mM Tris-HCl, pH 8.5; 0.15 M NaCl; 0.1 mM EDTA; 1 mM $MgCl_2$; 50 mM Dithiothretiol) and boiled for 10 min.[120] The supernatant of the boiled sample after centrifuging at 4000 ×g for 10 min was collected and transferred to a fresh tube and 100% chilled TCA was added to a final concentration of 20%. The mixture was then incubated at -20 °C for 2 hours. Samples were centrifuged at 16,000 × g for 30 min at 4 °C to remove the supernatant. The pellet was harvested after centrifuging at 16,000 ×g for 30 min at 4 °C and washed twice with 1 mL chilled acetone. The protein pellet was air-dried and then dissolved in solution buffer contains 7 M urea, 40 mM triszma base, 2 M thiourea, and 1% 3-(4-Heptyl)phenyl-3-hydroxypropyl dimethylammoniopropanesulfonate (C7BzO). The extracted protein was stored at -80°C prior to LC-MS/MS analysis.

For the total extracellular protein extraction, 50 mL supernatant of the bacterial culture medium was collected by centrifuging at 4000 ×g for 10 min. The collected supernatant was filtered through 0.2 μm filter to remove all bacterial cell and then 100% chilled TCA was added to a final concentration of 20%. The aforementioned steps after adding TCA were followed to extract the total extracellular proteins for proteomics analysis. Protein concentration was measured by Coomassie Protein Assay (Bradford) with bovine serum albumin (BSA) as standard.

4.2.7. MudPIT based shot-gun proteomics

The isolated total protein of *R. opacus* PD630 was analyzed by MudPIT (Multidimensional Protein Identification Technology) based shot-gun proteomics system as described in our previous publications.[121, 122] In summary, the extracted total proteins

were digested by mass spectometry grade trypsin with 1:40 w/w at 37 °C for 24 hours. The digested peptides were firstly desalted by a Sep-Pak C18 plus column and then loaded onto an in-house packed two phase column (constituted of strong cation exchange and C18 reverse phase) using a high pressure tank. The total peptides were separated by the two-dimensional liquid chromatography and analyzed by LTQ mass spectrometry (Thermo Finnegan) for MS/MS analysis.

4.2.8. Proteomics data analysis

The generated tandem mass spectras were extracted from the raw files and converted into the MS2 file. ProLuCID algorithm was used to search the MS2 file against the *R. opacus* PD630 protein database from previous publication.[123] The DTASelect1.9 was used to assess the validity of peptide/spectrum as described in our previous publication.[121] Proteins with more than two peptides were identified as detected and were recorded. PatternLab software was used for data analysis to calculate the protein expression abundance.[124] The cutoff of *p* value (BH q-value) and FDR (False Discovery Rate) were both set at 0.05. F-stringency was optimized automatically.

4.2.9. Cell growth and total lipid yield measurement

The cell growth of the bacteria grown on glucose was measured by reading the optical density at 600 nm, and that grown on lignin was measured by CFU. The total lipid of *R. opacus* PD630 was extracted in the form of FAME according to the method described in our previous publications.[104]

4.2.10. Laccase activity assay

Laccase activity was determined by oxidation of ABTS as a substrate. The absorbance increase at 420 nm by the oxidation of ABTS ($\mathcal{E}_{420}$ = 36,000 M^{-1} cm^{-1}) was measured in 3 min. The reaction was set up at room temperature by mixing 100 μL enzyme solution and 200 μL 50 mM sodium acetate buffer (pH 4.8) containing 6 mM ABTS. One unit of laccase activity was defined as the amount of enzyme that needed to oxidize 1 μmol of ABTS per minute.

4.3. Results and discussions

4.3.1. Proteomics analysis revealed lignin utilization capacity

Typically, the lignin-to-lipid conversion by microorganism should be achieved in three major steps: lignin depolymerization, aromatic compound degradation, and lipid production. To efficiently convert the lignin into lipid, the microorganism should be able to have the high capacity to coordinately carry out the three steps. Systematic proteomics analysis of *R. opacus* PD630 grown on 1% glucose or lignin as sole carbon source was carried to analyze its capacity and potential on lignin conversion into lipid (Figure 4-1, 4-2). These proteomics analysis results laid down the foundational system understanding to guide the biodesign of *R. opacus* PD630 for efficient lignin conversion into lipid.

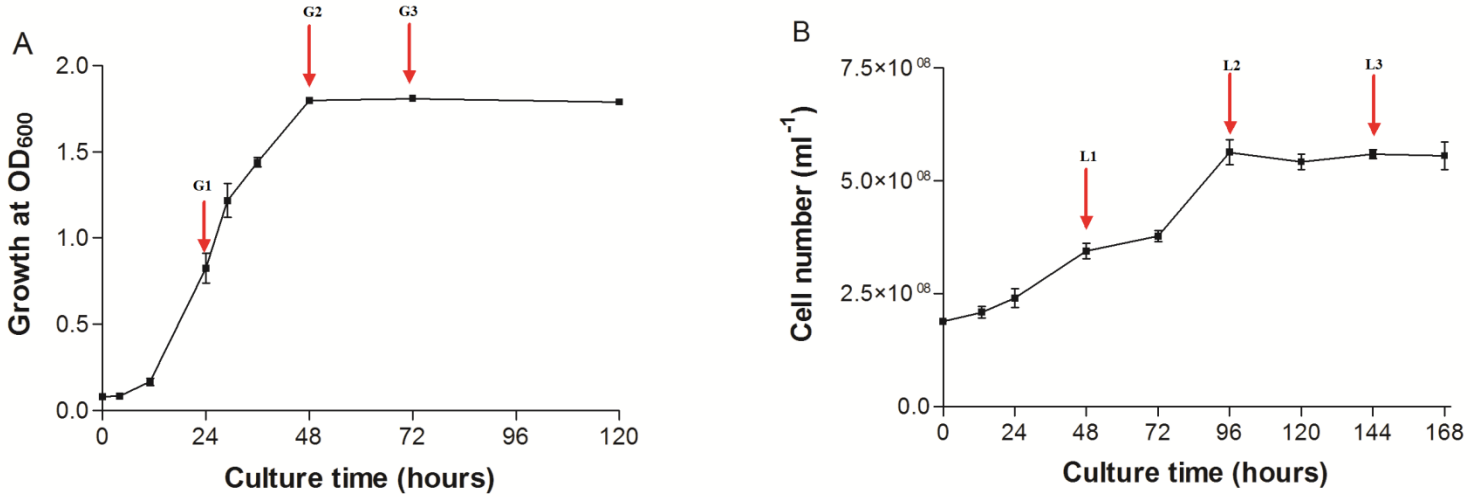

Figure 4- 1. The growth curve of *R. opacus* PD630 grown on 1% glucose (A) and 1% lignin (B) as sole carbon source. The red arrows indicated the time points of the bacterial samples collected for proteomics analysis.

Firstly, the system analysis of *R. opacus* PD630 suggested that the bacterium has very limited capacity on lignin depolymerization, which is the most important and challenged step for bacterial lignin conversion (Figure 4-2). There were only 18 proteins belonging to auxiliary activities (AA) class being detected from the total extracellular protein of *R. opacus* PD630 grown on lignin as sole carbon source (Table S1). AA class was widely accepted as a group of proteins cover the redox enzymes involving lignin and polysaccharide oxidative degradation. Among these AA proteins, only one protein (OPAG_06129) and one protein (OPAG_02267) was classified into AA1 and AA2 family respectively, which of both families were thought to be the groups containing the major lignolytic degradation enzymes. Detail sequence functional annotation indicated that OPAG_06129T0 encoded multicopper oxidase and OPAG_02267 encoded catalase/peroxidase. Both of these two proteins may not exhibit traditional major lignin degradation enzyme activity. The enzymatic assay of *R. opacus* PD630 grown on lignin also indicated that there were no detectable laccase or lignolytic peroxidase activity from the medium. These results were consistent with the growth assay of *R. opacus* PD630 that the bacteria could only have very limited biomass increase on lignin as sole carbon source (Figure 4-1).

Table 4-1. The proteins annotated to CAZy Auxiliary Activity (AA) families detected from *R. opacus* PD630 extracellular proteomics grown on lignin.

Sequence ID	Predicted Pfam Domains	CAZy Families	Detected Spectrum Count	Annotated Gene Name
OPAG_06129	Cu-oxidase_2	AA1	5	multicopper oxidase
OPAG_02267	Peroxidase	AA2	72	catalase/peroxidase HPI
OPAG_03034	GMC_oxred_C	AA3	3	choline dehydrogenase
OPAG_07298	Pyr_redox_2	AA3	2	NADH dehydrogenase
OPAG_05641	Pyr_redox_2	AA3	2	NADH dehydrogenase
OPAG_00358	GMC_oxred_N|GMC_oxred_C	AA3	2	choline dehydrogenase
OPAG_05112	FAD_binding_4|FAD-oxidase_C	AA4	2	glycolate oxidase
OPAG_02457	FAD_binding_4	AA4	2	alkylglycerone-phosphate synthase
OPAG_01861	FAD_binding_4|FAD-oxidase_C	AA4	13	vanillyl-alcohol oxidase
OPAG_00126	FAD_binding_4|FAD-oxidase_C	AA4	3	glycolate oxidase
OPAG_06111	YjgF_endoribonc	AA6	6	endoribonuclease
OPAG_09269	FAD_binding_4	AA7	2	oxidoreductase
OPAG_09230	FAD_binding_4	AA7	2	FAD-binding oxidoreductase
OPAG_01258	FAD_binding_4|BBE	AA7	2	oxidoreductase
OPAG_00178	FAD_binding_4|BBE	AA7	3	FAD-binding oxidoreductase

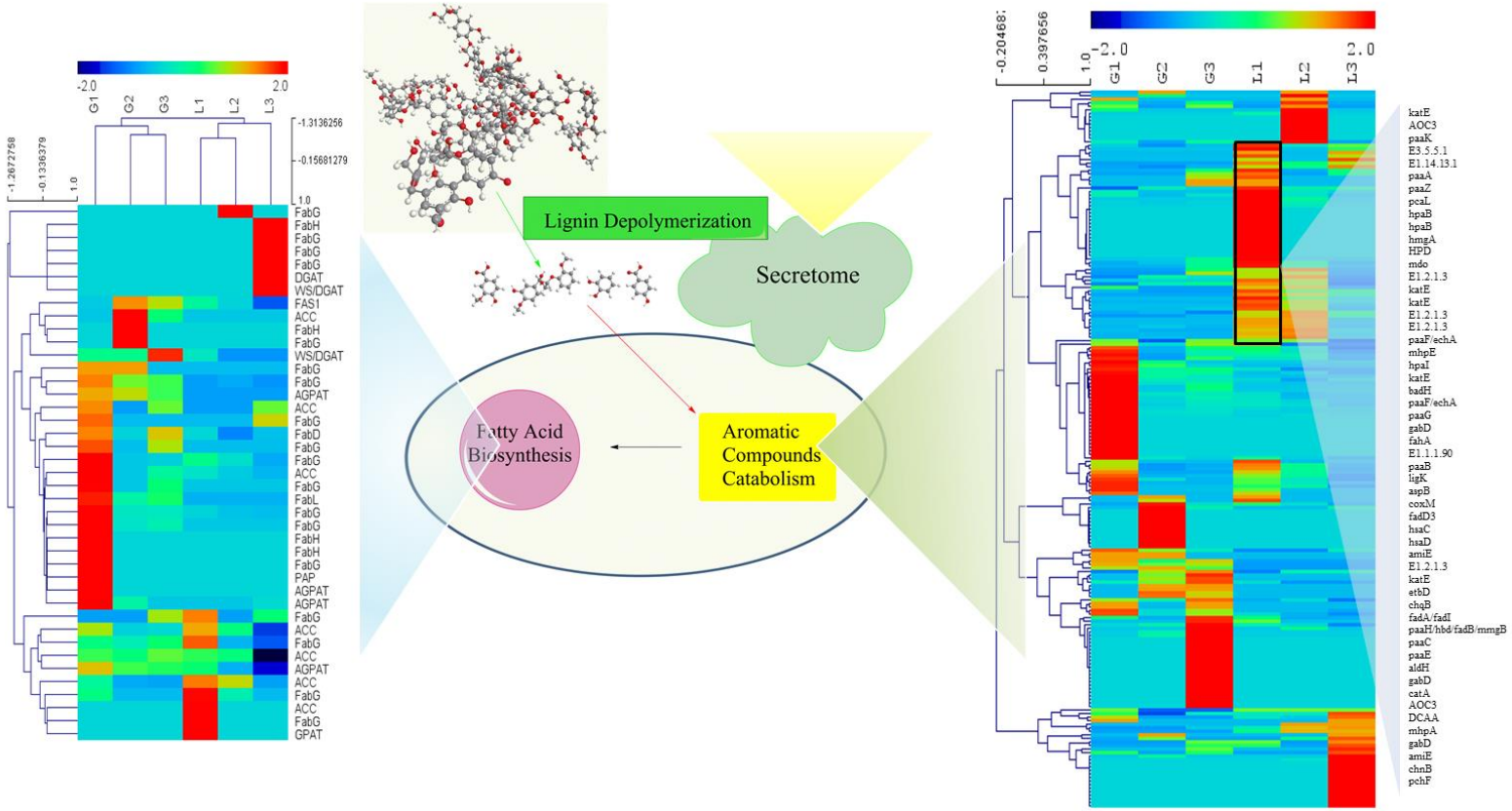

Figure 4-2. The system biological analysis of *R. opacus* PD630 for their capacity on lignin depolymerization, aromatic compound catabolism and lipid biosynthesis.

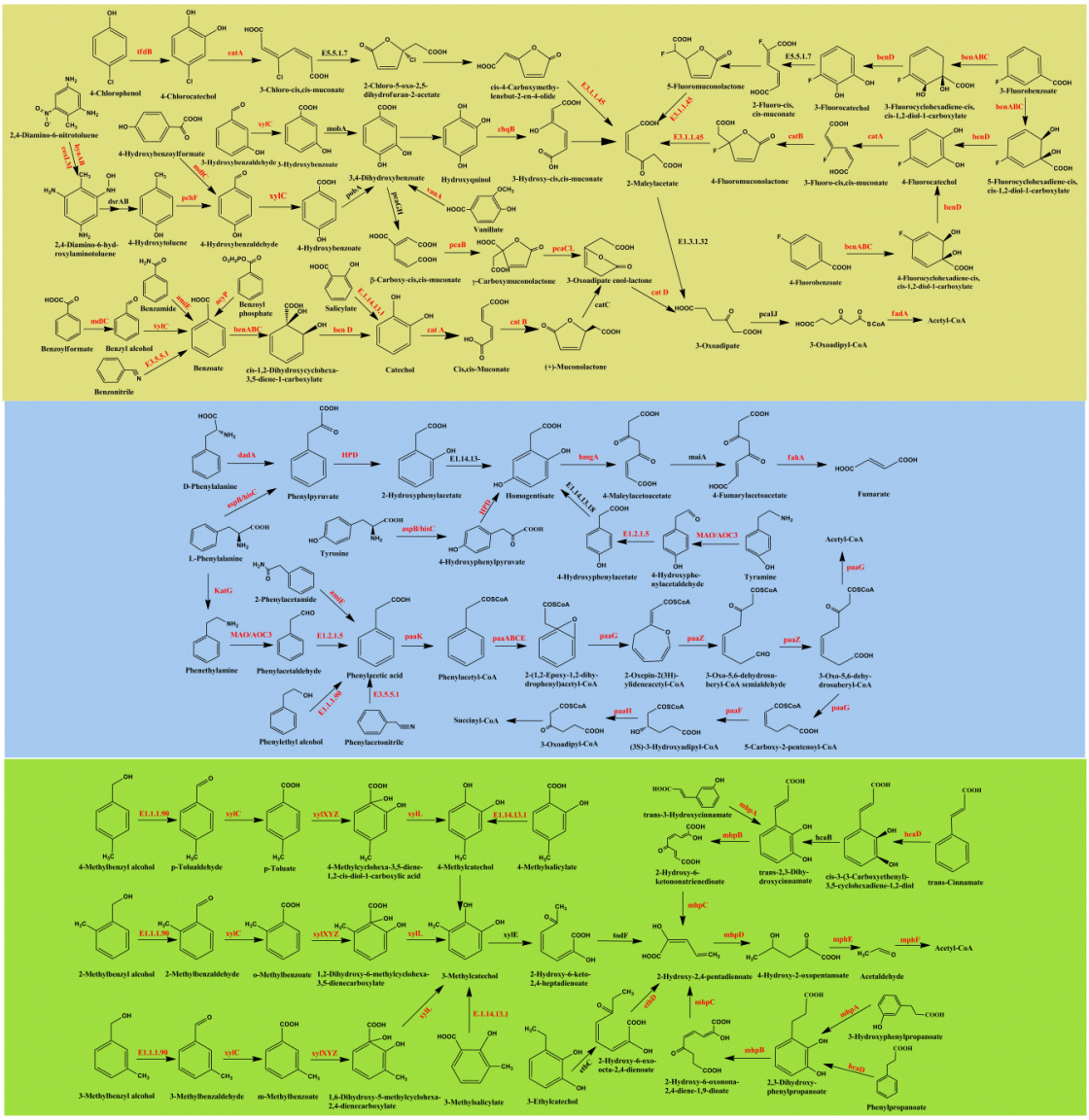

Figure 4-3. The proposed aromatic compound catabolism pathway in *R. opacus* PD630 for lignin derived aromatic compounds degradation. The red labeled genes were detected by proteomics analysis; the black labeled genes were presented in genome sequence while undetected by proteomics.

Secondly, the proteomics analysis suggested that *R. opacus* PD630 has broad aromatic compound degradation pathways to catabolize the lignin derived aromatic compounds. After depolymerization, the lignin will be degraded into mononuclear aromatic compounds or small molecular aromatic oligomers which could be transported into cell to be catabolized for growth energy. From the proteomics analysis of *R. opacus* PD630, several key enzymes were found to be involving the aromatic compounds degrading peripheral (upper) pathways and aromatic ring-cleavage central (lower) pathways were overexpressed in lignin condition.

Lignin is a complex of aromatic heteropolymer and thus the lignin depolymerization releases majority of aromatic compounds in different structures. According to proteomics and pathway reconstruction based on KEGG pathway database, it was found that *R. opacus* PD630 expressed various genes involving the aromatic compounds degrading peripheral (upper) pathways to convert broad aromatic compounds into several major compounds (Figure 4-2, 4-3). For example, nitrilase [E3.5.5.1] (OPAG_01914, OPAG_07408), xylC (OPAG_01252), amiE (OPAG_01575, OPAG_02742, OPAG_02996, OPAG_03179, OPAG_05074, OPAG_05770, OPAG_06458 and OPAG_07376), and acyP (OPAG_03528) could convert the benzonitrile, benzyl alcohol, benzamide and benzoyl phosphate into benzoate, respectively. amiE, nitrilase [E3.5.5.1], aryl-alcohol dehydrogenase [E1.1.1.90] (OPAG_01310 and OPAG_01864) and aldehyde dehydrogenase (NAD(P)+) [E1.2.1.5] (OPAG_00281) could convert 2-phenylacetamide, phenylacetonitrile, phenylethyl alcohol and phenylacetaldehyde into phenylacetic acid, respectively.

For aromatic ring-cleavage central (lower) pathways, three central aromatic catabolism pathways of β-ketoadipate pathway, phenylacetate (Paa) pathway and homogenisate pathways were significantly overexpression in *R. opacus* PD630 grown on lignin. The proteins involving the whole metabolism process from phenylacetic acid to acetyl-CoA in the phenylacetate (Paa) pathway were specifically overexpressed in the log phase grown on lignin, including the proteins of paaK (OPAG_01372), paaE (OPAG_01373), paaC (OPAG_01375), paaA (OPAG_01377), paaG (OPAG_01378, OPAG_03513 and OPAG_06886) and paaZ (OPAG_01382) (Figure 4-2, Table 4-2). Meanwhile, catA (OPAG_00937) and catB (OPAG_00935), the key enzymes of β-ketoadipate pathway, were significantly overexpressed in lignin condition (Figure 4-3, Table 4-2). The catA was overexpressed more than 15 folds in the log phase grown on lignin comparing to that grown on glucose. The catA has been well demonstrated for involving the cleavage of the aromatic ring of catechol and catechol derived aromatic compounds. The protein hmgA (OPAG_00871) of homogentisate 1,2-dioxygenase which cleaves the aromatic ring of homogenisate was also overexpreesed in lignin condition by over 10 folds. These proteomics results suggested that phenylacetic acid, catechol and homogenisate may be the three major central intermediates for lignin derived aromatic compounds catabolism in *R. opacus* PD630. Moreover, the enzymes involving in 3-hydroxyphenylacetate degradation pathway, including mhpA (OPAG_00403, OPAG_07925 and OPAG_07938), mhpB (OPAG_06578), mhpC (OPAG_09209) and mhpD (OPAG_06603) were also detected from the proteomics,

which suggested that these enzymes may also involving the aromatic ring-cleavage of the lignin derived aromatic compounds.

Recently study also found that the growth of *R. opacus* PD630 was increased by 10^6 fold (indicated by CFU) when grown on the lignin-derived compounds used as the sole carbon source compared to the cells grown on untreated kraft lignin, and the highest lipid yield could achieve to over 1 g/L. These results clearly indicated that *R. opacus* PD630 has strong capacity to catabolize the lignin-derived aromatic compounds, and β-ketoadipate pathway and Paa pathway may be the main pathways for central aromatic catabolism.

Table 4-2. The abundance of the protein related to aromatic compounds catabolism in *R. opacus* PD630 under different conditions.

Gene ID	Encoded protein	Protein relative abundance*					
		G1	G2	G3	L1	L2	L3
OPAG_00073	paaF	4	1.67	3.33	14.33	5	9
OPAG_00281	E1.2.1.5	1	1	1.67	2	2.33	1
OPAG_00336	E3.1.1.45	3	1	1	1	1	1
OPAG_00352	kynU	3.67	1	1	1	1	1
OPAG_00353	TDO2	5	1	1	1	1	1
OPAG_00365	hcaD	1	1	1.67	1	1	2.33
OPAG_00403	mhpA	1	1	1.67	2	1	1
OPAG_00416	nagL	1	1	1.67	1	1	1
OPAG_00417	FAHD1	1	1	1	1	1.67	1
OPAG_00426	chnB	2	1	2	1	3.33	1
OPAG_00546	gabD	12	4	2.33	7.33	4.33	1
OPAG_00569	MAO	1	1.67	1	1	1	1
OPAG_00652	hpaI	1	1	1	1	1	1.67
OPAG_00675	paaH	26	6.67	15.33	15.33	10.33	1.67
OPAG_00691	E6.3.4.6	1	1	1.67	1.67	1.67	1
OPAG_00692	atzF	1	1	1	1.67	1	1

Table 4-2. Continued

Gene ID	Encoded protein	Protein relative abundance*					
		G1	G2	G3	L1	L2	L3
OPAG_00708	adhP	1	1	1	1	1	2
OPAG_00710	dadA	17.67	1	1	15	7.67	1
OPAG_00829	E3.1.1.45	13.67	1.67	1.67	1	1.67	1
OPAG_00845	paaF	2	1	2	1	1	1
OPAG_00854	fadA/fadI	1.67	1	2.67	1.67	1	1
OPAG_00864	gcdH	6	4	8	2	3	1
OPAG_00869	fahA	4.33	1.67	2	17	4	2.67
OPAG_00871	hmgA	1.67	1	1	10.33	12	2.67
OPAG_00936	catB	1	1	1.67	2.33	4.33	4.67
OPAG_00937	catA	1	2	5.33	15.67	6	1
OPAG_00941	E3.1.2.23	1.67	2	4	2	1.67	1
OPAG_00945	hpaB	1.67	2	1	6	7	4
OPAG_00949	benA-xylX	1	5	8.67	1	1	1
OPAG_00950	benB-xylY	1	2	7.67	1	1	1
OPAG_00951	benC-xylZ	1	1.67	4.67	1	1	1
OPAG_00952	benD-xylL	1	1.67	2	1	1	1
OPAG_00976	frmA	1	10	10.33	1	1	1
OPAG_01080	chnB	1	1	1	1	2	1
OPAG_01085	frmA	4.67	5	5	14	11	1.67
OPAG_01086	E1.2.1.3	1	1	1	1	1.67	10.33
OPAG_01090	hipO	1	2.33	1	1	1	1
OPAG_01103	hpaB	1	1	1.67	6	7	4
OPAG_01104	catA	1	1	2	1	1	1
OPAG_01124	hcaD	1	2.33	2.67	1	1.67	1.67
OPAG_01196	AOC3	1	1	1.67	2.67	1	1.67
OPAG_01217	badH	1	1	1	2.67	1	1.67
OPAG_01224	atoD	1	1	1.67	1	1	1
OPAG_01250	mdlC	1	1	2.33	1	1	1
OPAG_01252	xylC	1	1	1	1	1.67	1.67
OPAG_01291	badH	1.67	1.67	1	1	1	1
OPAG_01303	aliA	1	1	1.67	1.67	1	2
OPAG_01309	hcaD	1	1	1.67	1	1	1
OPAG_01310	E1.1.1.90	1	1	1	1.67	1	1
OPAG_01349	frmA	1	1	1.67	1	1	1
OPAG_01352	AOC3	1	3.33	2.67	5	6	1
OPAG_01372	paaK	1	1	1	25	18.33	4.33
OPAG_01373	paaE	1	1	1	14.67	4	1

Table 4-2. Continued

Gene ID	Encoded protein	Protein relative abundance*					
		G1	G2	G3	L1	L2	L3
OPAG_01375	paaC	1.67	1	1.67	18.67	4	1
OPAG_01376	paaB	1	1	1	1.67	1	1
OPAG_01377	paaA	1	1	1	8	4.33	1.67
OPAG_01378	paaG	2.67	12.67	9.33	28.33	13	14
OPAG_01379	paaH	1	1	1	13	2.33	1
OPAG_01382	paaZ	10.67	1.67	2.33	105.33	59	48
OPAG_01431	nemA	1	1	1.67	1	1	1
OPAG_01575	amiE	1	1	1.67	1.67	1	1
OPAG_01615	DCAA	1	1	3	4	1	2.33
OPAG_01630	hpaE/hpcC	1	1	1	1	1	1.67
OPAG_01676	pcaC	1	2	1	1	1	1
OPAG_01717	E1.2.1.3	1	1	1	2.33	1.67	2
OPAG_01741	frmA	1.67	1	1	1.67	1.67	1.67
OPAG_01809	E1.2.1.3	1	1	1.67	1	1	1
OPAG_01861	pchF	1	1.67	1	1.67	1	1
OPAG_01864	E1.1.1.90	1	1	1	1	2	1
OPAG_01867	ligK	1	1	1	1.67	1	1
OPAG_01868	aspB	1	1	1	1.67	1	1
OPAG_01914	E3.5.5.1	3	1	1	1	1	1
OPAG_01949	E1.2.1.3	1	4	1.67	1	1	1.67
OPAG_01958	hpaI	1	1	1	1.67	1	1.67
OPAG_01965	aldH	1	1.67	1	1	1	1.67
OPAG_02036	adhP	1	1	1	1	1	2.67
OPAG_02067	katE	1	1	1	2	1	1.67
OPAG_02097	chnB	1	1.67	1	2	1	1
OPAG_02152	gnl	1	3.33	1	1	1	1.67
OPAG_02203	aldH	2.67	1.67	2.67	3	1	1
OPAG_02207	gabD	3.33	1	1.67	1.67	1.67	1
OPAG_02217	hpaI	1	1	1	1	1	1.67
OPAG_02267	katG	333.67	36	58.67	51	31.33	4.33
OPAG_02310	coxL	1.67	1	1.67	1	1	2.33
OPAG_02312	coxM	1	1	1	1.67	1	1
OPAG_02510	paaF	3.67	6.33	9.67	3	1	1
OPAG_02568	coxL	3	2.33	3	2.33	3.33	2.33
OPAG_02569	coxM	1	1.67	1	1	1	1
OPAG_02636	pcaC	1.67	1	1	1	1	1
OPAG_02742	amiE	1	1.67	1	1	1	1

Table 4-2. Continued

Gene ID	Encoded protein	Protein relative abundance*					
		G1	G2	G3	L1	L2	L3
OPAG_02784	adhP	1	1	2	1	1	1
OPAG_02861	CYP125A1	1	1.67	1	1	1	4
OPAG_02879	E1.2.1.3	1	1	1.67	1.67	1	2.33
OPAG_02882	pcaC	1	1.67	1	1	1	1
OPAG_02890	paaF	3	1	1.67	1	1	1
OPAG_02961	hyaA	1	1	2.33	1.67	1	1
OPAG_02969	fadD3	1	1	1	2.67	1	1
OPAG_02970	paaF	1.67	1	1.67	1	1	1
OPAG_02976	CYP142A1	1.67	1	1	1	1	1
OPAG_02996	amiE	17.67	4.33	4.67	4	1.67	2
OPAG_03015	E1.2.1.3	1.67	1	1	2	2	1
OPAG_03041	adh	4.67	1	1	3.33	2.67	1
OPAG_03045	gabD	8.33	1.67	1.67	5	3	1.67
OPAG_03047	hsaC	1	1	1	1.67	1	1
OPAG_03048	hsaD	1	1	1	1.67	1	1
OPAG_03053	mhpE	1	1	1	1.67	1	2
OPAG_03054	mhpF	1	1	1	1	1	1.67
OPAG_03056	kstD	1	1.67	1	1	1	1
OPAG_03179	amiE	1	1	1	1.67	1	1
OPAG_03181	hprT	50.33	14.33	9.67	2.67	1	1
OPAG_03187	paaF	66	3	6	4	1	1
OPAG_03211	E1.2.1.3	1	1.67	1	1	1.67	1
OPAG_03212	hcaD	1	1	2	1	1	1
OPAG_03247	cdd	1	1	1.67	1	1	1
OPAG_03248	deoA	10.67	2.67	7.33	1.67	1.67	1
OPAG_03279	E1.2.1.3	13.33	3	3	7	5	17
OPAG_03454	paaF	29.67	11	13.67	8.33	1	2
OPAG_03513	paaG	23.67	3	6	4.33	1	1
OPAG_03528	acyP	2.67	1	1	1	1	1
OPAG_03683	adh	7.67	5.33	7.33	1.67	1	1
OPAG_03805	fadA/fadI	21	3.67	8.33	11	6.67	1.67
OPAG_03859	atzF	1.67	1	1	1.67	2.33	1
OPAG_03970	paaF	1.67	1	2	7.33	5	9
OPAG_03976	E1.2.1.3	1	2	1	1	1.67	2.67
OPAG_03985	paaH	1	1	1	1	2	1
OPAG_04336	ureA	1	3.33	2.33	1	1	1
OPAG_04337	ureB	2.67	1	1	1	1	1

Table 4-2. Continued

Gene ID	Encoded protein	Protein relative abundance*					
		G1	G2	G3	L1	L2	L3
OPAG_04338	ureC	11.67	5.67	4.67	2.33	1	1.67
OPAG_04368	tesI	3.67	1	2.33	1.67	1.67	1
OPAG_04511	katE	4	12.67	15.33	25.67	20	2.33
OPAG_04615	katE	4.33	2.67	4	1	1	1
OPAG_04690	chnB	1	1	2.33	1	1	1
OPAG_04734	hcaD	7	5.33	6	1	1	1
OPAG_04740	kshB	1	3.33	3.33	1	1	1
OPAG_04741	mdo	4.33	5.67	4	198.67	218.33	21.67
OPAG_04797	E1.2.1.3	1	1	1	2.33	2.33	1
OPAG_04895	guaB	209	18.67	28.67	22.33	19.33	3
OPAG_04896	guaB	61.67	14.67	15.33	18.67	21.33	3
OPAG_04897	choD	5.33	2	2	1.67	1	1.67
OPAG_04898	guaA	45.33	15.33	20.33	7.67	4.67	2.33
OPAG_04962	pcaB	1	1	1	1	1	1.67
OPAG_04985	E1.2.1.3	1	1	1	1.67	1	1
OPAG_05038	paaH	3.33	1.67	1	1	1	1
OPAG_05074	amiE	1.67	1	1	1	3	1
OPAG_05101	katE	1	1	1	3.33	1	1
OPAG_05130	E1.14.13.40	1	1	1.67	1	1	1
OPAG_05184	DCAA	1	1	1.67	1	1	1
OPAG_05261	fadN	1	2	1	1	1	1
OPAG_05292	gabD	65.67	5.67	6.67	2.33	1	1
OPAG_05294	fadA/fadI	1	1.67	1	1	3	1
OPAG_05338	katE	1	1	1	1.67	1.67	1
OPAG_05363	E1.2.1.3	1	2.33	2	1	1	1
OPAG_05416	gabD	1	1	1.67	1.67	1	1
OPAG_05631	HPD	10.67	3.33	7.67	3.33	2	1
OPAG_05665	pcaL	1	1	1	2.67	2.33	1.67
OPAG_05666	pcaB	2	1	1.67	1.67	1.67	2.67
OPAG_05751	hisC	1	1	2.33	1	1	1
OPAG_05770	amiE	3	2.33	1.67	1	1	1.67
OPAG_05804	adhC	1.67	1	1	1	1	1
OPAG_05826	hisC	1	1	2.33	1	1	1
OPAG_05982	hisC	39.67	6.33	11.67	2.67	2	1
OPAG_06121	katE	1	1.67	1	8.33	8.67	1
OPAG_06159	paaF	1	1.67	1	1	1	1
OPAG_06217	paaF	1	1	1.67	1	1	1

Table 4-2. Continued

Gene ID	Encoded protein	Protein relative abundance*					
		G1	G2	G3	L1	L2	L3
OPAG_06220	fadJ	1.67	1	1	1	1	1.67
OPAG_06266	vanA	12.33	2.33	2.67	8.67	5.67	1
OPAG_06305	E3.1.1.45	1	1	1	1.67	4.67	1
OPAG_06339	hisC	3.67	1	1.67	1	1	1
OPAG_06340	paaF	18.67	7	7.33	3	4	1
OPAG_06458	amiE	2.67	1	1	1	1	1
OPAG_06488	E1.14.13.1	1.67	1	1	1	1	1
OPAG_06496	E1.2.1.3	1	1	1	1	1.67	1
OPAG_06519	fadA/fadI	14.33	3.67	3.67	8	6.33	2
OPAG_06526	gabD	2	1	1.67	5.67	1.67	1
OPAG_06577	aldH	1	1	1	1	1	2.67
OPAG_06578	mhpB	1	1	1.67	1	1	1
OPAG_06580	etbD	1	1	1	1.67	1	1
OPAG_06600	tfdB	1.67	1	1.67	1.67	1.67	1
OPAG_06603	mhpD	1.67	1	1	1	1.67	1
OPAG_06605	mhpE	1.67	1.67	1	1	1	1
OPAG_06629	chqB	1	1	1	1.67	1	1
OPAG_06657	fadA/fadI	1.67	1	1	2	1	1
OPAG_06750	E1.2.1.3	1	1	1	1	1.67	1
OPAG_06886	paaG	1	1	1.67	1	1	1
OPAG_06955	frmA	1	1	1	1	3	1
OPAG_07042	adh	1.67	1	2.33	1	1	1
OPAG_07067	E3.8.1.2	1	1	1.67	1	1	1
OPAG_07311	guaB	17	11	15	11	6	3.33
OPAG_07369	coxL	1	1	4.67	1	2	1
OPAG_07376	amiE	1	4.67	1.67	2.67	1.67	1
OPAG_07408	E3.5.5.1	1	1	1	3.67	2.67	1
OPAG_07409	E1.13.12.3	2.33	2	3	25.67	18.33	1
OPAG_07477	nagL	2.67	3	2.33	1	1	1
OPAG_07604	E3.1.1.45	8.67	4.33	1.67	1	1	1
OPAG_07804	fadA/fadI	1	1	1	1.67	1	1
OPAG_07826	phoD	1	1	1	1	1	1.67
OPAG_07840	gabD	58.33	10	15.33	16	13	6
OPAG_07868	AOC3	2	1	2.33	2	5	1
OPAG_07912	aldH	1	1	2	4.67	1	1
OPAG_07925	mhpA	1	2	1	1	1	1
OPAG_07938	mhpA	1	1	1	1	1	2.33

Table 4-2. Continued

Gene ID	Encoded protein	Protein relative abundance*					
		G1	G2	G3	L1	L2	L3
OPAG_07997	ligJ	1	2	1	1	1	1
OPAG_08008	hpaB	2.33	1	1	1.67	1	1
OPAG_08018	choD	1	22.67	18.33	1	1	1
OPAG_08214	gabD	13	1	2	16.67	8	1.67
OPAG_08218	gabD	1	1	1.67	3	1.67	1
OPAG_09046	HPD	1	1.67	1	21.33	26	3.33
OPAG_09075	HPD	1	1	1	1.67	2.33	2.33
OPAG_09087	paaF	11.67	1	1	1	1	1
OPAG_09096	gabD	16.33	1.67	3	19	9.33	1.67
OPAG_09141	paaH	29	8.67	6.33	11.67	6.33	3.33
OPAG_09152	hyaB	2.33	1	1	2	1	1
OPAG_09153	hyaB	1	1	1	1	1	2.33
OPAG_09173	gcdH	1	1	1	1	1	2
OPAG_09209	mhpC	1	1	2.33	1	1	1
OPAG_09229	gabD	1	1	1	1	1	3.33

*The protein relative abundance was generated by the program PatternLab with the ACFold method.

4.3.2. System biology guided design for extracellular lignin depolymerization

Based on aforementioned proteomics and growth analysis, it suggested that aromatic compound catabolism capacity should not be a limiting factor for lignin bioconversion into lipid by *R. opacus* PD630, while lignin depolymerization capacity may be the major hinder factor for efficient lignin conversion. Therefore, engineering a secretive ligninase system for efficiently depolymerizing lignin in *R. opacus* PD630 is required for lignin conversion to biofuels or valuable chemical compounds by microbe.[125, 126] To this end, laccase was chosen as the target ligninase for engineering in *R. opacus* PD630, as it has been discovered in our previous study that laccase-mediator system could synergy with bacteria cell for efficient lignin depolymerization to release aromatic compounds for microbial utilization. Considering that lignin depolymerization will need high level of enzyme produced by microbe which will require the carbon flux to protein product, a small laccase with high activity to broad substrates from *S. coelicolor* was selected to reduce the carbon consume for laccase production.[127, 128]

Even though heterologous expression of laccase has been studies for many years, few platforms could reach a really high extracellular laccase production due to the lack of well-established secretion system and the "toxicity property" of laccase to the cell. To reach the goal of producing high level of extracellular laccase for lignin depolymerization, *R. opacus* PD630 was engineered for laccase secretive expression system based on systemic design through optimizing the following four aspects: transcription/translation, signal peptide efficiency, membrane protein transporter capacity and cultivation condition (Figure 4-4).

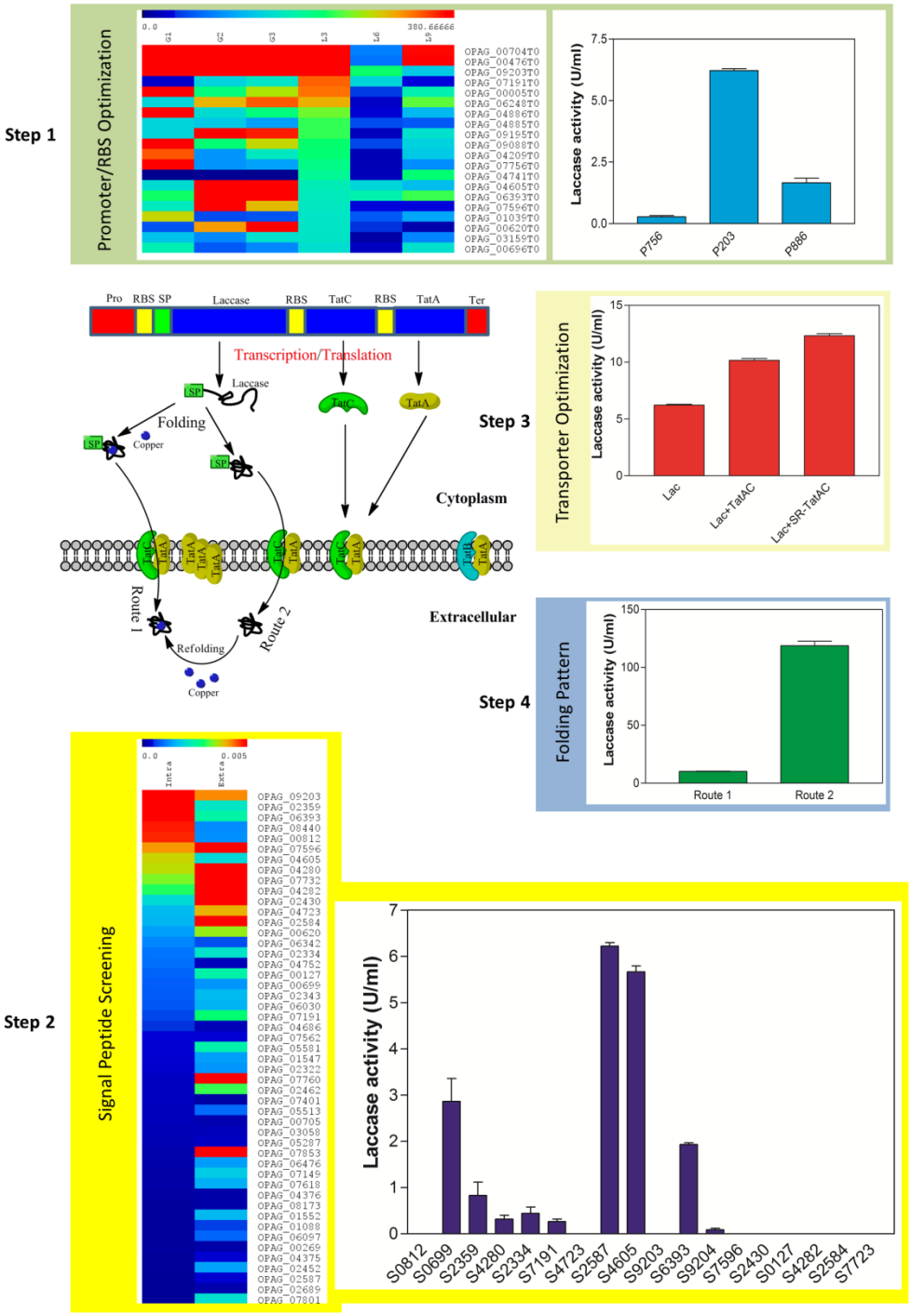

Figure 4-4. The biodesign for efficient laccase secretive expression in *R. opacus* PD630.

In step 1, the promoter/ribosomal binding site (RBS) were screened from the expression of laccase in *R. opacus* PD630 (Figure 4-4). The three promoters/RBSs tested here were chosen from three constitutively expressed proteins which represent three different expression levels in *R. opacus* PD630 based on our proteomics analysis. Under these promoters/RBSs, the laccase could be constantly expressed to display extracellular laccase activity which was needed to continually depolymerize the lignin to release carbon resource for microbe. At the meantime, it is noted that the laccase expression pattern under these promoters/RBSs was consistent to their native protein expression pattern, among which the promoter/RBS P203 from one of the most abundant protein OPAG_09203 also led to the highest extracellular laccase activity (Figure 4-4).

In step 2, the signal peptide for efficient laccase secretion was optimized. The small laccase from *S. coelicolor* used in this study is natively secreted by twin-arginine translocation (Tat) system, which normally transport folded protein and is thought to be the major protein transportation system in many gram-positive bacterial.[129, 130] Considering its easy self-folding property in the bacterial cytoplasm, the Tat system was chose as the target secretion system for laccase extracellular expression. I first screened 18 different predicted Tat system signal peptides from the highly secreted proteins based on our secretomics, among which the signal peptide of S2587 could lead to the most efficient laccase secretion (Figure 4-4). However, it seems that there was no correction of Tat system signal peptides efficiency in secreting laccase and its native protein. For example, many of the selected signal peptide could efficiently guide the transportation of their native proteins, while could not work on the laccase (Figure 4-4).

Heterologous expression of secretive laccase in high levels may lead to overloading of the protein membrane transporters, which will result in low efficiency of laccase secretion. What's more, the inefficient transportation of laccase from cytoplasm to extracellular will also cause the degradation of laccase unsecreted timely, which will in turn result in microbial energy and carbon source wastage. Therefore, the transportation capacity of the Tat system in *R. opacus* PD630 was optimized in step 3 by overexpression the key components of Tat system, TatA and TatC (Figure 4-4) [130]. The genes of *TatA* and *TatC* were integrated with laccase into the same operon (Figure 4-4). The overexpression of TatAC with their native RBSs could increase the extracellular laccase activity by over 60% compared to that without overexpression of TatAC grown in glucose (Figure 4-4). Besides this, the transportation capacity of Tat system was further increased by overexpressed TatA and TatC with two much stronger RBSs, R704 (the RBS from gene OPAG_00704) and R756 (the RBS from gene OPAG_07756) respectively, which resulted in further two folds increase of extracellular laccase activity (20 U/mL) compared to that overexpression of TatAC with their native RBS (Figure 4-4). Although the overexpression of TatA and TatC with strong RBSs could reach much higher extracellular laccase activity, it also extended the lag phase of engineered strain. Therefore, the strain engineered by TatAC with their native RBSs, which significantly increase laccase secretion and had no detectable effect on bacterial growth, was chosen for further lignin conversion experiments.

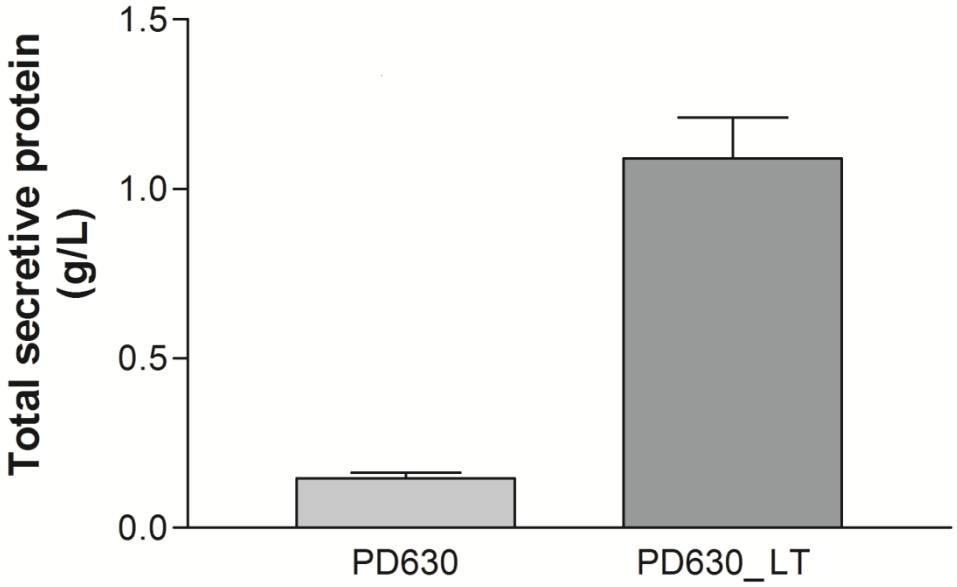

Figure 4-5. The comparison of the total secreted extracellular proteins of wild type and engineered *R. opacus* PD630 grown on 1% glucose after 4 days. PD630: the wild type of *R. opacus* PD630; PD630_LT: the *R. opacus* PD630 engineered with optimized laccase secretive expression system.

Considering the high activity of this small laccase to broad substrates, high level heterologous expression of the laccase in *R. opacus* PD630 may cause toxicity response to the cell which will decrease the laccase production. During the culture process, the laccase producing capacity of the engineered strain was much lower after several batches of cultivation grown in glucose. To overcome this barrier, the laccase was firstly produced in apoprotein form by cultivating the engineered strain in non-copper medium in step 4 of system optimization for laccase secretive expression. Without integrating with copper ions, the apoprotein has no any laccase activity and thus it has no toxicity to the cell. In this way, the engineered strain could produce 5-fold higher of extracellular total protein than wild type strain (Figure 4-5). The apoprotein could be refolded to recover its laccase activity by recruiting copper ions to its active sites when incubated with copper (Figure 4-4). This cultivation method could make the strain to be very stable on its laccase production capacity even after several batches of cultivation. More importantly, this method could also make the extracellular laccase activity reach to 120 U/mL after 4-days-grown in glucose, which is 7-fold higher than that directly cultured in the medium with copper (Figure 4-4). The carbon and nitrogen condition were further optimized for investing the secretive protein expression capacity of the engineered strain. The results showed that the engineered strain could secrete over 15 g/L total protein into culture medium when grown on 6% glucose for 7 days (Figure 4-6). This optimized secretive laccase heterologous expression system also made a breakthrough for microbial laccase heterologous expression.

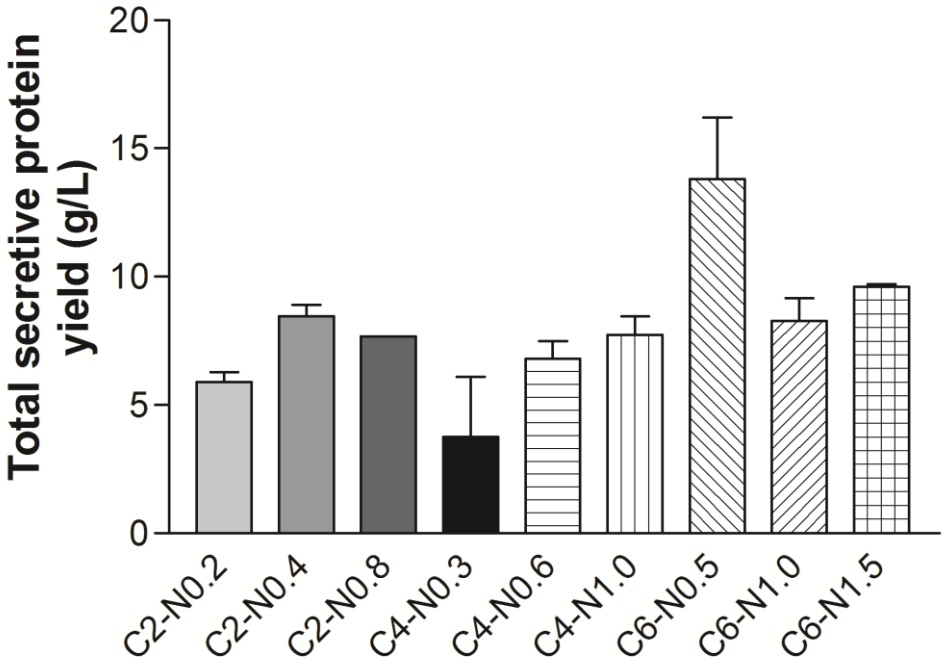

Figure 4-6. The total secretive protein yield of the engineered *R. opacus* PD630 with secretive expression system under different carbon and nitrogen condition after 7 days. C2-N0.2: 2% glucose and 0.2% $(NH_4)_2SO_4$.

4.3.3. Optimization of fatty acid biosynthesis pathway for high yield of lipid

Most of the aromatic compounds released from lignin after depolymerization will be metabolized to acetyl-CoA, which could either be used as substrates for citrate cycle pathway or fatty acid synthesis pathway. To increase the efficiency of lipid production from lignin, the TAG synthesis pathway to drive more carbon flux into fatty acid synthesis pathway was optimized. Based on the comparative proteomics analysis, it was found that two of the proteins, FASI (fatty acid synthase I) and atf2 which showed bifunctional wax ester synthase/acyl-CoA:diacylglycerol acyltransferase (WS/DGAT) activity, were significantly overexpression under high lipid production condition (Figure 4-7). Fatty acid synthase I in *R. opacus* PD630 is a highly integrated multienzyme, which contains seven functional domains, could catalyze all the fatty acid synthesis initiation and elongation reactions by coordinating with phosphopantotheinyl transferase (PTT) which was expressed in the same operon with *fasI*.[123, 131, 132] WS/DGAT encoded by *atf2* catalyzes the final step in biosynthesis of TAG which is the main storage form of lipid.

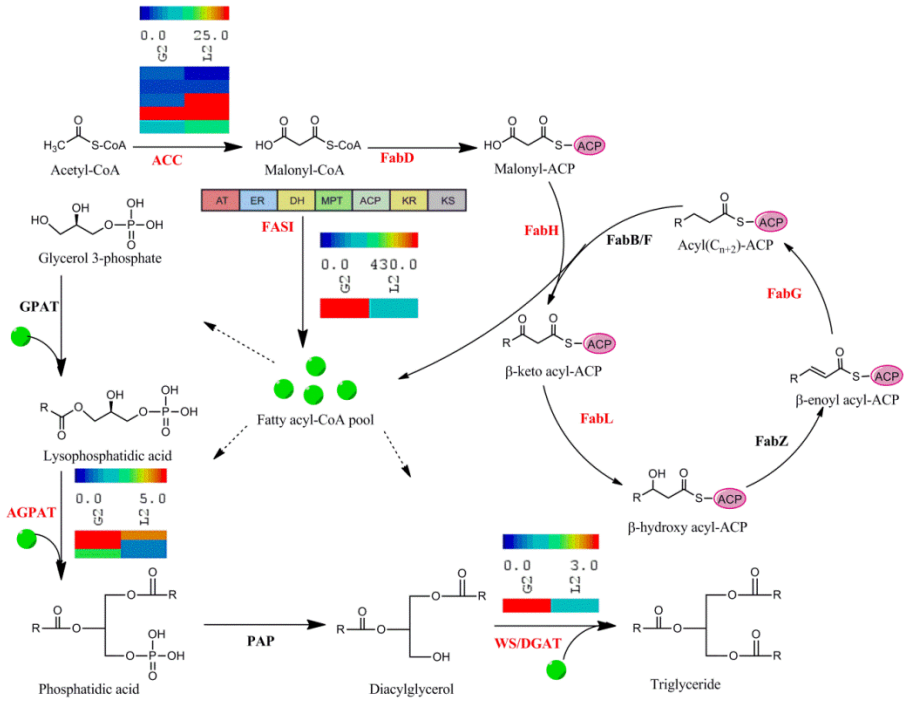

Figure 4-7. The comparison of protein expression in triacylglycerol biosynthesis pathway of *R. opacus* PD630 grown on 1% glucose and lignin. G2, L2 represent the protein expression in stationary phase grown on 1% glucose and 1% lignin, respectively. Each row of the heatmap represents one protein; each column of the heatmap represents one condition. The number in the heatmap represents the normalized spectral count of the detected protein. ACC, acetyl-CoA carboxylase; FabD, [acyl-carrier-protein] S-malonyltransferase; FabH, β-ketoacyl-[acyl-carrier-protein] synthase III; FabL, enoyl-[acyl-carrier-protein] reductases; FabZ, 3-hydroxyacyl-[acyl-carrier-protein] dehydratase; FabG, 3-oxoacyl-[acyl-carrier protein] reductase; FabB, 3-oxoacyl-[acyl-carrier-protein] synthase I; FabF, 3-oxoacyl-[acyl-carrier-protein] synthase II; FASI, fatty acid biosynthase I; GPAT, glycerol-3-phosphate acyltransferase; AGPAT, 1-acyl-sn-glycerol-3-phosphate acyltransferase; PAP, phosphatidate phosphatase; WS/DGAT, wax ester synthase/ acyl-CoA:diacylglycerol acyltransferase. The red highlighted protein name indicated that the proteins were detected on the condition; the protein name in black indicated that the protein were undetected on the condition.

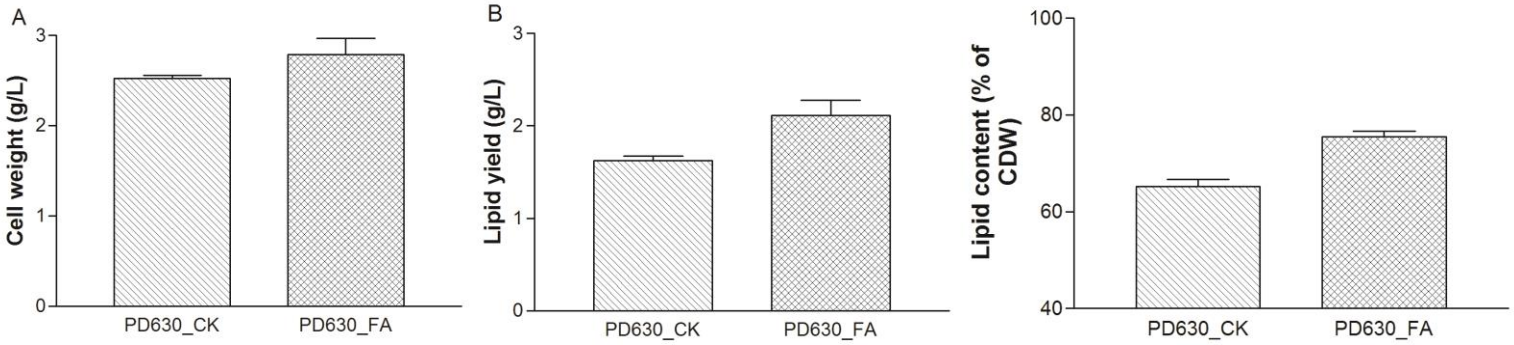

Figure 4-8. The cell growth (A), lipid yield (B) and lipid content (C) of R. opacus PD630 engineered with TAG biosynthesis module grown on 2% glucose after 4 days. PD630_CK: R. opacus PD630 transformed with empty plasmid as control; PD630_FA: R. opacus PD630 transformed with fasI operon and atf2.

Based on these analyses, it appears that overexpression of *fasI* operon and *atf2* would drive more carbon flux into lipid biosynthesis by recruiting more acetyl-CoA into fatty acid synthesis pathway instead of citrate cycle. We approved this hypothesis by overexpression both *fasI* operon and *atf2* in *R. opacus* PD630 (PD630_FA) with a benzoate-inducible promoter from *R. sp.* RHA1 as described by previous publication [133]. The engineered strain PD630_FA was first evaluated for its lipid production ability from glucose which could also be catabolized into acetyl-CoA for both citrate cycle and fatty acid synthesis pathway. PD630_FA performed significantly better in lipid accumulation from glucose compared to the wild type strain under test conditions (Figure 4-8). For example, PD630_FA made a total lipid yield to 2.916 g/L and lipid content to 54.76% after 4-days cultivation in glucose, while wild type strain only reached 0.915 g/L and 21.03%, respectively. However, it did not significantly change the cell biomass yield (Figure 4-8).

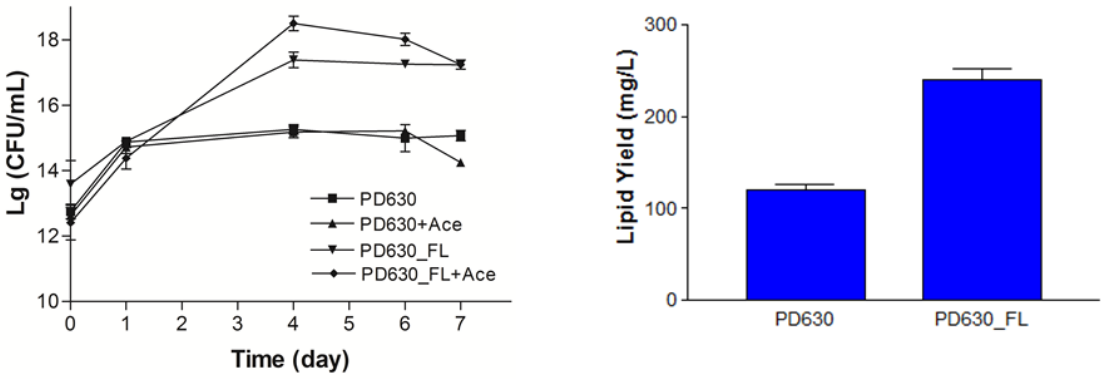

Figure 4-9. The growth curve and lipid yield of *R. opacus* PD630 integrated with both lignin depolymerization module and TAG biosynthesis module growth on 1% kraft lignin. PD630: *R. opacus* PD630 transformed with empty plasmid as control; PD630_FL: *R. opacus* PD630 transformed with both lignin depolymerization module and TAG biosynthesis module; Ace: acetosyringone.

4.3.4. Consolidated bioprocessing of lignin to lipid

After *R. opacus* PD630 was equipped with the highly laccase secretive system, the performance of this engineered strain (PD630_LT) was evaluated for lignin depolymerized. To make sure PD630_LT could maintain its original laccase production capacity before inoculating for lignin fermentation, the seed culture was prepared by cultivating PD630_LT in 0.5% glucose medium without copper for 4 days after all the glucose was consumed. Considering the laccase present in seed culture could be used for initial lignin depolymerization, the bacterial as well as its culture supernatant into lignin medium was inoculated for fermentation. As proven by our previous study, the presence of the right mediator could significantly improve the efficiency of lignin depolymerization by laccase. Here, acetosyringone was chosen as the redox mediator for the small laccase. After 7-days fermentation in kraft lignin medium, the CFU of PD630_LT was about 1000 folds higher than the control strain, and the total lipid yield could increase by 2 fold (Figure 4-7). All these results clearly highlighted that secreted laccase system could significantly improve lignin depolymerization and lignin conversion efficient in *R. opacus* PD630.

5. CONCLUSIONS AND PERSPECTIVES

The utilization of lignin-containing biorefinery waste stream for fungible bioproducts represents a critical challenge for integrated biorefinery. Inevitably, an effective biorefinery stream derived from the traditional biorefinery waste will increase the cost-effectiveness, carbon and energy efficiency to enable the lignocellulosic biofuel from both economic and sustainability aspects. In this study, the synergy between laccase and *R. opacus* PD630 for lignin depolymerization has demonstrated. The efficiency of lignin depolymerization by laccase could be enhanced by an efficient electron mediator. The Gram positive bacterium like *R. opacus* PD630 was also demonstrated to have high capacity for secretive protein expression. Based on the systems biology guided biodesign, an efficient laccase secretive system has been successfully established in *R. opacus* PD630, which could secrete protein into culture supernatant as high as 15 g/L. The engineered *R. opacus* PD630 by integrating both lignin depolymerization module and lipid biosynthesis module could significantly improve its lignin conversion into lipid.

Overall, several major challenges need to be addressed before such an integrated biorefinery strategy is viable. First, extensive process development and optimization need to be carried out to enhance the bioproduct titer for converting the lignin-containing waste stream. Second, extensive research has been carried out for engineering and screening microorganisms for cellulose and hemicellulose utilization. Similar efforts need to be implemented to derive effective microbes or a microbial consortium to effectively depolymerize and convert lignin to various fungible products. Third, the

utilization of lignin can be an integrated approach, where microbes utilize certain amount of aromatic compounds, leaving the rest to be used as carbon fiber or other materials. Last but not least, in order to build an integrated biorefinery schema, pretreatment needs to be optimized to both produce high ethanol yield and optimized production of multiple streams of bioproducts. Eventually, technoeconomic and life cycle analysis need to be carried out to evaluate the integrated biorefinery and to take the aforementioned issues into consideration.

REFERENCES

1. Ragauskas, A.J. et al. The path forward for biofuels and biomaterials. *Science* **311**, 484-489 (2006).
2. Yuan, J.S., Tiller, K.H., Al-Ahmad, H., Stewart, N.R. & Stewart, C.N., Jr. Plants to power: bioenergy to fuel the future. *Trends Plant Sci.* **13**, 421-429 (2008).
3. Yuan, J.S., Wang, X. & Stewart, C.N. Biomass feedstock: diversity as a solution. *Biofuels* **2**, 491-493 (2011).
4. Boerjan, W., Ralph, J. & Baucher, M. Lignin biosynthesis. *Annu. Rev. Plant Biol.* **54**, 519-546 (2003).
5. Chakar, F.S. & Ragauskas, A.J. Review of current and future softwood kraft lignin process chemistry. *Ind. Crops Prod.* **20**, 131-141 (2004).
6. Yang, B. & Wyman, C.E. Pretreatment: the key to unlocking low-cost cellulosic ethanol. *Biofuels, Bioprod. Biorefin.* **2**, 26-40 (2008).
7. Yuan, J.S., Galbraith, D.W., Dai, S.Y., Griffin, P. & Stewart, C.N., Jr. Plant systems biology comes of age. *Trends Plant Sci.* **13**, 165-171.
8. Wyman, C.E. What is (and is not) vital to advancing cellulosic ethanol. *Trends Biotechnol.* **25**, 153-157 (2007).
9. Schmer, M.R., Vogel, K.P., Mitchell, R.B. & Perrin, R.K. Net energy of cellulosic ethanol from switchgrass. *Proc. Natl. Acad. Sci. U. S. A.* **105**, 464-469 (2008).

10. Shabtai, J., Zmierczak, W., Chornet, E. & Johnson, D. Process for converting lignins into a high-octane blending component for gasoline. *U.S. Pat. Appl. Publ.* (2003).

11. Oasmaa, A., Alén, R. & Meier, D. Catalytic hydrotreatment of some technical lignins. *Bioresour. Technol.* **45**, 189-194 (1993).

12. Ben, H. & Ragauskas, A.J. Heteronuclear Single-Quantum Correlation–Nuclear Magnetic Resonance (HSQC–NMR) fingerprint analysis of pyrolysis oils. *Energy Fuels* **25**, 5791-5801 (2011).

13. Liu, W.-J., Jiang, H. & Yu, H.-Q. Thermochemical conversion of lignin to functional materials: a review and future directions. *Green Chem.* **17**, 4888-4907 (2015).

14. Shen, D. et al. Thermo-chemical conversion of lignin to aromatic compounds: Effect of lignin source and reaction temperature. *J. Anal. Appl. Pyrol.* **112**, 56-65 (2015).

15. Xu, Z. et al. Comparative genome analysis of lignin biosynthesis gene families across the plant kingdom. *BMC Bioinformatics* **8**, 1471-2105 (2009).

16. Xie, S., Syrenne, R., Sun, S. & Yuan, J.S. Exploration of Natural Biomass Utilization Systems (NBUS) for advanced biofuel-from systems biology to synthetic design. *Curr. Opin. Biotechnol.* **27**, 195-203 (2014).

17. Floudas, D. et al. The paleozoic origin of enzymatic lignin decomposition reconstructed from 31 fungal genomes. *Science* **336**, 1715-1719 (2012).

18. Geib, S.M. et al. Lignin degradation in wood-feeding insects. *Proc. Natl. Acad. Sci. U. S. A.* **105**, 12932-12937 (2008).

19. Bugg, T.D.H., Ahmad, M., Hardiman, E.M. & Singh, R. The emerging role for bacteria in lignin degradation and bio-product formation. *Curr. Opin. Biotechnol.* **22**, 394-400 (2011).

20. Shi, L. et al. Biochemical and molecular characterization of a novel laccase from selective lignin-degrading white-rot fungus *Echinodontium taxodii* 2538. *Process Biochem.* **49**, 1097-1106 (2014).

21. Xie, S. et al. Simultaneous conversion of all cell wall components by an oleaginous fungus without chemi-physical pretreatment. *Green Chem.* **17**, 1657-1667 (2015).

22. Sun, J.-Z. & Scharf, M.E. Exploring and integrating cellulolytic systems of insects to advance biofuel technology. *Insect Sci.* **17**, 163-165 (2010).

23. Ke, J. et al. In-situ oxygen profiling and lignin modification in guts of wood-feeding termites. *Insect Sci.* **17**, 277-290 (2010).

24. Watanabe, H., Noda, H., Tokuda, G. & Lo, N. A cellulase gene of termite origin. *Nature* **394**, 330-331 (1998).

25. Tartar, A. et al. Parallel metatranscriptome analyses of host and symbiont gene expression in the gut of the termite *Reticulitermes flavipes*. *Biotechnol Biofuels* **2**, 25 (2009).

26. Taprab, Y. et al. Symbiotic fungi produce laccases potentially involved in phenol degradation in fungus combs of fungus-growing termites in Thailand. *Appl. Environ. Microbiol.* **71**, 7696-7704 (2005).

27. Fernandez-Fueyo, E. et al. Comparative genomics of *Ceriporiopsis subvermispora* and *Phanerochaete chrysosporium* provide insight into selective ligninolysis. *Proc. Natl. Acad. Sci. U. S. A.* **109**, 5458-5463 (2012).

28. Martinez, D. et al. Genome sequence of the lignocellulose degrading fungus *Phanerochaete chrysosporium* strain RP78. *Nat. Biotechnol.* **22**, 695-700 (2004).

29. Eastwood, D.C. et al. The plant cell wall–decomposing machinery underlies the functional diversity of forest fungi. *Science* **333**, 762-765 (2011).

30. Yu, H.-B., Li, L., Zhang, X.-Y. & Huang, H.-Y. Effects of wood species and enzyme production on lignocellulose degradation during the biodegradation of three native woods by *Trametes versicolor*. *Forest Prod. J.* **58**, 62 (2008).

31. Martinez, A.T., Ruiz-Duenas, F.J., Martinez, M.J., Del Rio, J.C. & Gutierrez, A. Enzymatic delignification of plant cell wall: from nature to mill. *Curr. Opin. Biotechnol* **20**, 348-357 (2009).

32. Levasseur, A. et al. FOLy: an integrated database for the classification and functional annotation of fungal oxidoreductases potentially involved in the degradation of lignin and related aromatic compounds. *Fungal Genet. Biol.* **45**, 638-645 (2008).

33. ten Have, R. & Teunissen, P.J. Oxidative mechanisms involved in lignin degradation by white-rot fungi. *Chem. Rev.* **101**, 3397-3413 (2001).

34. Kersten, P. & Cullen, D. Extracellular oxidative systems of the lignin-degrading Basidiomycete *Phanerochaete chrysosporium*. *Fungal Genet. Biol.* **44**, 77-87 (2007).

35. Martinez, D. et al. Genome, transcriptome, and secretome analysis of wood decay fungus *Postia placenta* supports unique mechanisms of lignocellulose conversion. *Proc. Natl. Acad. Sci. U. S. A.* **106**, 1954-1959 (2009).

36. Hori, C. et al. Genomewide analysis of polysaccharides degrading enzymes in 11 white- and brown-rot Polyporales provides insight into mechanisms of wood decay. *Mycologia* **105**, 1412-1427 (2013).

37. Vanden Wymelenberg, A. et al. Comparative transcriptome and secretome analysis of wood decay fungi *Postia placenta* and *Phanerochaete chrysosporium*. *Appl. Environ. Microbiol.* **76**, 3599-3610 (2010).

38. Ryu, J.S. et al. Proteomic and functional analysis of the cellulase system expressed by *Postia placenta* during brown rot of solid wood. *Appl. Environ. Microbiol.* **77**, 7933-7941 (2011).

39. MacDonald, J. et al. Transcriptomic responses of the softwood-degrading white-rot fungus *Phanerochaete carnosa* during growth on coniferous and deciduous wood. *Appl. Environ. Microbiol.* **77**, 3211-3218 (2011).

40. Peralta-Yahya, P.P., Zhang, F., del Cardayre, S.B. & Keasling, J.D. Microbial engineering for the production of advanced biofuels. *Nature* **488**, 320-328 (2012).

41. Masai, E., Katayama, Y. & Fukuda, M. Genetic and biochemical investigations on bacterial catabolic pathways for lignin-derived aromatic compounds. *Biosci. Biotechnol. Biochem.* **71**, 1-15 (2007).

42. Shi, Y. et al. Characterization and genomic analysis of kraft lignin biodegradation by the beta-proteobacterium *Cupriavidus basilensis* B-8. *Biotechnol. Biofuels* **6**, 1 (2013).

43. Pieper, D.H. Aerobic degradation of polychlorinated biphenyls. *Appl. Microbiol. Biotechnol.* **67**, 170-191 (2005).

44. Ausec, L., Zakrzewski, M., Goesmann, A., Schlüter, A. & Mandic-Mulec, I. Bioinformatic analysis reveals high diversity of bacterial genes for laccase-like enzymes. *PLoS One* **6**, e25724 (2011).

45. Jing, D. & Wang, J. Controlling the simultaneous production of laccase and lignin peroxidase from *Streptomyces cinnamomensis* by medium formulation. *Biotechnol. Biofuels* **5**, 15 (2012).

46. Jing, D. Improving the simultaneous production of laccase and lignin peroxidase from *Streptomyces lavendulae* by medium optimization. *Bioresour. Technol.* **101**, 7592-7597 (2010).

47. McLeod, M.P. et al. The complete genome of *Rhodococcus sp.* RHA1 provides insights into a catabolic powerhouse. *Proc. Natl. Acad. Sci. U. S. A.* **103**, 15582-15587 (2006).

48. Yam, K., Geize, R. & Eltis, L. in Biology of *Rhodococcus*, Vol. 16. (ed. H.M. Alvarez) 133-169 (Springer Berlin Heidelberg, 2010).

49. Davis, J.R., Brown, B.L., Page, R. & Sello, J.K. Study of PcaV from S*treptomyces coelicolor* yields new insights into ligand-responsive MarR family transcription factors. *Nucleic Acids Res.* **41**, 3888-3900 (2013).

50. Iwagami, S.G., Yang, K. & Davies, J. Characterization of the protocatechuic acid catabolic gene cluster from *Streptomyces sp. strain* 2065. *Appl. Environ. Microbiol.* **66**, 1499-1508 (2000).

51. Kosa, M. & Ragauskas, A.J. Lignin to lipid bioconversion by oleaginous *Rhodococci*. *Green Chem.* **15**, 2070-2074 (2013).

52. Zhao, C. et al. Synergistic enzymatic and microbial lignin conversion. *Green Chem.* **18**, 1306-1312 (2016).

53. Linger, J.G. et al. Lignin valorization through integrated biological funneling and chemical catalysis. *Proc. Natl. Acad. Sci. U. S. A.* **111**, 12013-12018 (2014).

54. Vardon, D.R. et al. Adipic acid production from lignin. *Energy Environ. Sci.* **8**, 617-628 (2015).

55. Ahmad, M. et al. Identification of DypB from *Rhodococcus jostii* RHA1 as a lignin peroxidase. *Biochemistry* **50**, 5096-5107 (2011).

56. Kosa, M. & Ragauskas, A. Bioconversion of lignin model compounds with oleaginous *Rhodococci*. *Appl. Microbiol. Biotechnol.* **93**, 891-900 (2012).

57. Munk, L., Sitarz, A.K., Kalyani, D.C., Mikkelsen, J.D. & Meyer, A.S. Can laccases catalyze bond cleavage in lignin? *Biotechnol. Adv.* **33**, 13-24 (2015).

58. Christopher, L.P., Yao, B. & Ji, Y. Lignin biodegradation with laccase-mediator systems. *Front. Energy Res.* **2** (2014).

59. Pandey, M.P. & Kim, C.S. Lignin depolymerization and conversion: a review of thermochemical methods. *Chem. Eng. Technol.* **34**, 29-41 (2011).

60. Wang, H., Tucker, M. & Ji, Y. Recent Development in Chemical Depolymerization of Lignin: A Review. *J. Appl. Chem.* **2013**, 9 (2013).

61. Linger, J.G. et al. Lignin valorization through integrated biological funneling and chemical catalysis. *Proc. Natl. Acad. Sci. U. S. A.* **111**, 12013-12018 (2014).

62. Wei, Z. et al. Bioconversion of oxygen-pretreated Kraft lignin to microbial lipid with oleaginous *Rhodococcus opacus* DSM 1069. *Green Chem.* **17**, 2784-2789 (2015).

63. Chapple, C., Ladisch, M. & Meilan, R. Loosening lignin's grip on biofuel production. *Nat. Biotechnol.* **25**, 746-748 (2007).

64. Li, X. et al. Lignin monomer composition affects *Arabidopsis* cell-wall degradability after liquid hot water pretreatment. *Biotechnol. Biofuels* **3**, 1754-6834 (2010).

65. Chen, H.P. et al. Vanillin catabolism in *Rhodococcus jostii* RHA1. *Appl. Environ. Microbiol.* **78**, 586-588 (2012).

66. Patrauchan, M.A. et al. Roles of ring-hydroxylating dioxygenases in styrene and benzene catabolism in *Rhodococcus jostii* RHA1. *J. Bacteriol.* **190**, 37-47 (2008).

67. Hara, H., Eltis, L.D., Davies, J.E. & Mohn, W.W. Transcriptomic analysis reveals a bifurcated terephthalate degradation pathway in *Rhodococcus sp* strain RHA1. *J. Bacteriol.* **189**, 1641-1647 (2007).

68. Goncalves, E.R. et al. Transcriptomic assessment of isozymes in the biphenyl pathway of *Rhodococcus sp* strain RHA1. *Appl. Environ. Microbiol.* **72**, 6183-6193 (2006).

69. Navarro-Llorens, J.M. et al. Phenylacetate catabolism in *Rhodococcus sp* strain RHA1: a central pathway for degradation of aromatic compounds. *J. Bacteriol.* **187**, 4497-4504 (2005).

70. Patrauchan, M.A. et al. Catabolism of benzoate and phthalate in *Rhodococcus sp* strain RHA1: redundancies and convergence. *J. Bacteriol.* **187**, 4050-4063 (2005).

71. McLeod, M. & Eltis, L. in Microbial Biodegradation: genomics and molecular biology. (ed. Diaz) (Horizon Scientific Press, 2008).

72. Sainsbury, P.D. et al. Breaking down lignin to high-value chemicals: the conversion of lignocellulose to vanillin in a gene deletion mutant of *Rhodococcus jostii* RHA1. *ACS Chem. Biol.* **8**, 2151-2156 (2013).

73. Hara, H., Stewart, G.R. & Mohn, W.W. Involvement of a novel ABC transporter and monoalkyl phthalate ester hydrolase in phthalate ester catabolism by *Rhodococcus jostii* RHA1. *Appl. Environ. Microbiol.* **76**, 1516-1523 (2010).

74. Wang, W., Yang, S., Hunsinger, G.B., Pienkos, P.T. & Johnson, D.K. Connecting lignin-degradation pathway with pre-treatment inhibitor sensitivity of *Cupriavidus necator*. *Front. Microbiol.* **5**, 247 (2014).

75. Kurosawa, K., Laser, J. & Sinskey, A.J. Tolerance and adaptive evolution of triacylglycerol-producing *Rhodococcus opacus* to lignocellulose-derived inhibitors. *Biotechnol. Biofuels* **8**, 015-0258 (2015).

76. Otsuka, Y. et al. Efficient production of 2-pyrone 4, 6-dicarboxylic acid as a novel polymer-based material from protocatechuate by microbial function. *Appl. Microbiol. Biotechnol.* **71**, 608-614 (2006).

77. Yoneda, A. et al. Comparative transcriptomics elucidates adaptive phenol tolerance and utilization in lipid-accumulating *Rhodococcus opacus* PD630. *Nucleic Acids Res.* **44**, 2240-2254 (2016).

78. Fuchs, G., Boll, M. & Heider, J. Microbial degradation of aromatic compounds—from one strategy to four. *Nat. Rev. Microbiol.* **9**, 803-816 (2011).

79. Ragauskas, A.J. et al. Lignin valorization: improving lignin processing in the biorefinery. *Science* **344** (2014).

80. Shi, W., Syrenne, R., Sun, J.-Z. & Yuan, J.S. Molecular approaches to study the insect gut symbiotic microbiota at the 'omics' age. *Insect Sci.* **17**, 199-219 (2010).

81. Shi, W. et al. Comparative genomic analysis of the endosymbionts of herbivorous insects reveals eco-environmental adaptations: biotechnology applications. *PLoS Genet.* **9**, 10 (2013).

82. Wells, T., Wei, Z. & Ragauskas, A. Bioconversion of lignocellulosic pretreatment effluent via oleaginous *Rhodococcus opacus* DSM 1069. *Biomass Bioenergy* **72**, 200-205 (2015).

83. Ralph, J. et al. Lignins: natural polymers from oxidative coupling of 4-hydroxyphenyl- propanoids. *Phytochem. Rev.* **3**, 29-60 (2004).

84. Budini, R., Tonelli, D. & Girotti, S. Analysis of total phenols using the Prussian Blue method. *J. Agric. Food Chem.* **28**, 1236-1238 (1980).

85. Folch, J., Lees, M. & Sloane Stanley, G.H. A simple method for the isolation and purification of total lipides from animal tissues. *J. Biol. Chem.* **226**, 497-509 (1957).

86. Pu, Y., Cao, S. & Ragauskas, A.J. Application of quantitative 31P NMR in biomass lignin and biofuel precursors characterization. *Energy Environ. ScI.* **4**, 3154-3166 (2011).

87. Cao, S., Pu, Y., Studer, M., Wyman, C. & Ragauskas, A.J. Chemical transformations of *Populus trichocarpa* during dilute acid pretreatment. *RSC Adv.* **2**, 10925-10936 (2012).

88. Brune, A. Symbiotic digestion of lignocellulose in termite guts. *Nat. Rev. Micro.* **12**, 168-180 (2014).

89. Ben, H. & Ragauskas, A.J. NMR characterization of pyrolysis oils from kraft lignin. *Energ. Fuel.* **25**, 2322-2332 (2011).

90. Lund, M. & Ragauskas, A. Enzymatic modification of kraft lignin through oxidative coupling with water-soluble phenols. *Appl. Microbiol. Biotechnol.* **55**, 699-703 (2001).

91. Pu, Y., Anderson, S., Lucia, L. & Ragauskas, A.J. Investigation of the photo-oxidative chemistry of acetylated softwood lignin. *J. Photochem. Photobiol., A* **163**, 215-221 (2004).

92. Ghaffar, S.H. & Fan, M. Structural analysis for lignin characteristics in biomass straw. *Biomass Bioenergy* **57**, 264-279 (2013).

93. Babot, E.D. et al. Towards industrially-feasible delignification and pitch removal by treating paper pulp with *Myceliophthora thermophila* laccase and a phenolic mediator. *Bioresour. Technol.* **102**, 6717-6722 (2011).

94. Murugesan, K. et al. Enhanced transformation of triclosan by laccase in the presence of redox mediators. *Water Res.* **44**, 298-308 (2010).

95. Rico, A., Rencoret, J., del Rio, J., Martinez, A. & Gutierrez, A. Pretreatment with laccase and a phenolic mediator degrades lignin and enhances saccharification of Eucalyptus feedstock. *Biotechnol. Biofuels* **7**, 6 (2014).

96. Rodríguez Couto, S. & Toca Herrera, J.L. Industrial and biotechnological applications of laccases: A review. *Biotechnol. Adv.* **24**, 500-513 (2006).

97. Li, K., Xu, F. & Eriksson, K.-E.L. Comparison of fungal laccases and redox mediators in oxidation of a nonphenoliclignin model compound. *Appl. Environ. Microbiol.* **65**, 2654-2660 (1999).

98. Shiraishi, T., Sannami, Y., Kamitakahara, H. & Takano, T. Comparison of a series of laccase mediators in the electro-oxidation reactions of non-phenolic lignin model compounds. *Electrochim. Acta* **106**, 440-446 (2013).

99. Du, X. et al. Understanding pulp delignification by laccase–mediator mystems through isolation and characterization of lignin–carbohydrate complexes. *Biomacromolecules* **14**, 3073-3080 (2013).

100. Raj, A., Chandra, R., Reddy, M.M.K., Purohit, H. & Kapley, A. Biodegradation of kraft lignin by a newly isolated bacterial strain *Aneurinibacillus aneurinilyticus* from the sludge of a pulp paper mill. *World J.Microb. Biot.* **23**, 793-799 (2007).

101. Trajano, H.L. et al. The fate of lignin during hydrothermal pretreatment. *Biotechnol. Biofuels* **6**, 110 (2013).

102. Robert, D. in Methods in lignin chemistry 250-273 (Springer, 1992).

103. Kurosawa, K., Boccazzi, P., de Almeida, N.M. & Sinskey, A.J. High-cell-density batch fermentation of *Rhodococcus opacus* PD630 using a high glucose concentration for triacylglycerol production. *J. Biotechnol.* **147**, 212-218 (2010).

104. Xie, S., Sun, S., Dai, S.Y. & S.Yuan, J. Efficient coagulation of microalgae in cultures with filamentous fungi. *Algal Res.* **2**, 28-33 (2013).

105. Bourbonnais, R. & Paice, M.G. Oxidation of non-phenolic substrates: An expanded role for laccase in lignin biodegradation. *FEBS Lett.* **267**, 99-102 (1990).

106. Eggert, C., Temp, U., Dean, J.F.D. & Eriksson, K.-E.L. A fungal metabolite mediates degradation of non-phenolic lignin structures and synthetic lignin by laccase. *FEBS Lett.* **391**, 144-148 (1996).

107. Bourbonnais, R., Leech, D. & Paice, M.G. Electrochemical analysis of the interactions of laccase mediators with lignin model compounds. *BBA-Gen. Subjects* **1379**, 381-390 (1998).

108. Areskogh, D., Li, J., Gellerstedt, G. & Henriksson, G. Investigation of the molecular weight increase of commercial lignosulfonates by laccase catalysis. *Biomacromolecules* **11**, 904-910 (2010).

109. Constant, S. et al. New insights into the structure and composition of technical lignins: a comparative characterisation study. *Green Chem.* (2016).

110. Wen, J.-L., Sun, S.-L., Xue, B.-L. & Sun, R.-C. Recent advances in characterization of lignin polymer by solution-state nuclear magnetic resonance (NMR) methodology. *Materials* **6**, 359-391 (2013).

111. Reiter, J., Strittmatter, H., Wiemann, L.O., Schieder, D. & Sieber, V. Enzymatic cleavage of lignin [small beta]-O-4 aryl ether bonds via net internal hydrogen transfer. *Green Chem.* **15**, 1373-1381 (2013).

112. Rahimi, A., Ulbrich, A., Coon, J.J. & Stahl, S.S. Formic-acid-induced depolymerization of oxidized lignin to aromatics. *Nature* **515**, 249-252 (2014).

113. Niu, D., Zuo, Z., Shi, G.Y. & Wang, Z.X. High yield recombinant thermostable alpha-amylase production using an improved *Bacillus licheniformis* system. *Microb. Cell Fact.* **8**, 58 (2009).

114. Nakashima, N. & Tamura, T. Isolation and characterization of a rolling-circle-type plasmid from *Rhodococcus erythropolis* and application of the plasmid to

multiple-recombinant-protein expression. *Appl. Environ. Microbiol.* **70**, 5557-5568 (2004).

115. Hong, Y. & Hondalus, M.K. Site-specific integration of *Streptomyces* ΦC31 integrase-based vectors in the chromosome of *Rhodococcus equi*. *FEMS Microbiol. Lett.* **287**, 63-68 (2008).

116. Matsui, T., Saeki, H., Shinzato, N. & Matsuda, H. Characterization of *Rhodococcus-E. coli* shuttle vector pNC9501 constructed from the cryptic plasmid of a propene-degrading bacterium. *Curr. Microbiol.* **52**, 445-448 (2006).

117. Kalscheuer, R., Arenskötter, M. & Steinbüchel, A. Establishment of a gene transfer system for *Rhodococcus opacus* PD630 based on electroporation and its application for recombinant biosynthesis of poly(3-hydroxyalkanoic acids). *Appl. Microbiol. Biotechnol.* **52**, 508-515 (1999).

118. Na, K.-s. et al. Development of a genetic transformation system for benzene-tolerant *Rhodococcus opacus* strains. *J. Biosci. Bioeng.* **99**, 408-414 (2005).

119. Lessard, P.A., O'Brien, X.M., Currie, D.H. & Sinskey, A.J. pB264, a small, mobilizable, temperature sensitive plasmid from *Rhodococcus*. *BMC Microbiol.* **4**, 15 (2004).

120. Chourey, K. et al. Direct cellular lysis/protein extraction protocol for soil metaproteomics. *J. Proteome Res.* **9**, 6615-6622 (2010).

121. Zhang, Y. et al. Application of an improved proteomics method for abundant protein cleanup: molecular and genomic mechanisms study in plant defense. *Mol. Cell. Proteomics* (2013).

122. Zhang, Y., Liu, S., Dai, S. & Yuan, J. Integration of shot-gun proteomics and bioinformatics analysis to explore plant hormone responses. *BMC Bioinformatics* **13**, S8 (2012).

123. Holder, J.W. et al. Comparative and functional genomics of *Rhodococcus opacus* PD630 for biofuels development. *PLoS Genet* **7**, e1002219 (2011).

124. Carvalho, P.C., Fischer, J.S., Chen, E.I., Yates, J.R., 3rd & Barbosa, V.C. PatternLab for proteomics: a tool for differential shotgun proteomics. *BMC Bioinformatics* **9**, 1471-2105 (2008).

125. Stephanopoulos, G. Challenges in engineering microbes for biofuels production. *Science* **315**, 801-804 (2007).

126. Wargacki, A.J. et al. An engineered microbial platform for direct biofuel production from brown macroalgae. *Science* **335**, 308-313 (2012).

127. Machczynski, M.C., Vijgenboom, E., Samyn, B. & Canters, G.W. Characterization of SLAC: A small laccase from *Streptomyces coelicolor* with unprecedented activity. *Protein Sci.* **13**, 2388-2397 (2004).

128. Sherif, M. et al. Biochemical studies of the multicopper oxidase (small laccase) from *Streptomyces coelicolor* using bioactive phytochemicals and site-directed mutagenesis. *Microb. Biotechnol.* **6**, 588-597 (2013).

129. Widdick, D.A. et al. The twin-arginine translocation pathway is a major route of protein export in *Streptomyces coelicolor*. *Proc. Natl. Acad. Sci. U. S. A.* **103**, 17927-17932 (2006).

130. Palmer, T. & Berks, B.C. The twin-arginine translocation (Tat) protein export pathway. *Nat. Rev. Micro.* **10**, 483-496 (2012).

131. Lomakin, I.B., Xiong, Y. & Steitz, T.A. The crystal structure of yeast fatty acid synthase, a cellular machine with eight active sites working together. *Cell* **129**, 319-332 (2007).

132. Schweizer, E. & Hofmann, J. Microbial type I fatty acid synthases (FAS): major players in a network of cellular FAS systems. *Microbiol. Mol. Biol. Rev.* **68**, 501-517 (2004).

133. Gonçalves, E.R. et al. Transcriptomic assessment of isozymes in the biphenyl pathway of *Rhodococcus sp.* strain RHA1. *Appl. Environ. Microbiol.* **72**, 6183-6193 (2006).